Firmato digitalmente da LA REGINA GILDA
C=IT

DOTTORATO DI RICERCA IN

_____*SCIENZE BIOMEDICHE*_____

CICLO XXXVIII - PNRR NextGenerationEU

Dissecting the NRF2-mediated crosstalk between Cancer-Associated Fibroblasts (CAFs) and Non Small Cell Lung Cancer (NSCLC) cells for the development of targeted therapies

Settore Scientifico Disciplinare

MED-02/A

Dottorando/a

Dott.ssa *La Regina Gilda*

Supervisore

Prof.ssa *Bianchini Francesca*

Firmato digitalmente da:
Francesca Bianchini
Firmato il 30/12/2025 04:11
Seriale Certificato: 414088
Valido dal 08/12/2023 al 08/12/2026
Organizzazione: Università degli Studi di Firenze

Coordinatore

Prof. *Chiti Fabrizio*

Firmato digitalmente da FABRIZIO CHITI
Data: 17/04/2026 12:17:59 CEST

SUMMARY

1 INTRODUCTION

1.1 Lung Cancer

Lung cancer is one of the most frequently diagnosed cancers and the leading cause of cancer-related deaths worldwide. Despite advances in screening, diagnosis, and treatment, survival rates remain low, largely due to late-stage diagnosis and the aggressive nature of the disease. Lung cancer accounts for over 2 million new cases and nearly 1,8 million deaths annually, making it a major global health challenge [1]. Smoking is responsible for 89-90% of cases, but other factors include passive smoking, exposure to radon, asbestos, air pollution and family history or genetic predisposition [2], [3], [4]. Incidence and mortality rates vary by region, gender, and socioeconomic status, with higher rates in men and in countries with high smoking prevalence. However, the growing number of cases in women is also alarming [5], [6] [7].

The two main types of lung cancer are non-small cell lung cancer (NSCLC, ~85% of cases) and small cell lung cancer (SCLC, ~15%) [7]. According to the classification criteria by WHO NSCLC includes different forms of lung neoplastic diseases such as adenocarcinoma (LUAD), squamous cell carcinoma (LUSC), and large cell carcinoma (LCC). The classification has a great impact in term of biological behavior, prognosis and clinical management. However, the histopathological classification requires extensive medical expertise and involve invasive biopsy of tissues [7] (Fig1). Adenocarcinoma (LUAD) arises from glandular cells, often shows glandular or papillary structures, and is associated with driver mutations in specific genes such as Epidermal Growth Factor Receptor (EGFR), Anaplastic Lymphoma Kinase (ALK), and Kirsten Rat Sarcoma viral oncogene homolog (KRAS). The identification of these targetable mutations allowed the development of specific drugs for precision medicine approach [8], [9]. This form is more common in women and non-smokers, often presents as peripheral nodules, and generally has better prognosis than LUSC or LCC [10], [11]. Squamous cell carcinoma (LUSC) originates from bronchial epithelial cells. Lesions are characterized by keratinization and intercellular bridges, and frequently harbour alterations in genes like Phosphatidylinositol-4,5-bisphosphate 3-kinase catalytic subunit alpha (PIK3CA), SOX2: A SRY-Box Transcription Factor 2 (SOX2), and Fibroblast Growth Factor Receptor 1 (FGFR1) [8]. LUSC is less likely to have targetable mutations but shows high glucose uptake and glycolytic activity[12] . LUSC is more common in men and smokers. Lesions develop in the central area of the lungs, and symptoms like cough and sputum are associated with higher rates of infection and worse prognosis than ADC [11][13]. Large Cell Carcinoma (LCC) is defined by lack of glandular or squamous differentiation; often is the consequence of an exclusion diagnosis. Indeed, LCCs can be reclassified as poorly differentiated LUAD or LUSC using immunohistochemistry and molecular

profiling [14], [15], [16]. LCC is more aggressive and shows the poorest prognosis among the three types of NSCLC. Lastly, LCC lesions are often revealed at an advanced stage [11].

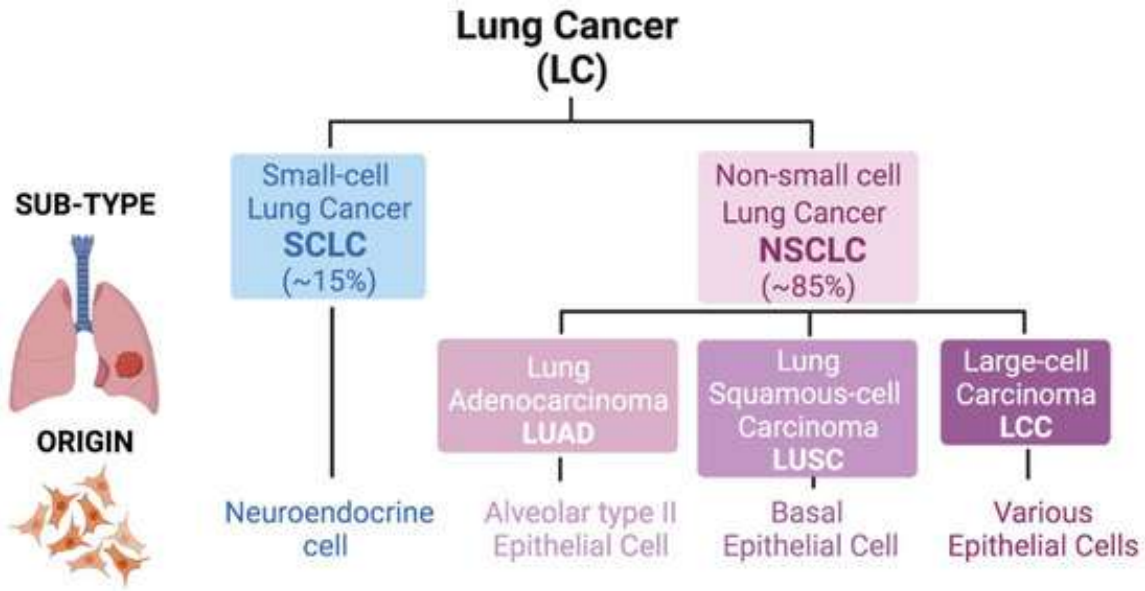

Figure 1 :Classification of lung cancer (Sánchez-Ortega, Miriam, Ana Clara Carrera, and Antonio Garrido. 2021. "Role of NRF2 in Lung Cancer" Cells 10, no. 8: 1879. https://doi.org/10.3390/cells10081879)

1.2 MOLECULAR PATHOGENESIS AND THERAPEUITC LANDSCAPE OF NSCLC

The assesment of specific gene mutations represents the most established set of biomarkers used in clinical practice for NSCLC prediction and prognostication. Common mutations include EGFR, KRAS, ALK, ROS1, BRAF,MET, RET, and HER2. Tumor suppressor genes such as TP53, STK11/LKB1 and KEAP1 are frequently altered, affecting cell cycle regulation, apoptosis and therapy resistance [17], [18], [19], [20]. NSCLC tumors often exhibit high tumor mutation burden (TMB), copy number variations and chromosomal instability, wich are associated with aggressive behavior and metastasis [21], [22], [23]. Another characteristic feature of NSCLC is the role of microRNA and long non-coding RNAs. It has been demenstrated that both microRNA and lncRNAs modulate gene expression, affecting tumor progression and therapy response [24], [25]. However, the principal and more frequently affected biological pathways involved in NSCLC pathogenesis are PI3K-Akt, Notch, mTOR and p53 [26], [27].

The management of NSCLC has rapidly evolved, with a strong emphasis on personalized and precision medicine. Current strategies are tailored to tumor stage, molecular profile and patient characteristics, in order to integrate surgery, systemic therapies and treatments with novel agents [28]. Complete surgical resection remains the gold standard, offering the best chance for cure and local/regional control in NSCLC, especially as advancements in minimally invasive techniques and

enhanced recovery protocols have reduced associated morbidity [29]. Th indications for surgery are continually evolving and expanding beyond early-stage disease. This expansion is directly driven by the introduction of powerful new therapeutic modalities including treatments like immune checkpoint inhibitors (with or without chemotherapy) and targeted systemic therapies or ablative techniques options such as stereotactic radiotherapy (SBRT)[30], [31]. Personalized treatment approaches for NSCLC, incorporating genomic analyses and predictive biomarkers, could potentially cure early disease and improve outcomes[32] the identification of genomic mutations lead to the development of targeted therapies based on the use of tyrosine kinase inhibitors (TKIs), or blocking antibodies in both early and advanced stages [28], [7], [32] , [33]. Newly developed agents, including third-generation TKIs and antibody-drug conjugates (ADCs), address inherited and acquired resistance and expand treatment options for rare mutations [34], [35]. Finally, Immune Checkpoint Inhibitors (ICIs) targeting PD-1/PD-L1 or CTL-4 are a mainstay for patients without actionable mutations. The PD-L1 expression has recently enriched with other emerging biomarkers for ICs [36], [7], [33]. These treatments are increasingly used in both advanced and early-stage cancers following specific schedule settings, in combination with chemotherapy [31][35][34]. However, the development of drug resistance remains a major hurdle, prompting research toward the development of novel agents.

1.3 THE TUMOR MICROENVIRONMENT

The tumor microenviroment (TME) is a complex, dynamic ecosystem of cancer cells, stromal cells, immune cells, blood vessels, extracellular matrix (ECM) and signaling molecules. The TME actively drives tumor progression, metastatic diffusion, immune evasion and therapy resistance [37], [38], [39]. The TME is composed by cellular elements such as cancer associated fibroblasts (CAFs), immune cells (macrophages, T cells, B cells, neutrophils, and dendritic cells), endothelial cells, pericytes, adipocytes and neuroendocrine cells [38]. In addition, non-cellular elements, like growth factors, cytokines, chemokines and exosomes are fundamental components of the TME [37]. Finally, physical and chemical features such as hypoxia, the acidic extracellular pH, the increased matrix stiffness and the abnormal vasculature are common, prompt tumor cell toward a more aggressive phenotype [40], [41].

The TME provides growth factors and survival signals, supporting cancer cell proliferation and resistance to apoptosis [42]. Soluble factors released in the TME are crucial for the maintenance of angiogenic stimuli. Tumor and stromal cells secrete pro-angiogenic factors (e.g., VEGF), stimulating new blood vessel formation to supply nutrients and oxygen diffusion [43]. In addition, other soluble factors, such as chemokines and other growth factors recruit and reprogram immune cells, often

creating an immunosuppressive environment that allows tumor cells to evade host immune defences [44]. On the other hand, cellular elements of the TME such as cancer associated fibroblasts (CAFs) exert a key role in the promotion of cancer cell invasiveness and metastatic diffusion through the remodelling of the ECM. The continuos remodelling of the ECM facilitates cancer cell migration and invasiveness [39] [38], Furthermore, TME supports cancer cell dissemination, survival in circulation and colonization at distant sites, through the promotion of hypoxia-induced adaptations and the interactions with platelets or with other immune cells [41][45]. Finally, TME leads to therapy resistance, the increased ECM stiffness hinders drug delivery, and promotes the acquisition of resistance to chemotherapy, radiotherapy and immunotherapy [39], [42], [43].

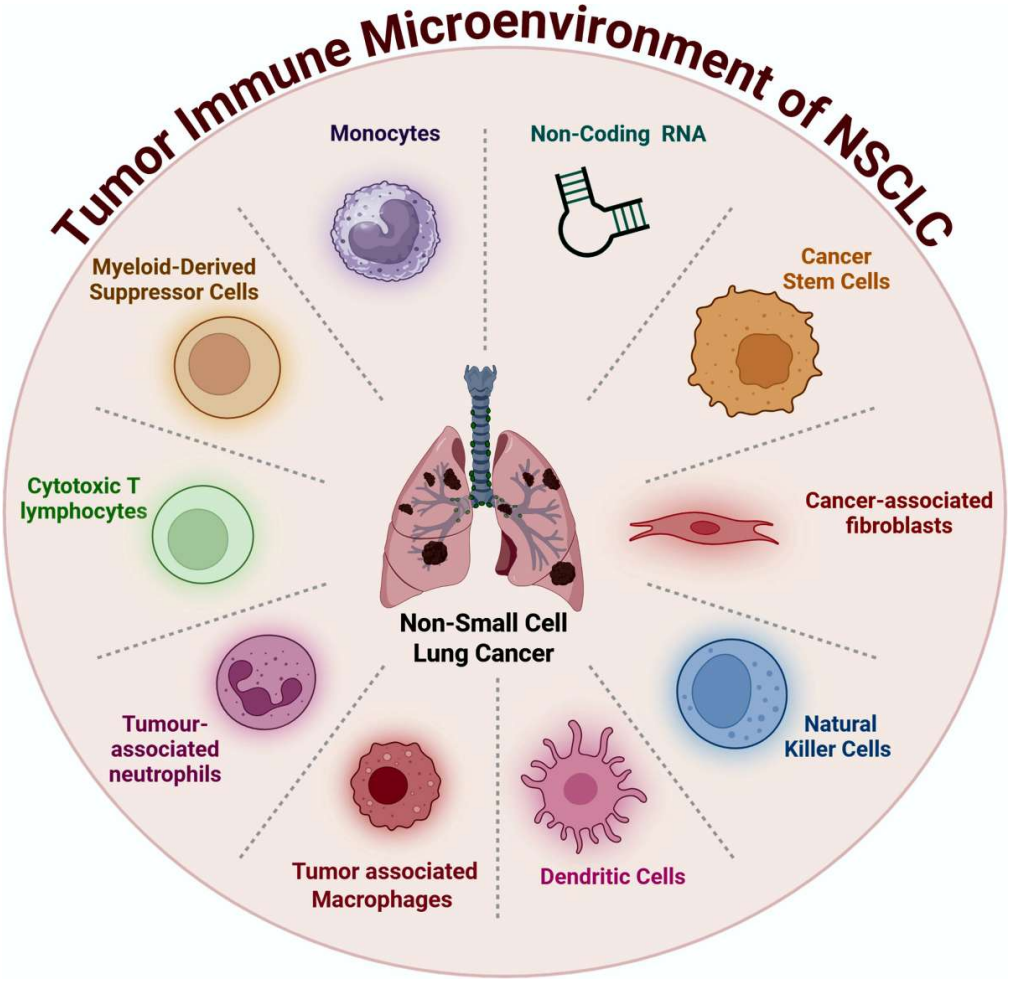

Figure 2 :Components of the TME, image taken from "Bharadwaj, S., Mierzwicka, J.M., Vaňková, L. et al. Unraveling the molecular-pathological characteristics and cellular complexity of the tumor immune microenvironment in metastatic non-small cell lung cancer. Cell Commun Signal 23, 400 (2025). https://doi.org/10.1186/s12964-025-02410-w"

It has been demonstrated that the TME in NSCLC often becomes immunosuppressive, limiting the effectiveness of immune checkpoint inhibitors (ICIs). Genetic alterations such as KEAP1,

SMARCA4, and PTEN mutations drive immune evasion by reducing T-cell infiltration, impairing antigen presentation, and fostering an immunosuppressive cytokine milieu. These changes are linked to poor outcomes and resistance to immunotherapy, regardless of PD-L1 status or tumor mutational burden [46], [47], [48], [49]. Regulatory T cells (TREG), myeloid-derived suppressor cells (MDCDs) and tumor associated macrophages (TAMs) are abundant in the NSCLC TME, suppressing anti-tumor immune responses and promoting tumor growth [48], [50]. Taken together, the TME is no more considered a passive bystander but a critical driver of tumor progression, of metastatic diffusion and therapy resistance. Targeting the TME in all its complexity and components is a promising strategy for improving cancer treatment outcomes.

1.3.1 CAF and fibrosis: critical components of the pro-tumorigenic TME

Cancer-associated fibroblasts (CAFs) are central players in the tumor microenvironment, orchestrating intratumoral fibrosis and profoundly influencing tumor progression, immune evasion and therapy resistance [51]. CAFs are the primary source of extracellular matrix (ECM) components, such as collagen, leading to dense, fibrotic stroma characteristic of many solid tumors. This fibrosis not only provides structural support but also creates a physical barrier that impedes drug delivery and immune cell infiltration, contributing to poor prognosis and resistance to therapy [52], [53]. Desmoplastic tumors, in which CAF-driven fibrosis is prominent, present an aggressive tumor behavior [54], [55], [56]. The phenotypic heterogeneity of CAFs and their dynamic interactions with cancer and immune cells make these cells both a challenge and an opportunity for targeted therapies[57]. CAFs are commonly identified by the expression of markers such as alpha-smooth muscle actin (α-SMA) (ACTA2), fibroblast activation protein alpha (FAP-α), Platelet-Derived Growth Factor Receptor (PDGFR), fibroblast growth factor receptor (FGFRalpha/beta), CD90, integrin β1 and others. However, it became clear that no single marker is specific, and that a panels of markers and gene signatures need to be used to distinguish CAF subtypes and differentiate them from normal fibroblasts [58], [59], [60], [61]. Another strategy to characterize and identify primary CAFs is to combine traditional biomarkers with lineage exclusion, so long as primary CAFs should be negative for epithelial cell adhesion molecule (EpCAM) [62].

Transforming growth factor-beta (TGF-β) is the central signaling molecule driving the activation, function, and tumor-promoting activities of CAFs in the TME. TGF-β is a potent inducer of the transition from normal fibroblasts or precursor cells (such as adopose-derived stromal cells) into CAFs [63]. This process involves upregulation of CAF markers (e.g., alpha-SMA, FAP, vimentin) and is mediated by both canonical (SMAD-dependent) and non-canonical signaling pathways [64],

[65], [66]. TGF-β also stimulates CAF proliferation and survival, often through autocrine and paracrine loops [64], [66].

Extensive evidence demonstrates that CAFs and fibrosis are pivotal components of tumor progression, invasion, and metastasis in NSCLC. CAFs expressing CD248 increase collagen I production, leading to a stiffer ECM. This enhanced stiffness activates the Hippo pathway and connective tissue growth factor, directly promoting NSCLC cell infiltration, migration, and metastasis. Knockout of CD248 in fibroblasts significantly reduces lung tumor metastasis in animal models, confirming a causal role [67]. In orthotopic NSCLC models, tumors enriched with CAFs show an increased fibrotic tissue, collagen deposition and higher rates of mediastinal lymph node metastasis, while targeting CAFs reduces both fibrosis and metastatic spread [68].

CAFs secrete cytokines (e.g.,IL-6), growth factors that induce the epithelial-mesenchymal transition (EMT) in cancer cells, which is the key event that promote cancer cell invasiveness and metastatic potential [69], [70]. it has been demonstrated that high expression of CAF markers and fibrosis-related genes in NSCLC correlates with advanced tumor stage, increased invasion, distant metastasis and poor prognosis [71], [72].

Targeting CAFs and their fibrotic activity is promising but complex therapeutic approach. Strategies under investigation include the disruption of CAF-cancer cell signaling cross-talk, the modulation of ECM remodeling, and the selective targeting of tumor-promoting CAF subtypes [51], [73], [74]. Indeed, advances in single-cell sequencing and imaging are improving the identification and characterization of CAF subpopulation, paving the way for more precise interventions [51], [52], [57].

1.3.2 NRF2 role and basal regulation mechanisms

The protein Nrf2 (nuclear factor erythroid 2-related factor 2) is a key transcription factor regulating antioxidant and cytoprotective genes. Indeed, the Nrf2 pathway is reported as the most important strategy that cell adopt against oxidative stress [75] . Nrf2 regulates the expression of hundreds of genes involved in antioxidant defence like NQO1(NAD(P)H Quinone Oxidoreductase1), GCL (Glutamate-Cysteine Ligase), GSTs (Glutathione S-Tranferase), HO-1 (Heme Oxygenase-1), in drug detoxification (MRP1 and MRP2, multidrug resistace efflux proteins) and in glutathione metabolism. Moreover, Nrf2 regulates inflammatory response, autophagy (p62) and mitochondrial functioning. In the complex Nrf2 exert a central role in cellular homeostasis and stress adaptation control [76], [77].

Nrf2 is ubiquitously expressed in a wide range of tissue and cell types and belongs to a subset of basic leucine zipper genes (bZIP) sharing a conserved structural domain designated as a cap'n'collar domain. The basic region, just upstream of the leucine zipper region, is responsible for DNA binding and the acidic region is required for transcriptional activation. Nrf2 binds to antioxidant response elements (AREs), ARE sequence is present in the promoter region of genes involved in the antioxidant and detoxifying response, but also cellular proliferation, metabolism, immune response, signaling, cell survival and cellular cycle[78]. ARE-mediated transcriptional activation requires heterodimerization of Nrf2 with other bZIP proteins including Jun (c-Jun, Jun-D, and Jun-B) and small Maf (MafG, MafK, MafF) proteins [79], [80] . Nrf2 contains seven conserved Nrf2-ECH homology (Neh) domains (Neh1-Neh7), each mediating specific regulatory and functional roles. The Neh2 domain binds to KEAP1, its direct regulator. Neh1 contains the DNA-binding basic leucin zipper motif, while Neh3, Neh4 and Neh5 act as transactivation domains. Neh6 and Neh7 domains further modulate Nrf2 stability and repression through interaction with beta-TrCP and RXRalpha, respectively[81], [82] (Fig.3).

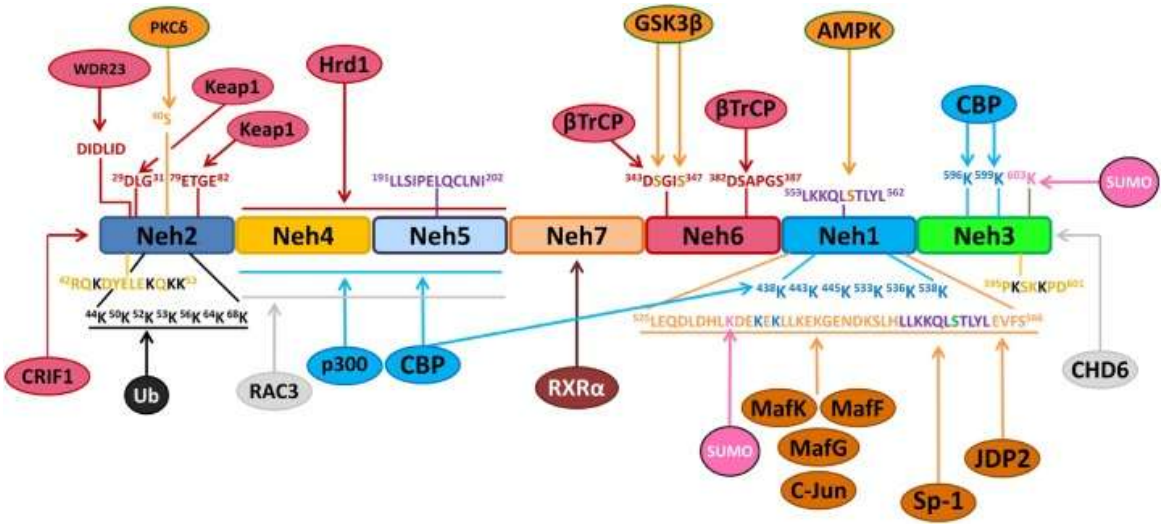

Figure 3 : Nrf2 protein structure from Homo sapiens. https://doi.org/10.1016/j.phrs.2018.06.013

Nrf2 is negatively regulated by KEAP1, which targets it for degradation under normal conditions, the main function of KEAP1 is as adapter for the Cullin3/RingBox1 (Cul3/Rbx1) E3 ubiquitin ligase complex, so under homeostatic conditions, KEAP1 binds Nrf2 in the cytoplasm facilitating its ubiquitination and subsequent degradation. Oxidative or electrophilic stress modifies KEAP1 cysteine residues, distrupting this interaction, allowing Nrf2 to accumulate and translocate to the nucleus and activate gene transcription [83], [84], [85]. The regulation of Nrf2 is also intrinsically linked to the cellular degradation process of autophagy via the protein p62 (SQSTM1), p62 is a

multifunctional scaffold protein that acts in autophagic degradation mechanisms and also it acts as a positive regulator of NRF2. Critically p62 possesses a Keap1-binding domain (KIR) that allows it to directly compete with NRF2 for binding to the Keap1 protein, indeed increased expression or aggregation of p62 sequesters Keap1, thereby reducing the availability of Keap1 to bind NRF2. This competitive inhibition stabilizes NRF2 for the translocation to the nucleus. Furthermore, this interaction establishes a positive feedback loop because the p62 gene itself contains an ARE in its promoter; consequently, the stabilized NRF2 directly transcribe and increase the expression of p62. This reciprocal relationship amplifies the antioxidant response and sustains NRF2 activation [86], [87], [88].

NRF2 is regulated not only by the canonical KEAP1-CUL3 pathway but also through several non – canonical KEAP1-indipendent mechanisms. These alternative pathways provide additional layers of control over NRF2 stability, localization and activity and are increasingly recognized as important in both physiological conditions and in diseases. Glycogen synthase kinase 3beta (GSK3b) phosphorylates NRF2 creating an active site recognized by the E3 ubiquitin ligase adapter beta-TrCP, which targets NRF2 for ubiquitin-mediated proteasomal degradation via the CUL1 complex, this pathway primarily regulates NRF2 in the nucleus and is especially important for terminating the NRF2 response after stress, rather than controlling its basal levels [89], [90].

Furthermore, WDR23, as a part of the DDB1-CUL4E3 ligase complex, binds directly to the Neh2 domain of NRF2 (at the DIDLID sequence, not the KEAP1-binding motifs) and promotes its degradation. This pathway operates independently of KEAP1 providing an alternative route for NRF2 turnover [91].

NRF2 activity is tightly regulated by numerous protein kinases that act as upstream sensors for stress, nutrient availability and growth factor signaling. NRF2 contains many serine, threonine and tyrosine residues, which may provide sites for phosphorylation by different kinases and this phosphorylation of NRF2 can impact its stability, nuclear translocation and transcriptional activity[92]. Thus, a number of different pathways have been explored including mitogen-activated protein kinase cascades (MAPK), the phosphatidylinositol 3-kinase (PI3K/AKT) pathway, protein kinase C (PKC) and the extracellular signal-regulated kinase (ERK) signalling pathways. Specifically, phosphorylation of NRF2 at Serine-40 (S40) in the Neh2 domain by Protein Kinase C (PKC) is a key activating event, leading to the dissociation of the NRF2/KEAP1 complex and subsequent nuclear translocation [93].

Moreover, NRF2 activity is finely tuned through the phosphorylation by a panel of MAP kinases family that exhibit complex and sometimes contradictory roles [94]. Studies involving inducers like butylated hydroxyanisole (BHA) have highlighted the involvement of JNK (cjun N-terminal kinase 1/2) and ERK. BHA was shown to increase the phosphorylation of both ERK1/2 and JNK 1/2,

leading to NRF2 release from Keap1 and subsequent nuclear translocation under the control of these pathways [95]. Conversely, p38 activity has been sown to inhibit NRF2 by a phosphorylation that promotes its association with Keap1, thereby preventing its nuclear translocation. Interestingly, this inhibitory effect was reversed by sulforaphane, proposing a mechanism for its NRF2-inducing action [96]. Other regulatory pathways have been identified by studying the interaction between NRF2 and proteins other than Keap1. Indeed, beyond p62[97] there are alternative route that involves a growing set of proteins such us DPP3, WTX, p21 and BRCA1[98] [99]. These non-canonical activators through their binding distrupts the Keap1-NRF2 complex, thereby preventing NRF2 ubiquitination and degradation. The net result is an increase in NRF2 nuclear translocation and activation. This extensive repertoire of factors involved in the post-translational modification of NRF2 underscores the pathway's intricate and highly regulated nature, elucidating the precise cross-talk between these various signaling pathways is crucial for advancing our understanding of cellular defence mechanisms and identifying viable therapeutic targets.

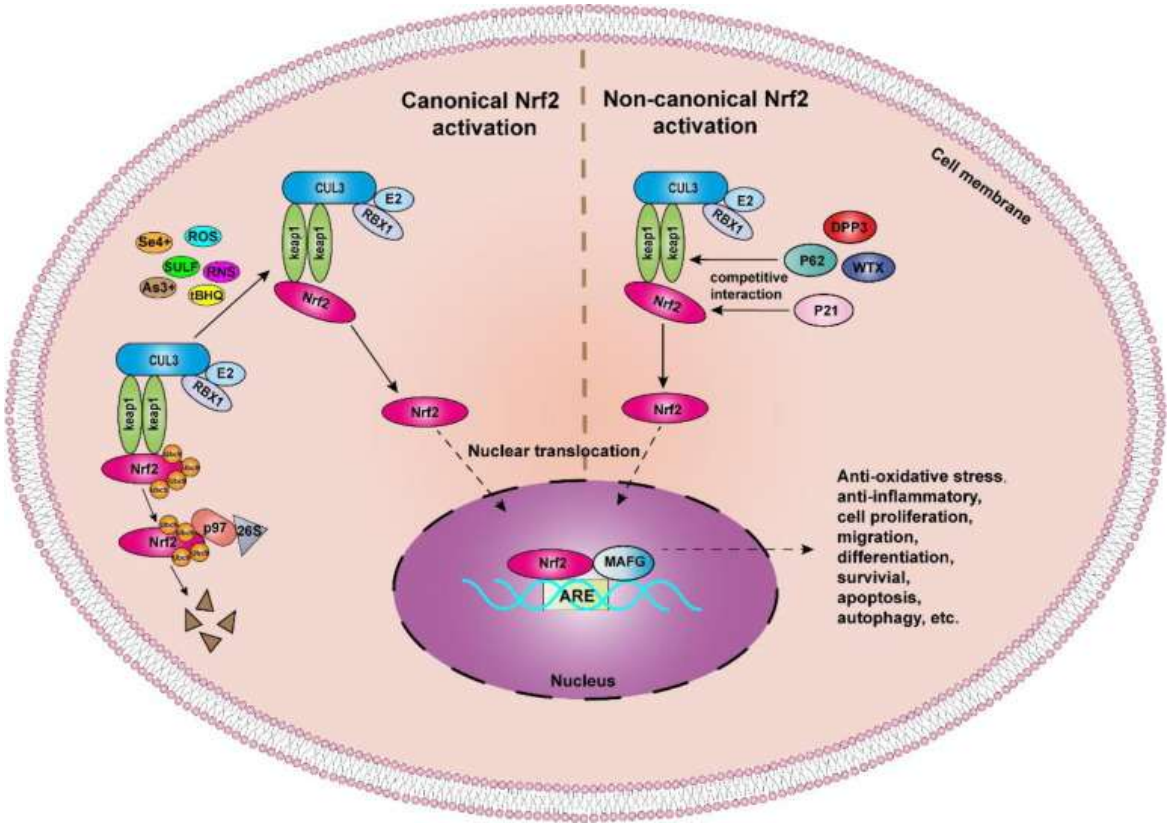

Figure 4 : Canonical and non-canonical mechanisms of NRF2 activation

1.3.3 NRF2 in cancer

NRF2 initially acts as a beneficial defending mechanism, shielding healthy cells from damage. However, in malignant settings, this pathway is frequently exploited by cancer cells to support tumor progression and evade the effects of various therapeutic interventions[100], [101] .

Regarding the prevention of carcinogenesis, in normal and early-stage cancer cells, NRF2 activation protects against DNA damage, oxidative stress and inflammation, thereby reducing the risk of malignant transformation [102], [103].Moreover, NRF2 upregulates antioxidant and detoxification genes, maintaining redox homeostasis and preventing genome instability[104] . In established tumors, persistent or aberrant NRF2 activation (often due to mutations in KEAP1 or NRF2 itself) supports cancer cell survival, proliferation, and metabolic reprogramming, angiogenesis and metastasis [105], [106]. In particular, NRF2 upregulates glutathione synthesis, thioredoxin and other ROS-scavenging systems, lowering oxidative stress that would otherwise limit tumour cell survival and mutagenic tolerance [107]. NRF2 drives pathways that supply nucleotides, amino acids and NADPH: it promotes ribonucleotide synthesis and serine biosynthesis and redirects carbon flux to support proliferation and redox balance and by increasing anabolic and autophagic programs NRF2 helps maintain biomass and survival during stress facilitating rapid tumour growth [100], [101]. Persistent NRF2 activation commonly co-occurs with KRAS or PI3K/AKT pathway activation; NRF2 can potentiate PI3K signaling and downstream kinase networks to boost growth and survival in certain cancers [108]. In the context of immune modulation and evasion NRF2 activity shapes the tumor immune microenvironment, diminishing cytotoxic immune responses and correlating with reduced responses to anti-PD-1 therapies in some tumors [109]. Constitutive NRF2 increases detoxification and DNA (?)repair capacity and is mechanistically linked to resistance to chemotherapy, radiotherapy and targeted agents across solid tumors [108], [110]. In some cases, cancers become dependent on high NRF2 activity for growth and survival, making NRF2 a potential therapeutic target [102], [111].

Genetically mutations in the NRF2 gene (NFE2L2) are increasingly recognized as important drivers in various cancers. These mutations often lead to persistent activation of NRF2, which profoundly influences tumor behaviour, therapy response and patient prognosis. Most cancer-associated NRF2 mutations cluster in the DLG and ETGE motifs of the protein, which are critical for its interaction with the negative regulator KEAP1. Mutations at positions like R34 and D29 are frequent in lung, bladder, and uterine cancers. These mutations disrupt KEAP1 binding, preventing NRF2 degradation and resulting in its constitutive activation [112], [113], [114], [115]. NRF2 mutations are associated with aggressive tumour growth, higher mutating burden, and poor prognosis in cancers such as non-small cell lung cancer (NSCLC), esophageal squamous cell carcinoma, and hepatoblastoma [116], [117], [118].

In lung cancer, NRF2 plays a complex, context-dependent role, acting as both a tumor suppressor and a promoter of tumor progression and therapy resistance [119]. The maintenance of the malignant phenotype in lung cancer cells is highly dependent on the NRF2 pathway, a mechanism referred to as NRF2 addiction [120].

In NSCLC, NRF2 acts in two different and opposite ways[119] (Fig.5). On one side, NRF2 acts as a tumor suppressor, and contributes to preventing DNA damage by regulating the expression of NQO1. NQO1 is required for controlling the mRNA levels of the repair proteins BRCA1 and RAD51[121] These proteins regulate homologous recombination (HR) during the repair of double-strand breaks (DSB) [122]. Indeed, NRF2-null mice are more susceptible to acute DNA damage [123]. In addition, NRF2 activation in normal human lung fibroblasts reduces DSB levels after irradiation [124]. These defending mechanisms against tumorigenesis have been confirmed in other animal studies [125], [126], [127]. NRF2 can modulate the inflammatory and immune response at the tumor site through the decreases in pro-inflammaory cytokines expression such as tumor necrosis factor alpha (TNF-alpha), interleukin 1-beta (IL-1beta) or IL-6 [102]. NRF2 is also able to recruit Natural Killer (NK) cells that secrete the isoform D of IL-17, promoting tumor rejection [128].

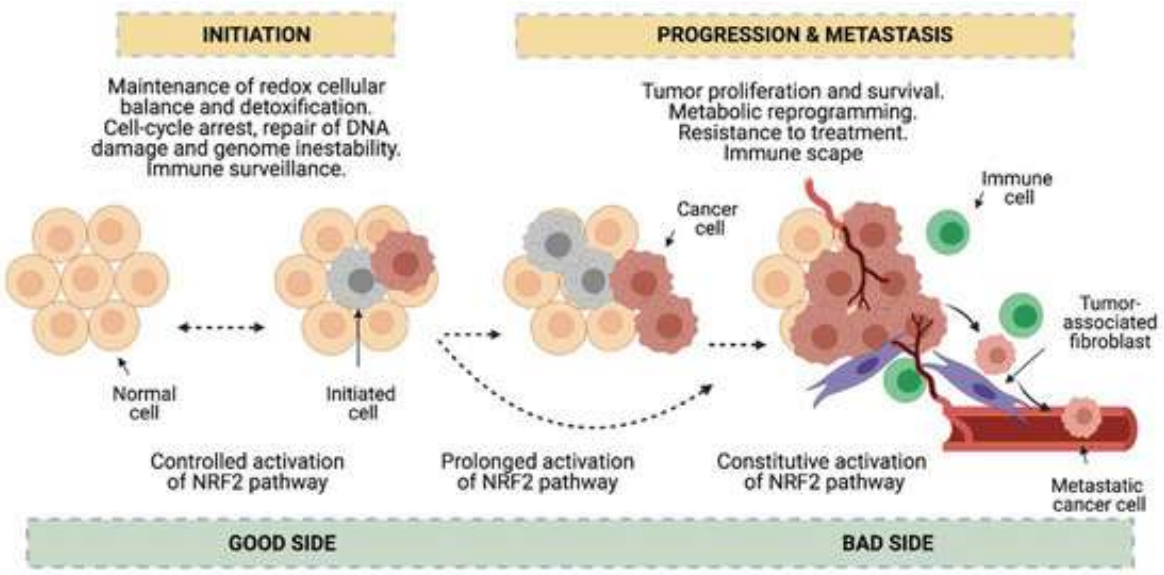

Figure 5 : Dual role of NRF2 in cancer (Sánchez-Ortega, Miriam, Ana Clara Carrera, and Antonio Garrido. 2021. "Role of NRF2 in Lung Cancer" Cells 10, no. 8: 1879. https://doi.org/10.3390/cells10081879)

On the other side, NRF2 acts as a pro-oncogene. Activating mutations in NRF2 provide advantageous conditions for cancer progression [129]. Elevated NRF2 protein levels were found in several malignancies including lung cancer [126][130], [131]. *NFE2L2/KEAP1* is a commonly mutated

pathway in NSCLC [132]. Gain-of-function mutations in *NFE2L2* or loss-of function mutations in *KEAP1* are frequently observed [129]. KEAP1 mutations are found in 17% of LUAD and 12% of LUSC tumors, NFE2L2 mutations are more frequent in LUSC (15%) than LUAD (3%); globally, 26% of NSCLC tumors show increased nuclear NRF2 expression [133], [134]. The oncogenic action of NRF2 in NSCLC involves regulating enzymes related to metabolic reprogramming, promoting aerobic glycolysis (the so-called Warburg effect) [120] [116]. NRF2 overexpression significantly impacts amino acid metabolism, enabling cancer cell survival and proliferation under stress [131], [120]; KEAP1/NRF2 mutant NSCLC cells show increased sensitivity to glutaminase inhibition, which sensitizes these cells to radiotherapy [135], [136]. Constitutive NRF2 activation correlates with increased tumor cell survival and proliferation [137] , NRF2 increases levels of IGF1, PDGFC, and VEGFC [102] and high NRF2 nuclear level is associated to a shortening in progress-free survival in NSCLC patients [134]. Finally, high expression levels of the NRF2 target gene NQO1 are also linked to worse prognosis [138].

The over activation of NRF2 is linked also to metastatic diffusion, indeed, NRF2 overexpressing cancer cells show an increased ability to grow in an anchorage-independent manner and have high metastatic potential [139]; It has been also observed that some of NFE2L2 and KEAP1 mutations are highly expressed in NSCLC metastatic lesions [140]. NRF2-driven antioxidant responses are highly active in cancer-associated fibroblasts and pericytes within the TME, supporting tumor survival under oxidative stress [141]; NRF2 also reprograms tumor and stromal cell metabolism, facilitating adaptation to hypoxia and nutrient deprivation, and promoting cancer cell proliferation and invasion [142][143].

Moreover, NRF2 contributes to immune escape in the TME, not only by controlling cytokine expression but also through KEAP1 mutation that is associated with a reduced leukocyte infiltration [144] and, finally, NFE2L2 mutant tumors show low expression of immune response markers [145].

There are preclinical evidences that highlight the role of NRF2 in fostering immunosuppressive TME through its activity on tumor-associated macrophages (TAMs). NRF2 suppresses pro-inflammatory cytokine production, increases expression of immune checkpoint molecules like PD-L1 and promotes anti-inflammatory macrophage phenotypes, all of which dampen anti-tumor immune responses [146], [147], [148]. NRF2 also protects immunosuppressive myeloid-derived suppressor cells (MDSCs) from oxidative stress, further inhibiting T cell activity [103]. In some contexts, NRF2 activation in immune cells can reduce tumor growth by enhancing immune surveillance but in established tumors it often supports immune evasion [119], [149]. Remaining in the context of the TME, NRF2-driven antioxidant responses are highly active in cancer-associated fibroblasts and pericytes within the TME, supporting tumor survival under oxidative stress [141]; NRF2 also

reprograms tumor and stromal cell metabolism, facilitating adaptation to hypoxia and nutrient deprivation, and promoting cancer cell proliferation and invasion [142], [143].

In conclusion, in NSCLC, NRF2 expression is linked to resistance against chemotherapy (e.g., platinum-based drugs, cisplatin) and targeted therapies (e.g., EGFR-TKIs) [150], [151]; this effect is due to the NRF2 derived expression of genes that counteract drug-induced oxidative stress and ferroptosis reducing treatment efficacy [152], [153] several studies showed that inhibiting NRF2 or its downstream pathways can restore drug sensitivity in resistant NSCLC cells [154], [155].

Thus, targeting NRF2 stability, its regulatory partners or downstream metabolic vulnerabilities is being explored as an innovative therapeutic strategy [156].

2 AIM OF THE STUDY

Non-Small Cell Lung Cancer remains one of the most challenging malignancies to treat, characterized by high mortality rates and a complex landscape of therapeutic resistance. While research has traditionally focused on the genetic landscape of tumor cells, the Tumor Microenvironment has increasingly been recognized as a primary driver of malignancy. Among the various cellular components of the TME, Cancer-Associated Fibroblasts (CAFs) play a predominant role, orchestrating a persistent desmoplastic reaction that not only provides a physical scaffold for the tumor itself but also acts as a dynamic signalling hub that promotes progression and resistance to drug.

In the context of NSCLC, this aberrant fibrotic response does not merely alter the tissue architecture; it creates a hostile and high-pressure environment that forces both stromal and neoplastic cells to a continuous adaptation, orchestrating the acquisition of new survival strategies in cancer cells. A cornerstone of this adaptation is the ability to withstand oxidative stress and maintain cellular integrity, a process largely governed by the transcription factor NRF2 (Nuclear factor erythroid 2-related factor 2). The regulation of NRF2 is traditionally described through its canonical, KEAP1-dependent degradation pathway. However, in the complex milieu of the lung stroma, NRF2 is often modulated via non-canonical pathways triggered by internal and external factors. TGF-beta which is a master regulator of the fibrotic response, driving the activation of CAFs is a key modulator of non-canonical NRF2 activation. Aalthough the pro-fibrotic effects of TGF-beta are well-documented, the molecular mechanisms underlying the crosstalk between CAFs-derived TGF-beta and the NRF2 antioxidant response in the NSCLC TME remains poorly understood.

The overarching goal of this study was to elucidate the molecular mechanisms by which the TME promotes cancer progression and treatment resistance in a preclinical model of human NSCLC, with a specific focus on the interplay between fibrotic signalling and redox homeostasis. By transitioning from simplified cytokine-based models to complex 3D co-culture, the present research aimed to validate the TGF-beta/NRF2 axis as a key mediator of stromal-tumor crosstalk.

The research plan of the present study was organized into the following sequential aims:

1. Evaluation of the role of key components of the TME on NSCLC cells. Assessment of the role of TGF-beta, and other inflammatory and fibrotic cytokines on NRF2 expression in three different NSCLC cell lines.

2. Effect of the antifibrotic drug pirfenidone (PFD) on CAFs phenotype. PFD (an antifibrotic drug traditionally used in clinical practice for idiopathic pulmonary fibrosis) inhibits TGF-beta signalling. We explored whether PFD reduce the expression of CAF markers of activation and "normalize" CAF phenotype. PFD treatment may be used as a strategic tool to dismantle the stromal support system in TME. CAF have been established from three different patients. These cells were characterized via a flow cytometry and immunofluorescence to ensure the establishment of a robust primary cell model that accurately reflects the stromal heterogeneity of the lung TME.
3. Role of the canonical and non-canonical NFR2 activation in NSCLC. We established an *in vitro* microenvironment model using conditioned medium collected from CAFs to analyse whether the secretome of CAFs affects NRF2 expression.
4. Evaluation of the effect of profibrotic/antifibrotic CAF secretome on tumor cell viability, proliferation and aggressiveness.
5. Evaluation of the effect of NRF2 loss-of-function on NSCLC survival and invasiveness. The study involved the use of siRNA-mediated silencing.
6. Development of a 3D multicellular co-culture model (3D multicellular tumor spheroid, MCTS). The MCTS were obtained by co-culturing NSCLC cells and primary CAFs. MCTS were established as a biomimetic platform for future studies, providing a superior tool for testing stromal-targeting strategies in an architecturally complex environment.

3 MATERIALS AND METHODS

3.1 CELL LINE AND CULTURE CONDITIONS

A549, H1975 and H1299 cancer cells and MRC5 human lung fibroblast cell line was obtained by ATCC. Cells were cultured in DMEM High Glucose medium (EuroClone, Milan, Italy) supplemented with 10% of fetal bovine serum (FBS, EuroClone) and maintained at 37°C in humidified atmosphere containing and 5% CO_2. Subconfluent cultures were harvested by incubation with a trypsin-EDTA solution (EuroClone), and propagated every three days. Viability of the cells was determined by trypan blue exclusion test. The cultures were regularly tested for mycoplasma contamination.

3.2 PRIMARY CANCER ASSOCIATED FIBROBLAST CELL CULTURE

All primary CAF lines were established from fresh tumor tissue samples obtained from NSCLC patients undergoing surgery at Careggi Hospital, under an institutional review board-approved protocol, informed consent was obtained from all patients prior to sample collection. Fresh tumor samples were immediately transferred to the laboratory in sterile PBS supplemented with antibiotics. The tissue was macroscopically separated from adjiacent normal tissue and surrounding fat, then carefully minced into small fragments (1-3 m^3), using a sterile scalpel. Fibroblasts are characterized by their rapid adherence to the plastic surface. After 24 hourse, non adherent cells (primarily epithelial and immune cells) were removed by aspirating the medium and replacing it with fresh complete medium. This step helps in the selective enrichment of the adherent CAF population. The fragments recovered from the lesions were incubated for 2 weeks until they developed a homogeneous population characterized by CD90 expression and EpCAM negative. CAFs were maintained in DMEM High Glucose medium (EuroClone Milan, Italy) supplemented with 20% of FBS and maintained at 37°C in humified atmosphere containing 5% CO_2. Experiments were conducted using CAFs between passages 3-10 to ensure a homogeneous and stable phenotype.

3.3 FACS ANALYSIS

The isolated primary CAF were characterized by flow cytometry to confirm their phenotype, specifically through the expression of the fibroblast marker CD90 (Thy-1). CAFs were

cultured in 6well plates and were detached using a mild detachment solution (e.g., 0.25% Trypsin/EDTA or Accutase), collected, and washed once with cold PBS supplemented with 2% FBS. To minimize non-specific antibody binding, cells were blocked for 15 minutes at 4°C in PBS supplemented with 1% Bovine Serum Albumin (BSA). Following the blocking step, cells were incubated in the dark at 37 °C for 1 hour with the following target antibody: CD90-PE (Milteny biotec 130114902) and CD326 (EpCAM)-APC (Milteny biotec 130111117) a dedicated sample of cells was incubated in FACS buffer alone, without any conjugated antibody to establish the intrinsic cellular autofluorescence and optimize the flow cytometer voltage and compensation settings. Following incubation, cells were washed twice with FACS buffer to remove unbound reagents and resuspended in a final volume of 300 ul of FACS buffer. Samples were immediately acquired using a flow cytometer (BD- FACSCanto II) , a minimum of 10,000 events were recorded per sample. Data analysis was performed using flow cytometry software (FlowJo).

3.4 IMMUNOFLUORESCENCE

Immunofluorescence staining was performed on adherent cell cultures to visualize the expression and localization of specific proteins. Cells were seeded onto sterile appropriate culture plates (Ibidi 15um-SLIDE 8 well, 80826) at a density of 20.000 and subjected to experimental treatments. Cells were washed with PBS and then fixed with 4% paraformaldehyde (PFA) in PBS for 15 minutes at room temperature. Following fixation, cells were washed again with PBS and permeabilized using 0.1% Triton X-100 in PBS for 10 minutes. After a wash with PBS cells were incubated with a Blocking Buffer (1% BSA) for 30 minutes at room temperature to prevent non-specific binding of antibodies. Than cells were incubated with the primary antibody alphaSMA (Invitrogen MA1-06110) diluted in blocking buffer at the manufacturer's recommended concentration, overnight at 4°C. The cells were washed for 5 minutes with PBS and were incubated with the appropriate fluorescently-conjugated secondary antibody and Falloidin 543 (Biotium 00043) and nuclei counterstained (Hoechst 33258) for 1 hour at room temperature in the dark. Images were acquired using confocal microscope (Leica SP8) and image analysis and quantification were performed using ImageJ.

3.5 PREPARATION AND USE OF CONDITIONED MEDIUM (CM)

CAFs were seeded in T75 flasks and allowed to adhere overnight in complete medium. Once the CAF monolayers reached about 80% confluence, the complete medium was removed. The cells were washed twice with sterile PBS and then incubated in serum-free DMEM. This step ensures that the collected CM contains primarly factors secreted by the CAFs and minimizes contamination by external growth factors from FBS. The CAF were allowed to condition the medium for 24 and 48 hours in the presence or absence of Pirfenidone, the antifibrotic drug. Following the conditioning period, the medium was collected, immediately filtered through a 0.22 um sterile syringe filter, the resulting CM was aliquoted and stored at -80°C until use.

3.6 MTT ASSAY

Cell viability was assessed using the MTT (3-(4,5-dimethylthiazol-2-yl)-2,5-diphenyl tetrazolium bromide) reduction assay (M5655, Sigma Aldrich, Milan, Italy). For the assay 2000 cells were seeded per well in 100 ul of complete DMEM into a 96-well plate. Three technical replicates were prepared for each condition. After cell adherence (typically overnight), the culture medium was removed from the wells, and fresh complete DMEM containing the specific experimental treatments was added. Following 24 or 48 hours of treatment the medium was removed and 100 ul of MTT reagent solution was added to each well. The MTT working solution was prepared by diluting a 5 mg/mL stock solution 1:10 in DMEM specifically formulated without the pH indicator phenol red, which can interfere with colorimetric quantification. The plate was incubated at 37°C for 4 hours. During this period, metabolically active cells reduce the yellow MT salt into blue/purple insoluble formazan crystals, catalyzed by the mitochondrial enzyme succinate dehydrogenase. At the end of the incubation, the MTT solution was removed and replaced with 100 uL of dimethyl sulfoxide (DMSO, Sigma Aldrich) to dissolve the formazan crystals. The absorbance of the solubilized formazan solution was measured at 550 nm using a microplate reader (Bio-Rad, Milan, Italy).

3.7 WESTERN BLOTTING ANALYSIS

Cells were washed with ice cold PBS containing 1 μM Na_4VO_3, and lysed in 100 μL of cell RIPA lysis buffer (Merck Millipore, Vimodrone, Milan, Italy) containing PMSF (Sigma-Aldrich), sodium orthovanadate (Sigma-Aldrich) and protease inhibitor cocktail

(Calbiochem). The protein assay was performed using the Bradford reagent (Thermo Fisher, 23236) prepared according to the manufacturer's instructions. Bovine Serum Albumin (BSA) standard was used to generate the standard curve. Aliquots of supernatants containing equal amounts of protein (25-50ng) in Laemmli buffer were separated on Bolt® Bis-Tris Plus gels 4-12% precast polyacrylamide gels (Life Technologies, Monza, Italy). Fractionated proteins were transferred from the gel to a PVDF (polyvinylidene difluoride) membrane using iBlot 2 system (Life Technologies, Monza, Italy). Membranes were blocked for 1 h, at room temperature, with Odyssey blocking buffer (Dasit Science, Cornaredo, Milan, Italy). Subsequently, the membrane was probed at 4 ◦C overnight with primary antibodies diluted in a solution of 1:1000 in Odyssey blocking buffer/T-PBS buffer. The primary antibodies used are the following: alphaSMA (Invitrogen MA1-06110), p-NRF2 (S40, Biorbyt ORB506122), Vinculin (Santa Cruz, SC-73614), GAPDH (Cell Signaling, 97166), Col1A1 (Invitrogen, MA5-50846), TGFbeta (Invitrogen, MA5-15065), NQO1 (Santa Cruz, sc-32793), p62 (Phospho-SQSTM1/p62, Cell Signaling, #13121), p21 (Cell signaling 2947s). The membrane was washed in T-PBS buffer, incubated for 1 h at room temperature with goat anti-rabbit IgG Alexa Flour 750 antibody or with goat anti-mouse IgG Alexa Fluor 680 antibody (Invitrogen) (1:10000), and then visualized by an Odyssey Infrared Imaging System (LI-COR® Bioscience, Lincoln, NE, USA). GAPDH or Vinculin mouse anti h/m/r mAb (Santa Cruz sc-8035) (1:1000) was used to assess equal amount of protein loaded in each lane. Western blot membranes were imaged using Odyssey Infrared Imaging System (LI-COR® Bioscience, Lincoln, NE, USA); the relative expression levels of target proteins were determined by densitometric analysis of the acquired images using the public domain software ImageJ (NIH, Bethesda, MD, USA).

3.8 RNA EXTRACTION AND QUANTITATIVE PCR

Total RNA from cells was extracted using the Trizol reagent. The first-strand cDNA was synthesized using the iScript cDNA Synthesis Kit (Biorad #1708891) following instructions provided. Quantitative real-time polymerase chain reaction (RT-PCR) was carried out using Applied Biosystems SYBR Green PCR Master Mix (#4309155). The sequences of the primers used are. Gapdh (F: 5'-CAAGGCTGTGGGCAAGGT-3'; R: 5'-GGAAGGGCCATGCCAGTGA-3'), TGFbeta (F: 5'-TACCTGAACCCGTGTTGCTCTC; R: 5'-GTTGCTGAGGTATCGCCAGGAA) and Col1A1 (F:5'-GATTCCCTGGACCTAAAGGTGC; R: 5'- AGCCTCTCCATCTTTGCCAGCA).

The results were analyzed on the (Biorad CFX96 qPCR Instrument). Values were normalized to GAPDH and all the results were obtained from at least three technical triplicates.

3.9 TRANSFECTION PROTOCOL

Gene silencing was performed on NSCLC cell line (A549, H1975 and H1299) using small interfering RNA (siRNA).

Cells were seeded in 6 well-plates at a density of 2x105 cells/well in complete DMEM, aiming for 60-70% confluence at the time of transfection. After a period of starvation in serum-free medium, cells were transfected with a specific siRNA targeting human NRF2 (Silencer Select, siRNA ID#s9493, Life technologies) and a non-targeting control siRNA (Scramble), used as a negative control to exclude non-specific effects of the transfection process. Transfection was performed using Lipofectamine 3000 (Invitrogen) according to the manufacturer's instruction. Briefly: siRNA and Lipofectamine reagent were diluted separately in Opti-MEM reduced serum medium, the two solutions were combined and incubated for 10 minutes at room temperature to allow the formation of siRNA-lipid complex.

The complexes were added dropwise to the cell in a final siRNA concentration of 10, 50, 100 nM. After an incubation of 6 hours at 37 ◦C, the medium was replaced with fresh complete DMEM.

3.10 CELL INVASION ASSAY

Cell invasive capacity was determined in vitro by assessing the cell' ability to migrate through and degrade a synthetic extracellular matrix 8ECM) barrier. The assay was performed using Transwell inserts (Sarstedt) with 8 um pores, placed within a 24-well plate. The upper surface of the Transwell filters was coated with 50 uL of a Geltrex solution prepared at a concentration of 15 ug/mL in sterile PBS. Geltrex (Gibco A14132-01,Reduced Growth Factor Basement Membrane Matrix) served as the synthetic matrix rich in ECM proteins. The Geltrex layer was allowed to dry under sterile conditions at room temperature for 2 hours to form a stable, thin barrier. After the 24-hour drying period, 50000 cells/transwell were seeded in 400 uL of complete DMEM in the upper chamber of the Transwell insert. An additional 600 uL of DMEM was added to the bottom of the well (under the Transwell), acting as a chemoattractant. The plates were subsequently incubated for 24 hours at 37°C in 5% CO2 , humidified incubator, allowing invasive cells to degrade the Geltrex and migrate to the lower chamber. After incubation, the test was stopped, and the medium was aspirated from the Transwells. Cells that had not invaded were removed by gently scrubbing the upper side of the filter with

a cotton swab. The invasive cells present on the lower side of the filter were fixed using 1 ml of 20% Mrethanol for 20 minutes. Following the fixation, a wash was performed with 1 X PBS for 2 minutes; cells were then stained using a 0.5% Crystal Violet working solution for 15 minutes (prepared from a 20% stock solution in ethanol, diluted in 1XPBS). Images of the stained cells on the filters were acquired using a digital microscope (OPTIKA) and quantification of invaded cells was performed on 4 different fields of the transwell using ImageJ analysis software.

3.11 3D CELL CULTURE

Multicellular Tumor Spheroid (MCTS) were generated using the liquid overlay method on non-adherent surfaces, promoting cell-cell aggregation and minimizing cell-substrate interaction. A 2% Agarose solution was prepared by dissolving the powder in sterile PBS and sterilizing the solution by autoclaving. The solution was kept molten at approximately 60°C until use; 50 ul of the molten 2% Agarose solution was quickly added to each well of a sterile 96-well plate, the plate was allowed to solidify at room temperature O.N . NSCLC cell lines (A549, H1975 and H1299) and CAFs (pre-treated or untreated, as specified) were harvested and resuspended at the required total cell concentration in complete DMEM. The cells were mixed at a 2:1 ratio (CAF:NSCLC cell line), ensuring that the final suspension volume was homogeneous. The mixed cell suspension was immediately plated onto the pre-coated 96-well plates at a final density of 1.500 cells/well in a final volume of 200 uL of medium per well. The plates were transferred to a 37°C , 5% CO_2 incubator. MCTS formation was verified after 24 hours and images were acquired using an inverted microscope coupled with an imaging system (OPTIKA). Spheroid diameter was measured using ImageJ by averaging the longest and shortest diameters of selected spheroids per condition.

3.12 STATISTICAL ANALYSIS

All quantitative data are expressed as means ± standard errors of the mean (SEM) depicted by vertical bars from representative experiment of at least three independent experiments. For the statistical analysis, differences between two experimental groups were assesses using the unpaired two-tailed Student's t-test. For comparison involving three or more groups, or multiple treatment conditions, statistical significance was determined by One-way Analysis of Variance (ANOVA) or Two-way ANOVA, following a significant ANOVA result, specific group comparisons were performed using appropriate post hoc tests, such as the Tukey's test

or the Bonferroni correction, to adjust for multiple comparison. Statistical significance was defined as a p-value less than 0.05 ($p < 0.05$). The following notation was used to denote significant levels: * $p < 0.05$; ** $p < 0.01$; *** $p < 0.001$; **** $p < 0.0001$.

4 RESULTS

4.1 EVALUATION OF THE EFFECT OF CYTOKINES REPRESENTATIVE OF THE TUMOR MICROENVIRONMENT ON NRF2 EXPRESSION IN NSCLC CELL LINES

Cytokines and growth factors of the TME, such as TGF-β and TNF-α play a significant role in cancer progression and in cross-talk between cancer cells and stromal cells. We exposed two NSCLC cell lines (A549 and H1975) to these agents mimicking TME conditions. Both TGF-β and TNF-α at 48h of exposure significantly increased the protein expression of the active phosphorylated form of NRF2 (pNRF2), while the NRF2 inhibitor K67 did not show a significant effect. When K67 was used in combination with TGF-β or TNF-α caused an strongly inhibition the modulatory effect of the two cytokines on NRF2 expression, as showed using western blot assay. Furthermore, we found a reduction in p21 protein expression, a negative regulator of the cell cycle, when NSCLC cells were exposed to TGF-β or TNF-α. This reduction correlates with the increase in NRF2. Conversely, when cells were exposed to K67, in the presence of the two cytokines, we found an increase in p21 and an inhibition of NRF2 (Fig.6). This effect was more pronounced after the treatment with TGF-β.

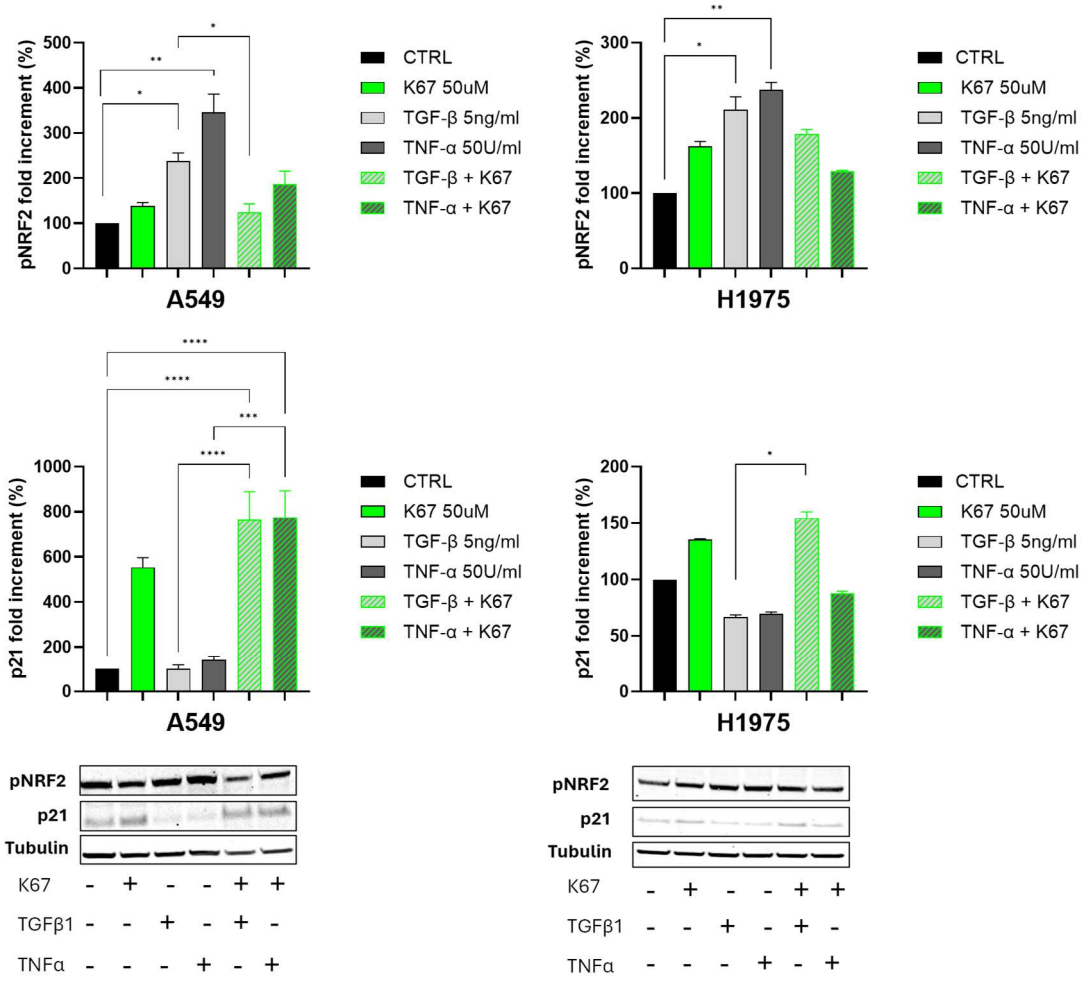

*Figure 6: A549 and H1975 NSCLC cell lines were exposed for 48 hours to the NRF2 inhibitor K67 [50uM] and to the cytokines TGF-β [5ng/ml] and TNF-α [50U/ml] alone or in combination with NRF2 inhibitor. Data from western blot analysis are normalized to untreated cells (CTRL) and Tubulin, results are represented as a mean ± SEM, ****P ≤ 0.0001,***P ≤ 0.001, **P<0.01, and *P<0.05.*

K67 has a weak inhibitory effect on the interaction between Keap1 and Nrf2. However, K67 competitively binds to the p-p62 binding site on Keap1, leading to the inhibition of over-activation of the p62-dependent Nrf2 pathway. To exclude any toxicity effects of the Nrf2 inhibitor K67 we performed a viability assay both at increasing doses of the inhibitor alone and in combination with the cytokines at the highest dose and no effects on cell viability were observed (Fig.7).

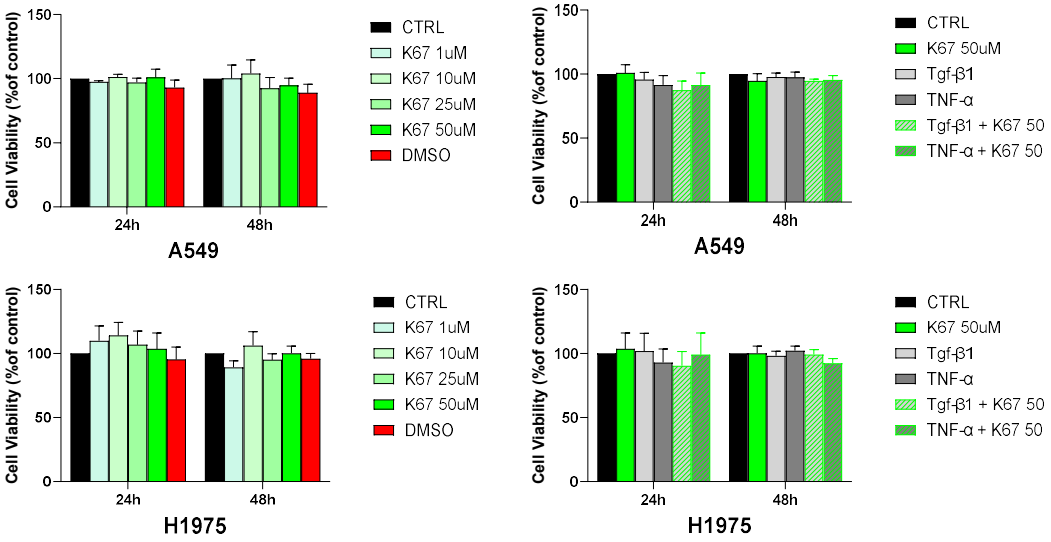

Figure 7: Time-dose dependent cell viability assessed by MTT assay, the data shown are normalized to the untreated condition (CTRL)

In addition, our investigations revealed that cytokine exposure did not affect NSCLC cells viability.

4.2 ISOLATION AND CHARACTERIZATION OF CANCER-ASSOCIATED FIBROBLASTS FROM HUMAN ADENOCARCINOMA

Our initial findings established that TGF-β, a prominent TME-associated cytokine, significantly upregulates the expression of NRF2 in two distinct NSCLC cell lines. Given that TGF-β is not only a crucial mediator of TME fibrosis but also a pivotal agent in the cross-talk between cancer-associated fibroblasts and tumor cells, we focused our efforts on the isolation and characterization of different CAF populations from NSCLC patients.

4.2.1 Identification of CAF population by CD90 expression via flow cytometry

To develop a more physiologically relevant model, we successfully isolated primary CAFs from human adenocarcinoma tissue samples obtained from three different patients. Prior to their use in co-culture experiments, the isolated cells were characterized to confirm their phenotype. CAF identity was validated by flow cytometry, which confirmed the expression of the specific surface marker CD90 and the lack of expression of the epithelial cell-specific marker CD326.

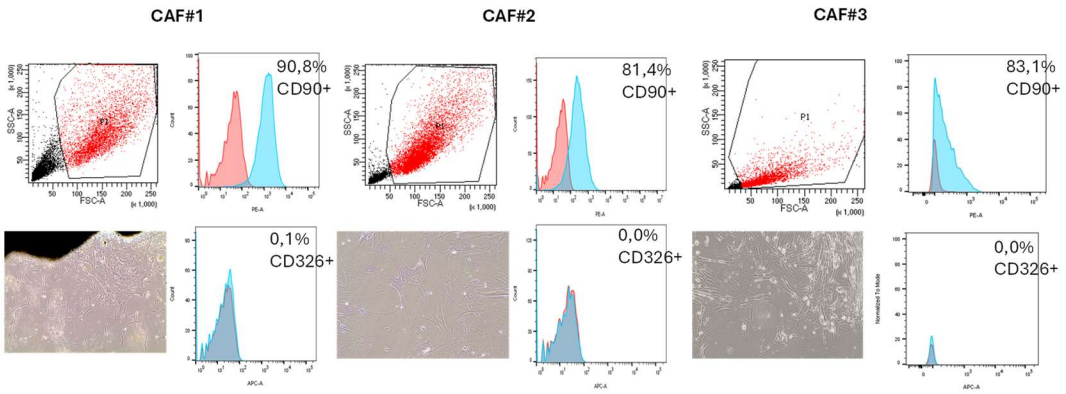

Figure 8 Representative flow cytometry plots demonstrating the gating strategy and expression profile of CD90 (a mesenchymal/fibroblast marker) and CD326 (a epithelial specific marker) in the three patient-derived isolates (CAF#1, CAF#2, and CAF#3).

4.2.2 Confirmation of activated myofibroblast phenotype through alphaSMA expression and stress fibres formation

To further validate the activated cancer-associated phenotype of the isolated CAFs, we compared the expression of α-SMA (alpha-Smooth Muscle Actin), a canonical myofibroblast activation marker, with that of a normal fibroblast cell line.

We utilized MRC5 cells, a normal human lung fibroblast cell line, as a non-malignant comparator. Western blot analysis revealed a markedly elevated basal expression of α-SMA across all three patient-derived isolated cell populations (CAF#1, CAF#2 e CAF#3) compared to the MRC5 control cells (Fig.9A)

The myofibroblast phenotype was visually confirmed by immunofluorescence (IF) staining for α-SMA. The images demonstrated that the three CAF populations presented a highly distinct, elongated, and contractile morphology characterized by prominent cytoplasmic α-SMA stress fibres. In sharp contrast, MRC5 cells exhibited minimal α-SMA staining and lacked the well-organized stress fibre architecture (Fig.9B).

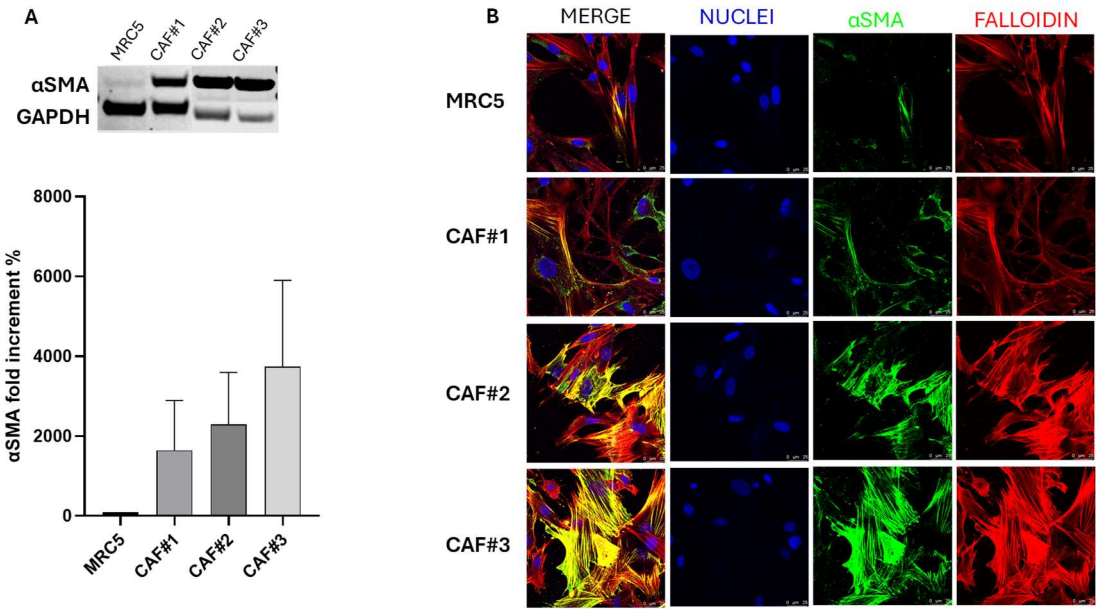

Figure 9 (A) Representative Western blots showing the basal protein expression levels of α-SMA in the three CAFs isolates compared to MRC5 normal fibroblast cell line. GAPDH was used as the loading control. Densitometric quantification of alphaSMA Data are presented as three independent experiments and show a significantly higher expression of the protein target.(B) Representative immunofluorescence (IF) images for α-SMA (green) in MRC5 and CAF isolates. Nuclei were counterstained with DAPI (blue), stress fibres with Phalloidin (red). Scale bar 25 uM.

This significantly higher α-SMA expression and the characteristic stress fibre architecture confirm that our isolated CAF populations exhibit a spontaneously activated myofibroblast phenotype, a key characteristic distinguishing them from quiescent fibroblasts and justifying their role as a central component of the tumor microenvironment in our subsequent functional assays.

4.3 TARGETING THE TUMOR MICROENVIRONMENT: ANTI-FIBROTIC EFFECTS OF PIRFENIDONE ON PATIENT-DERIVED CANCER-ASSOCIATED FIBROBLASTS

To investigate the therapeutic potential of targeting the TGF-β signaling axis in the NSCLC tumor microenvironment, we evaluated the effects of an antifibrotic drug, Pirfenidone. Pirfenidone is a clinically approved anti-fibrotic agent used for treating Idiopathic Pulmonary Fibrosis (IPF), primarily through the inhibition of TGF-β signaling. Given its mechanism of action and the critical role of TGF-β in CAF function, we exposed the isolated patient-derived CAFs to Pirfenidone.

The CAFs from all three patients were treated with a concentration of 1.5 mg/mL (a dosage consistent with previous literature) for 24 and 48 hours. The subsequent fibrotic and activation status of the CAFs was analysed by assessing the expression of key markers via Western blot and real-time PCR.

The Western blot analysis provided molecular evidence of reduced fibrotic component activation following Pirfenidone treatment, though notable inter-patient variability was observed (Fig.10). The primary target, TGF-β expression, exhibited a significant decrease across all three patient-derived, validating the drug's mechanism of action. However, the kinetics of this response differed: CAFs from Patient 1 showed a delayed but robust downregulation of, which became significant only at the 48 hour time point. In contrast, CAFs from Patient 2 and Patient 3 displayed a faster response, with TGF-β expression already significantly reduced at the 24 hour time point (Fig. 10B). The response of Collagen I (Col1A1) expression further highlighted the heterogeneity of the CAFs, CAF#1 and CAF#2 showed the expected significant decrease in Collagen I protein levels after 48 hours of treatment. Conversely, CAF#3 exhibited a counter-intuitive increase in Collagen I production at both the 24hour and 48hour time points. This suggests that CAF population in CAF#3 may possess an underlying, TGF-β -independent mechanism driving ECM synthesis, or that the TGF-β inhibition in this patient leads to a compensatory feedback loop (Fig.10C). The myofibroblast differentiation marker, α-SMA, was consistently and effectively suppressed by Pirfenidone treatment in all three CAFs isolates, indicating a successful inhibition of the CAF activation status (Fig.10A).

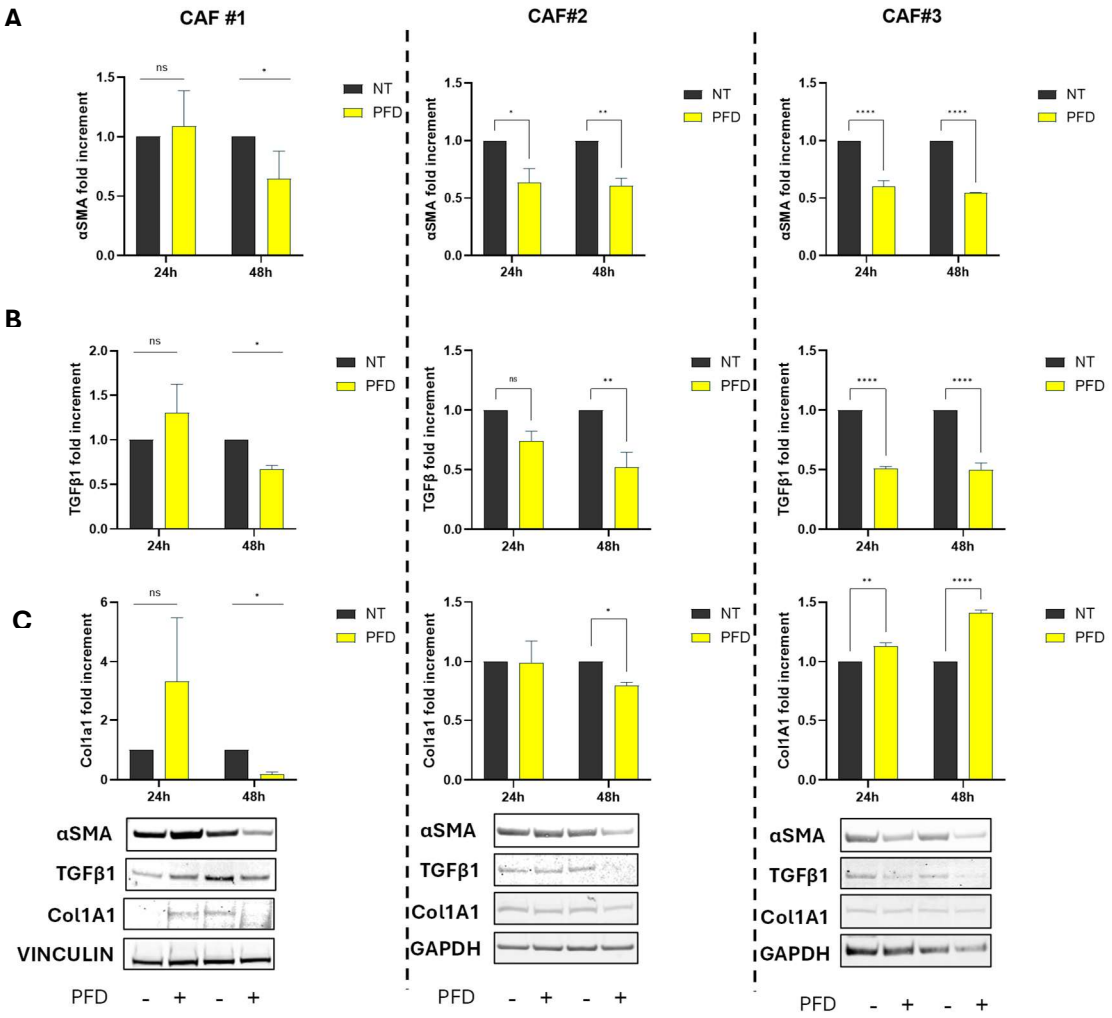

*Figure 10 : Representative Western blots showing the protein expression levels of TGF-β, α-SMA, and Collagen I in CAFs .CAFs were treated with 1.5 mg/mL Pirfenidone for 24 and 48 h. Data from western blot analysis are normalized to untreated cells (NT) and VINCULIN or GAPDH, results are represented as a mean ± SEM, ****P ≤ 0.0001,***P ≤ 0.001, **P<0.01, and *P<0.05.*

To complement the Western blot data and determine whether Pirfenidone's effects were regulated at the transcriptional level, we analysed the mRNA expression of TGF-β and COL1A1 in the treated CAFs (Fig.11). TGF-β transcript levels show compensatory upregulation in stark contrast to the significant reduction observed in TGF-β protein levels via Western blot, the real-time PCR analysis revealed a robust and significant increase in TGF-β mRNA transcript levels in all three CAFs isolates (Fig.11A). Unlike the complex regulation seen for TGF-β, the transcriptional levels of the key extracellular matrix component, Collagen I (COL1A1), showed a consistent and significant downregulation in response to Pirfenidone across all three CAFs isolates (Fig.11B).

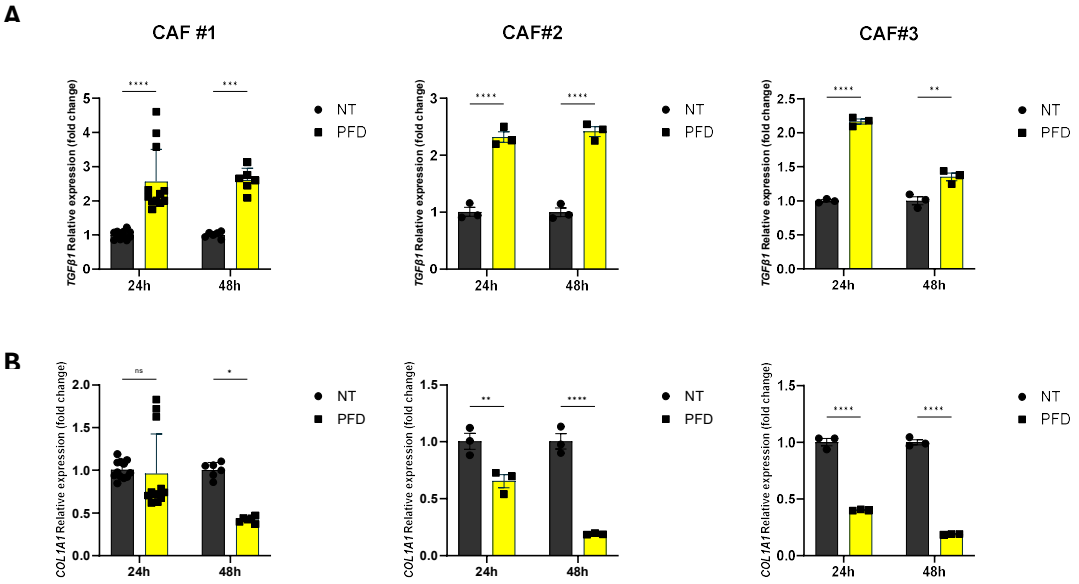

*Figure 11 : Expression of TGF-β and COL1A1 mRNA transcript levels in CAFs by RT-PCR, data are normalized to untreated cells (NT) and GAPDH. results are represented as a mean ± SEM ****P ≤ 0.0001 ,***P ≤ 0.001, **P<0.01, and *P<0.05 vs untreated (NT).*

4.4 TRANSITION TO FUNCTIONAL IN VITRO CO-CULTURE MODELS: ASSESSING CAF-MEDIATED EFFECTS ON NSCLC CELLS VIA CONDITIONED MEDIUM

Given the critical role of secreted factors in mediating CAF– tumor cell cross-talk within the TME, we utilized CAF-derived conditioned medium (CM) isolated from the three patients populations to mimic the complexity of the microenvironment in vitro. This CM was generated from CAFs that were either treated with Pirfenidone (PFD) or without (as an untreated control). Subsequently, this conditioned medium was applied to three distinct NSCLC cell lines A549, H1975 and H1299, allowing us to investigate how Pirfenidone's anti-fibrotic effect on CAFs and on the TME perturbation functionally impacts the tumor cells themselves. It is important to note that the CAFs were treated with PFD for the duration of the conditioning period, and this CM was subsequently used directly on the NSCLC cells. Consequently, the CM contains residual, unquantified PFD. Therefore, the observed effects on NSCLC cells depend on the combined result of the altered CAF phenotype and may be also on the effect of the “remaining” PFD drug.

4.4.1 Evaluation of NSCLC cell viability in response to CAF-derived conditioned medium

To evaluate the functional consequences of Pirfenidone treatment on CAFs, we assessed the impact of the resulting CM on the viability and proliferation of three distinct NSCLC cell lines A549, H1975, and H1299 using the MTT assay.

The basal effect of the untreated CAF (CM-CAF) on NSCLC viability was largely non-significant across most combinations of isolates and cell lines. However, the findings from CAF#3 highlighted a pronounced inter-patient heterogeneity, demonstrating a pro-proliferative effect, A549 and H1299 cells showed a significant increase in viability when exposed to CM-CAF#3 $p < 0.05$. The kinetics of this effect differed by cell line: the increase was evident at 48 hours for A549 cells, but appeared earlier, at 24 hours, for H1299 cells. H1975 cells, however, remained largely unaffected by any untreated CM.

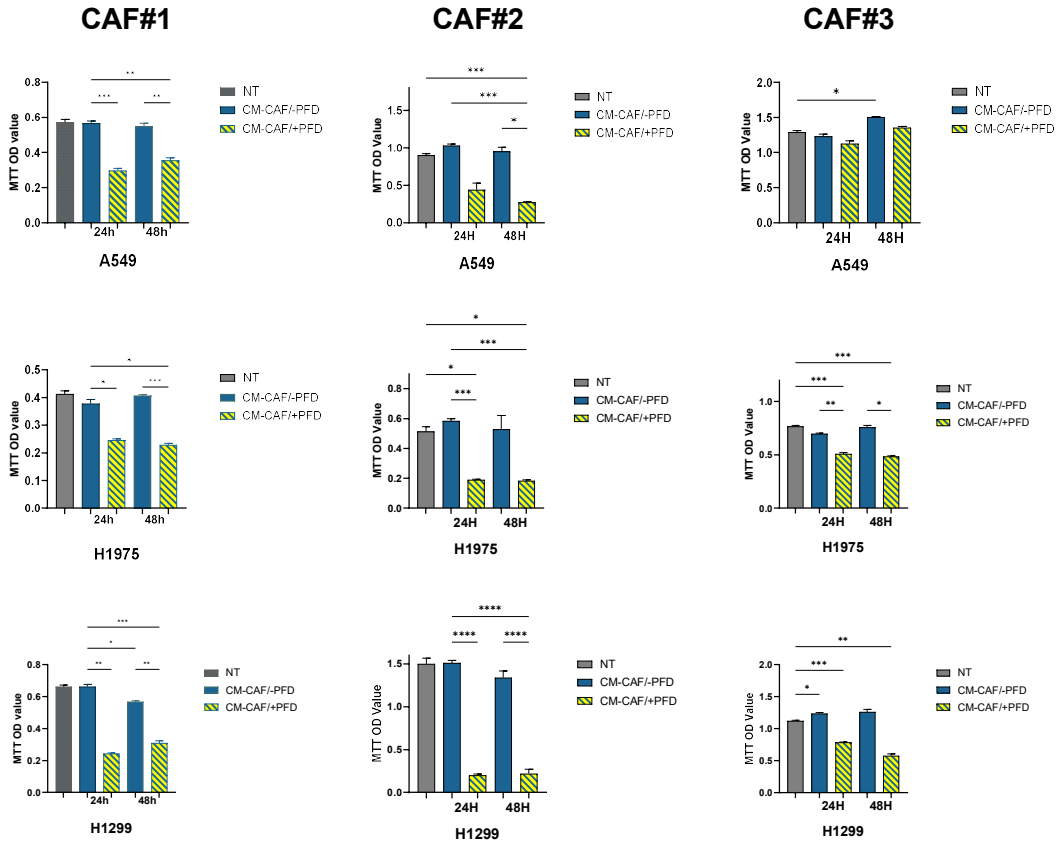

Figure 12 : MTT assay results showing the quantification of viable A549, H1975, and H1299 cells after 24h/48h of exposure to primary CAF-derived conditioned media (CM). Treatment conditions include CM from untreated CAFs (CM-CAF/-PFD) and Pirfenidone-treated CAFs (CM-CAF/+PFD), data are represented as Optical Density

*(OD). Results are represented as a mean ± SEM ****P ≤ 0.0001 ,***P ≤ 0.001, **P<0.01, and *P<0.05 vs untreated (NT)*

In striking contrast to the basal effects, CM derived from Pirfenidone-treated CAFs (CM CAF/+PFD) generally had significantly impaired the viability of NSCLC cells across the three cell lines and the CAF populations. However, the CAF#3 isolate continued to display unique characteristics: the anti-proliferative effect of CM CAF#3/+PFD is evident in H1975 and in H1299 cells, but failed to show a significant reduction in the viability of A549 cells, which remained statistically similar to the untreated CM CAF#3/-PFD. Despite the highly varied response kinetics observed with the CAF#3 isolate, the overall data suggest that the PFD-mediated modulation of CAFs is largely successful at suppressing the release of pro-tumorigenic factors, thus promoting an anti-proliferative phenotype in the NSCLC cells. The non-response in A549 exposed to CM CAF\#3 +PFD highlights the need for a mechanistic investigation into the specific secretome signature of CAF\#3 that confers resistance to PFD's indirect effects on the A549 line.

4.4.2 Pirfenidone exerts limited cytotoxicity on NSCLC cells but fails to directly modulate NRF2 signaling in NSCLC cells

To distinguish the indirect, CAF-mediated effects of Pirfenidone from any potential direct effects on NSCLC cells, we first evaluated its direct cytotoxicity and then its influence on NRF2 signaling.

We assessed the cytotoxicity of Pirfenidone on the three NSCLC cell lines A549, H1975, and H1299 using the MTT assay (Fig.13).

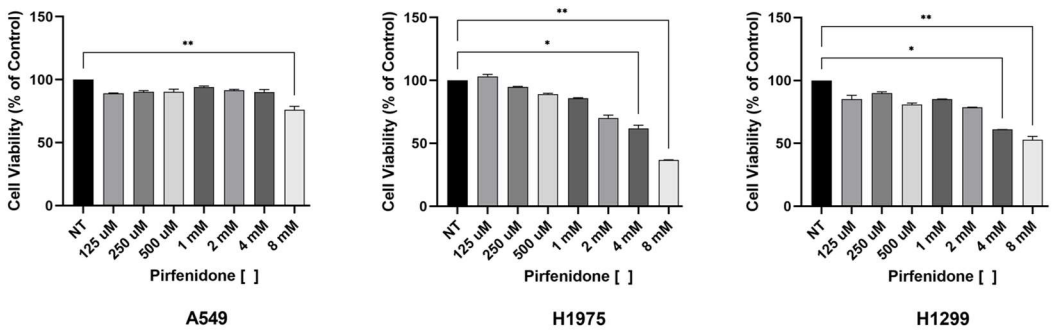

*Figure 13 MTT assay results showing the percentage of viable A549, H1975, and H1299 cells after exposure to PFD at various concentrations. Results are represented as a mean ± SEM ****P ≤ 0.0001 ,***P ≤ 0.001, **P<0.01, and *P<0.05 vs untreated (NT)*

The results confirmed that Pirfenidone exhibits limited, concentration-dependent cytotoxicity across all three lines, with the calculated half-maximal inhibitory concentration IC50 being approximately 2 mM (Fig.14).

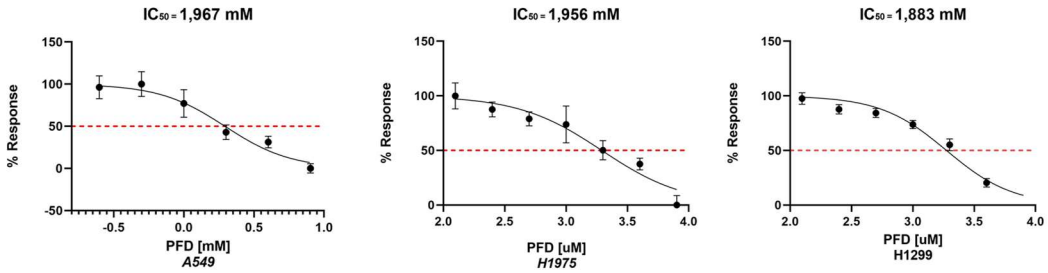

Figure 14 Determination of Pirfenidone IC_50 values across NSCLC cell lines. Dose-response curves represent the effect of increasing concentrations of Pirfenidone (PFD) on the viability of A549, H1975, and H1299 cells after treatment. The half-maximal inhibitory concentration IC_50 was calculated using a non-linear regression model (log[inhibitor] vs. normalized response). Data points represent the mean ± SD of at least three independent experiments.

This IC50 value served as the upper threshold for direct treatment, contrasting sharply with the 1.5 mg/mL, the PFD dose used for CAF modulation, which is closer to 8 mM.

Based on the IC_50 data, we selected two distinct concentrations for testing the direct modulation of NRF2 signaling: the IC_50 dose (2 mM) and the high CAF-modulating dose (8 mM). Western Blot analysis on A549, H1975, and H1299 cells revealed that direct treatment with Pirfenidone at either 2 mM or 8 mM failed to induce any detectable change in the expression levels of the active form p-NRF2. These findings collectively demonstrate that, while Pirfenidone possesses a minor, direct cytotoxic effect on NSCLC cells at high concentrations, the modulatory effect on the NRF2 pathway was not observed (Fig.15)

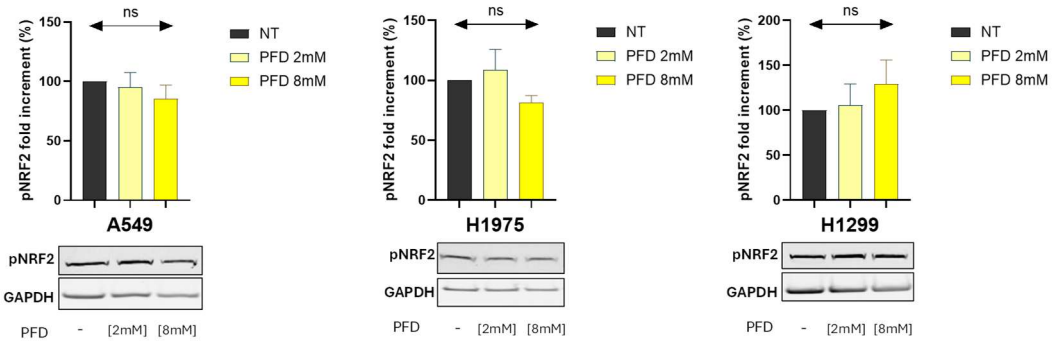

*Figure 15 : Representative Western blots showing the protein expression levels of pNRF2. Data from western blot analysis are normalized to untreated cells (NT) and GAPDH, results are represented as a mean ± SEM, ****P ≤ 0.0001,***P ≤ 0.001, **P<0.01, and *P<0.05.*

4.4.3 Conditioned medium from CAFs modulates NRF2 signaling in NSCLC cells

To investigate the molecular mechanisms underlying the observed changes in NSCLC cell viability and to elucidate the CAF-mediated modulation of tumor cell fate, we examined the NRF2 pathway, as a critical mediator of cellular survival and resistance, in response to the CAF-derived conditioned medium (CM). This analysis was conducted under the hypothesis that the CAF secretome, from a myofibroblast phenotype (Section 4.4.2) would contain factors that activate the NRF2 pathway in NSCLC cells. One of these agents is TGF-β, a key regulator of CAF function that we showed to be inhibited by PFD in CAFs. Given our finding that PFD alone does not directly modulate NRF2 signaling (Section….), we focused solely on the CAF-mediated effects. We analysed the expression of the stabilized and active form of NRF2 (p-NRF2 S40), the canonical downstream target NQO1, and the upstream regulator p62 after exposure to untreated CM (CM CAF/-PFD) and PFD-modulated CM (CM-CAF/ +PFD) from all three patient isolates.

The NRF2 pathway response in A549 cells (Fig.16) to the CAF conditioned media was characterized by significant inter-patient heterogeneity, confirming the diverse nature of the CAF secretomes. Analysis of the untreated CM revealed that the basal activation of the NRF2 pathway was highly specific to the CAF isolate. p-NRF2 expression, showed a significant increase only when A549 cells were exposed to CM CAF\#3 -PFD, while isolates CAF\#1 and CAF\#2 did not induce a statistically significant activation of this factor. This pattern of heterogeneity extended to the downstream targets: NQO1 upregulation was observed with CM

CAF\#1 -PFD and CM CAF\#3 -PFD, but not CM CAF\#2 -PFD. Furthermore, the upstream regulator p62 was uniquely affected, showing a significant increase with CM CAF\#2 -PFD but a significant reduction with CM CAF\#3-PFD. The CM derived from PFD-treated CAFs showed distinct suppressive patterns when compared to their respective untreated controls. p-NRF2 expression was the most consistently modulated component, showing significant downregulation by CM-CAF/+PFD from all three isolates. However, the downstream response was, again, heterogeneous. Suppression of the target gene NQO1 and the regulator p62 was significantly observed only with CM-CAF\#1 +PFD and CM-CAF\#2 +PFD. Crucially, the CM CAF\#3 +PFD failed to downregulate both NQO1 and p62 expression. This lack of suppression of the NRF2 downstream targets NQO1 and p62 CM CAF\#3 +PFD correlates directly with the failure of this specific conditioned medium to inhibit A549 cell viability in the MTT assay (Section 4.4.1). This molecular pattern suggests a functional link between the degree of CAF-mediated modulation of NRF2 targets and the ultimate proliferative outcome of the A549 cells.

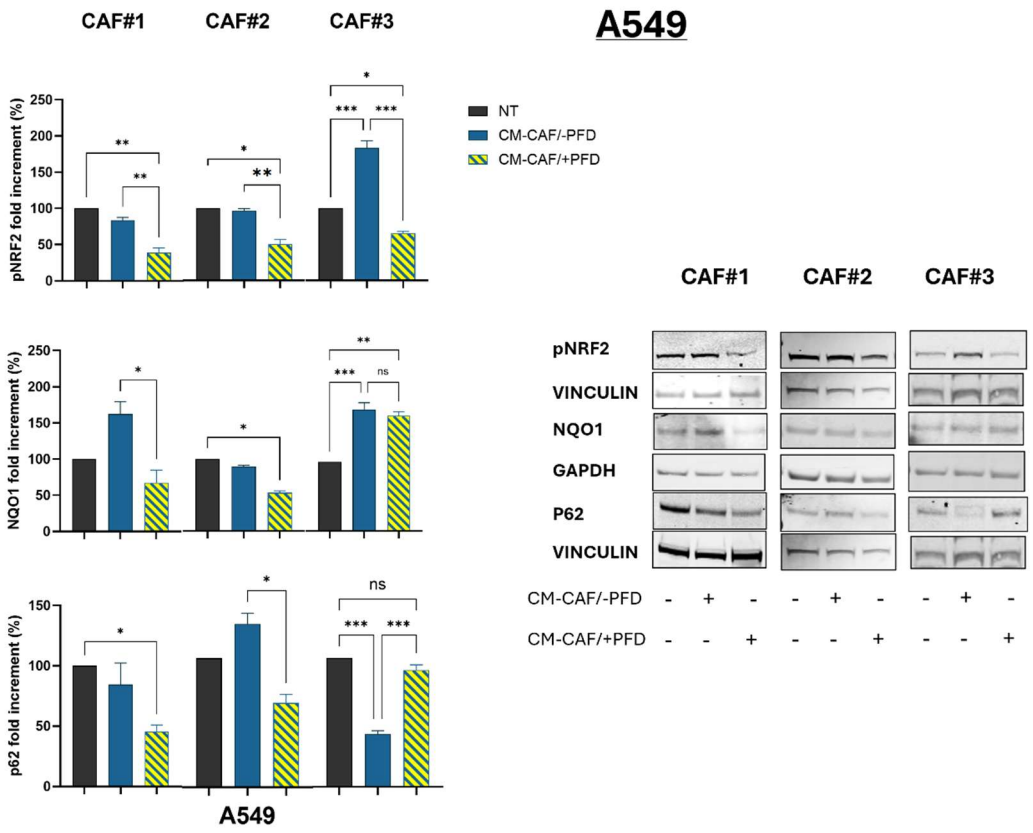

*Figure 16 Representative Western blots showing the protein expression levels in A549 cells of pNRF2, NQO1 and p62. Data from western blot analysis are normalized to untreated cells (NT) and GAPDH or Vinculin, results are represented as a mean ± SEM, ****P ≤ 0.0001,***P ≤ 0.001, **P<0.01, and *P<0.05.*

The NRF2 pathway response in H1975 cells (Fig.17) highlighted inter-patient variability in the basal activation state but generally demonstrated a broader susceptibility to PFD modulation.

Basal exposure to untreated CM led to a significant activation of p-NRF2 in H1975 cells, specifically with CM derived from CAF\#2 and CAF\#3 isolates. The CM from CAF\#1, however, did not show a statistically significant effect on p-NRF2 stabilization. Interestingly, unlike the A549 line, the expression of the downstream target NQO1 remained unaltered by the CM from all three CAF isolates. For the expression of p62, only the CM CAF\#3 -PFD caused a significant increase.

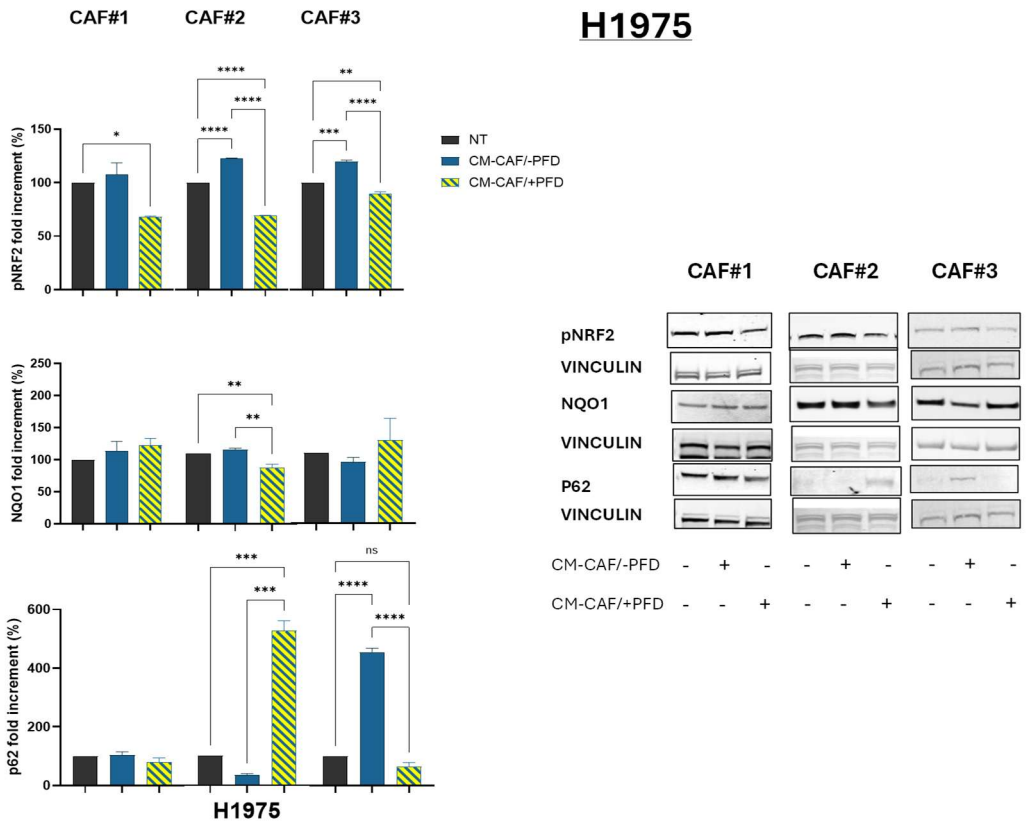

*Figure 17 Representative Western blots showing the protein expression levels in H1975 cells of pNRF2, NQO1 and p62. Data from western blot analysis are normalized to untreated cells (NT) and GAPDH or Vinculin, results are represented as a mean ± SEM, ****P ≤ 0.0001,***P ≤ 0.001, **P<0.01, and *P<0.05.*

The CM derived from PFD-treated CAFs showed a general tendency toward suppression. The most uniformly suppressed component was p-NRF2, whose expression was significantly downregulated by CM-CAF/+PFD from all three isolates CAFs, compared to their respective controls. This indicated a consistent suppression of NRF2 stabilization regardless of the CAF origin. Despite this robust apical suppression, the downstream target NQO1 was significantly reduced only by CM-CAF\#2 +PFD, while CAF\#1 and CAF\#3 failed to elicit a change. Finally, p62 expression showed a complex and bidirectional regulation: CM-CAF\#2+PFD induced an increase in p62, whereas CM CAF\#3 +PFD caused a significant decrease in p62 when compared to the treatment with CM CAF\#3 -PFD.

The NRF2 pathway response in H1299 cells (Fig.18) was distinct from the other two lines, demonstrating a lower basal susceptibility to CM-mediated NRF2 activation but high sensitivity to PFD modulation.

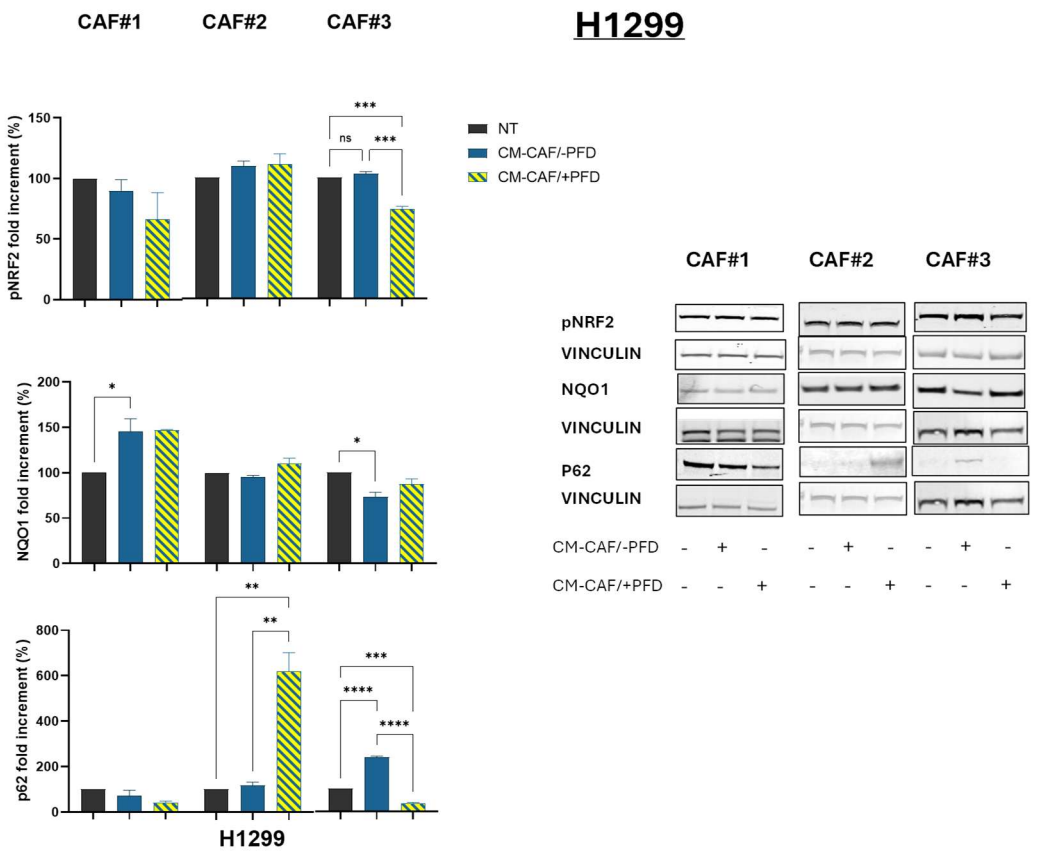

*Figure 18 : Representative Western blots showing the protein expression levels in H1299 cells of pNRF2, NQO1 and p62. Data from western blot analysis are normalized to untreated cells (NT) and GAPDH or Vinculin, results are represented as a mean ± SEM, ****P ≤ 0.0001,***P ≤ 0.001, **P<0.01, and *P<0.05.*

Analysis of the untreated CM revealed that the H1299 line was significantly less responsive to basal CAF signaling. Specifically, no significant increase in the phosphorylated form of NRF2 was observed when exposed to the CM from any of the three CAF isolates. This suggests that the activating factors present in the CM were not sufficient or appropriate to induce NRF2 stabilization in this specific cell line. Despite the lack of p-NRF2 increase, the downstream target NQO1 still showed a complex regulation: levels increased significantly with CM CAF\#1 -PFD but decreased significantly with CM CAF\#3 -PFD. The expression of p62 mirrored the same complex, isolate-specific patterns observed in the H1975 cells.

4.4.4 Pirfenidone-Modulated CAFs impair cell proliferation: correlation with NRF2 and p21 modulation

To directly measure the anti-proliferative effect of the PFD-modulated CAF secretome and to investigate its association with the NRF2 pathway, cell counts and analysis of the cell cycle inhibitor p21 were performed.

To establish NRF2 as a crucial mechanistic link in the anti-proliferative effect, we introduced ML385 as a pharmacological tool. ML385 is a potent, non-competitive small molecule inhibitor highly specific for NRF2, functioning by distrupting its ability to bind to the antioxidant response elements (ARE). By comparing the effects of the CM-CAFs/+PFD (which suppresses NRF2 via the secretome) with ML385 (which suppresses NRF2 directly), we aimed to functionally validate whether the suppression of NRF2 is sufficient to drive the observed reduction in proliferation in each NSCLC line. To ensure optimal pharmacological targeting of NRF2 in NSCLC cells, we first determined the effective inhibitory concentration of ML385 across all three cell lines. A Western Blot analysis using two concentrations of ML385 (10 μM and 20 μM) was done to evaluate the inhibitory effect on NRF2, and the modulatory effect on p21 and p62. The results showed that 20 μM of ML385 was the optimal concentration required to consistently achieve a significant downregulation of pNRF2 across all three NSCLC lines. Consequently, the 20 μM concentration was selected for subsequent experiments.

Cell counting assays were performed on NSCLC cell lines (A549, H1975 and H1299) exposed to CM over 24 and 48 hours. Across all three NSCLC lines and all three patient isolates, CM derived from PFD-treated CAFs consistently and significantly reduced the proliferation rate compared to the untreated CM control. Conversely, the basal CM control exhibited a pro-proliferative effect in several combination.

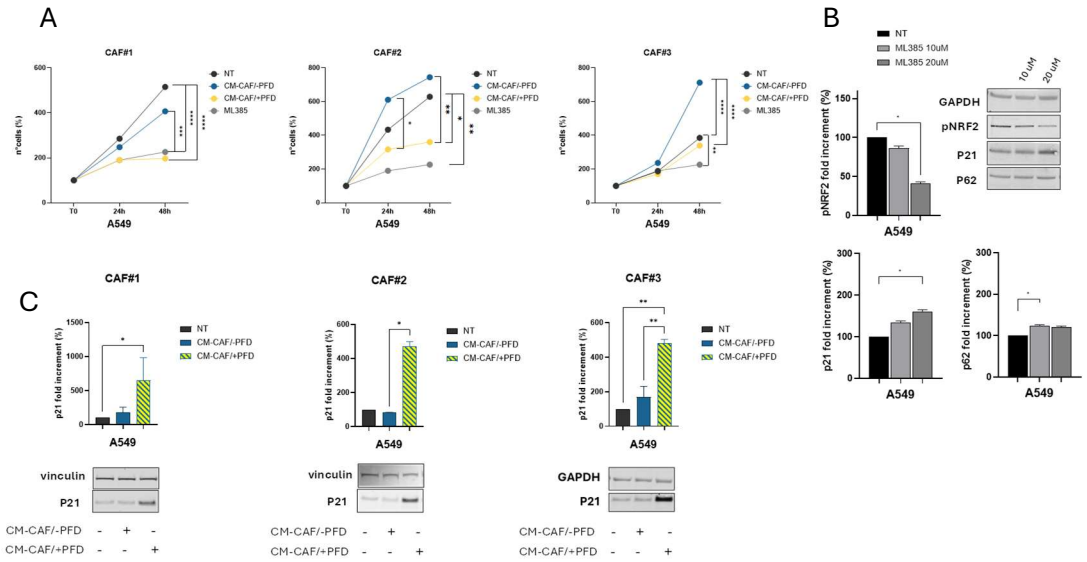

*Figure 19: Quantification in percentage of A549 cell numbers under the indicated experimental conditions (CAF-conditioned media +/- PFD and ML385) (A). Representative Western blots showing the protein expression levels in A549 cells of pNRF2, p21 and p62 under ML385 exposure at different concentrations (B). Representative Western blots showing the protein expression levels in A549 cells of p21 under the indicated experimental conditions (CAF-conditioned media +/- PFD) (C). Data are normalized to untreated cells (NT) and GAPDH or Vinculin, results are represented as a mean ± SEM, ****P ≤ 0.0001,***P ≤ 0.001, **P<0.01, and *P<0.05.*

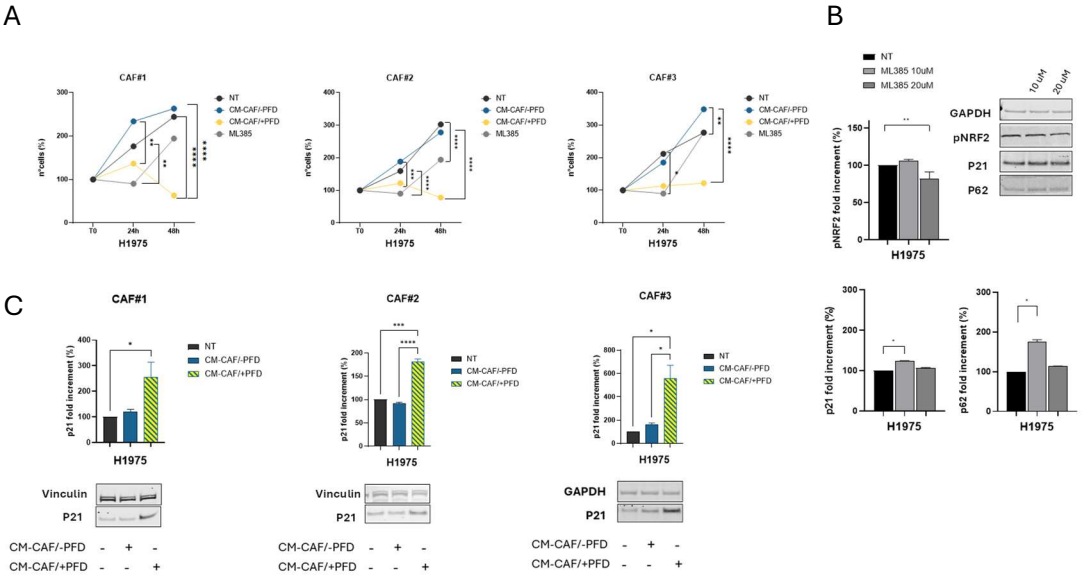

*Figure 20: Quantification in percentage of H1975 cell numbers under the indicated experimental conditions (CAF-conditioned media +/- PFD and ML385) (A). Representative Western blots showing the protein expression levels in H1975cells of pNRF2, p21 and p62 under ML385 exposure at different concentrations (B). Representative Western blots showing the protein expression levels in H1975cells of p21 under the indicated experimental conditions (CAF-conditioned media +/- PFD) (C). Data are normalized to untreated cells (NT) and GAPDH or Vinculin, results are represented as a mean ± SEM, ****P ≤ 0.0001,***P ≤ 0.001, **P<0.01, and *P<0.05.*

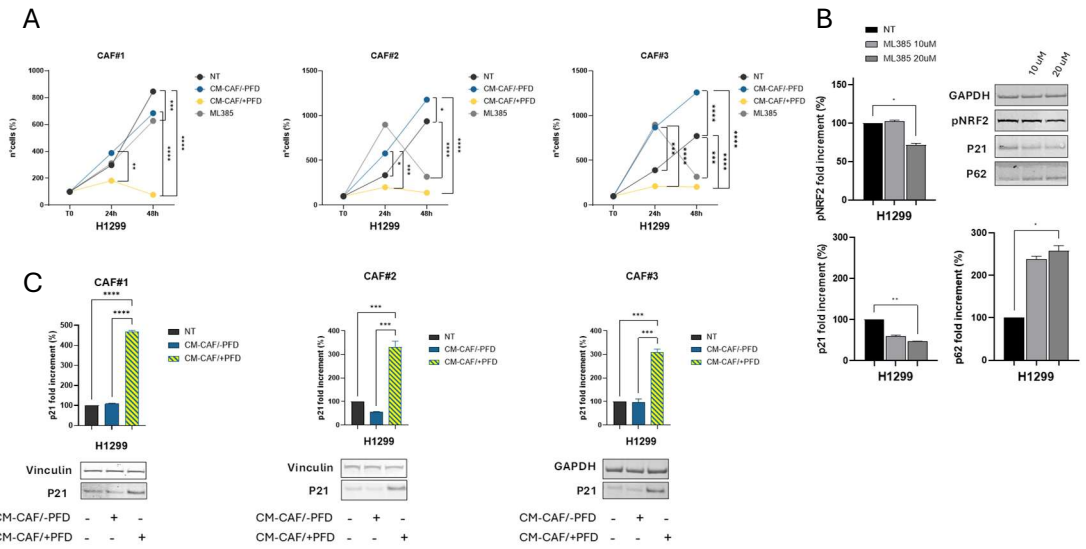

*Figure 21 Quantification in percentage of H1299 cell numbers under the indicated experimental conditions (CAF-conditioned media +/- PFD and ML385) (A). Representative Western blots showing the protein expression levels in H1299 cells of pNRF2, p21 and p62 under ML385 exposure at different concentrations (B). Representative Western blots showing the protein expression levels in H1299 cells of p21 under the indicated experimental conditions (CAF-conditioned media +/- PFD) (C). Data are normalized to untreated cells (NT) and GAPDH or Vinculin, results are represented as a mean ± SEM, ****P ≤ 0.0001,***P ≤ 0.001, **P<0.01, and *P<0.05.*

In A549 and H1975 cells the treatment with ML385 resulted in a significant reduction in cell proliferation, in contrast ML385 failed to induce a significant inhibitory effect on H1299 cell proliferation.

We investigated the downstream cell cycle regulation by analysing the CDK inhibitor p21. Western blot analysis across all responsive NSCLC lines showed that CM-CAFs/+PFD treatment led to a significant increase in p21 protein levels, a pattern expected of cell cycle inhibition. To directly link this induction to NRF2 status, we analysed p21 expression following ML385 treatment:

A549 and H1975 under ML385 exposure led to a significant downregulation of pNRF2 and consequently a marked increase in p21 expression. This confirms a functional NRF2-p21 regulatory axis in these lines.

In the H1299 cell lines, consistent with the absence of a functional anti-proliferative effect, ML385 treatment did not induce any significant increase in p21 expression. While the potential contribution of residual PFD in the conditioned medium cannot be excluded, the differential response to ML385 provides strong evidence for the existence of parallel mechanisms of proliferation control.

4.4.5 Validation of NRF2 silencing with siRNA as a specific tool for functional assays

To achieve highly specific modulation of the NRF2 pathway, complementing the pharmacological inhibitor ML385, and to secure more precise tool for subsequent functional assays in combination with the CM, we optimized genetic silencing via siRNA targeting exon 4 of the Nrf2 transcript. The choice to target exon 4 (which encodes the Neh3 domain) is critical: this domain is essential for NRF2's stability and its ability to recruit co-activators, thereby directly impacting the activation of gene transcription. This precise approach allows us to specifically ablate the NRF2 protein's transcriptional function, offering a focused method to study its role.

To guarantee maximum efficacy while minimizing potential off-target effects, a dose optimization study was conducted over time across all three NSCLC cell lines. We tested scalar concentrations (10nM, 50nM and 100 nM) for Nrf2siRNA and the high concentration for the scrambled siRNA (NegCTRL) and analysed them via western blot at 24h, 48h and 72h for the expression of pNRF2 and the key transcriptional target NQO1.

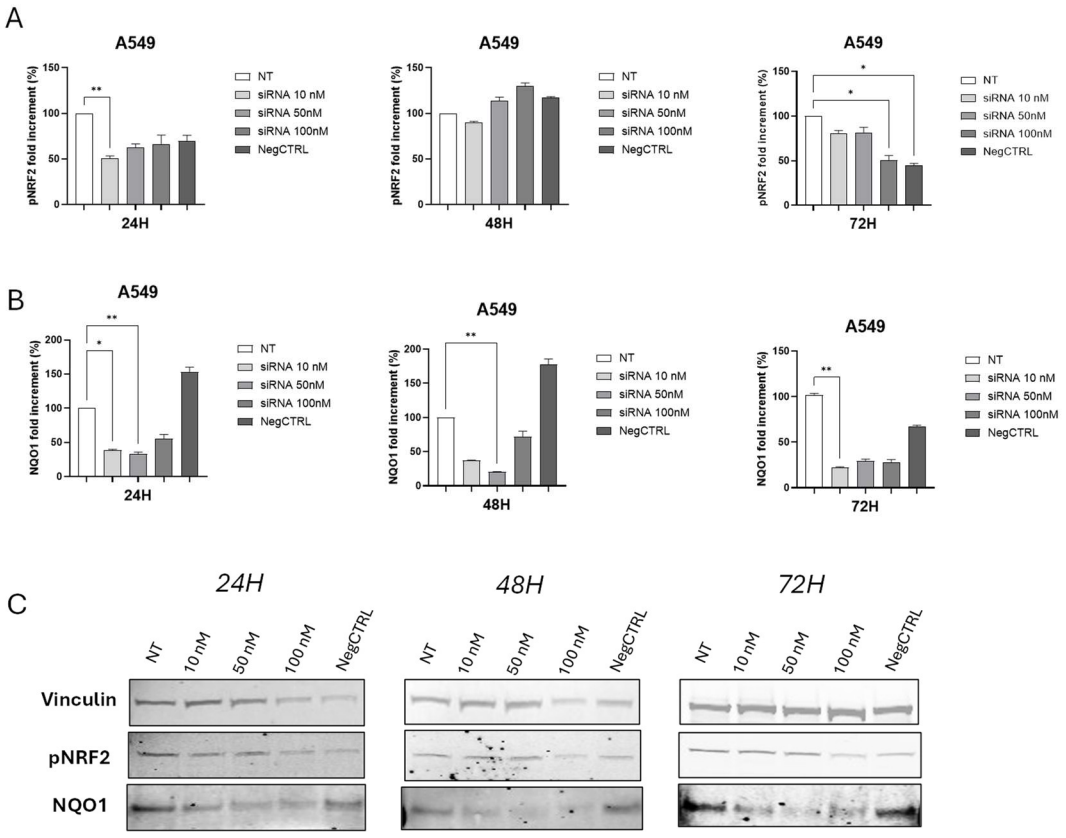

Figure 22 : Western blot evaluation of NRF2 silencing. Protein expression of pNRF2 (A) and NQO1 (B)in A549 cells transfected with different concentrations of siRNA at different time points. Representative Western blots

*showing the protein expression levels (C). Data are normalized to untreated cells (NT) and GAPDH or Vinculin, results are represented as a mean ± SEM, ****P ≤ 0.0001,***P ≤ 0.001, **P<0.01, and *P<0.05.*

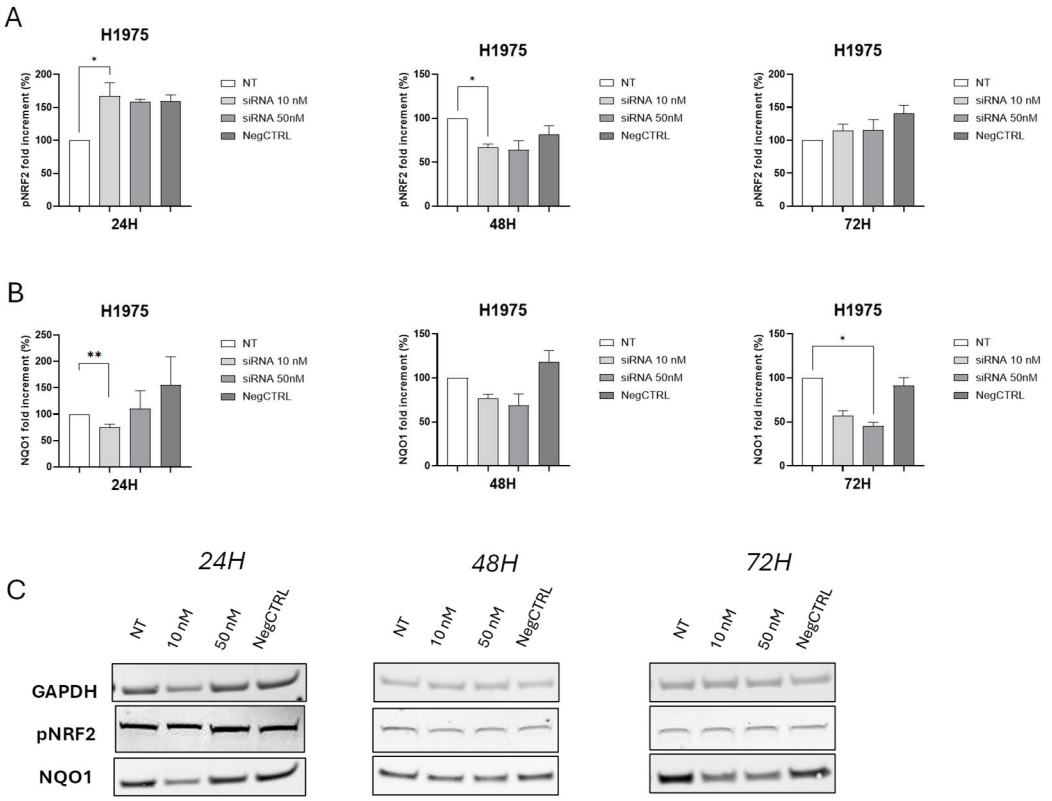

*Figure 23: Western blot evaluation of NRF2 silencing. Protein expression of pNRF2 (A) and NQO1 (B)in H1975 cells transfected with different concentrations of siRNA at different time points. Representative Western blots showing the protein expression levels (C). Data are normalized to untreated cells (NT) and GAPDH or Vinculin, results are represented as a mean ± SEM, ****P ≤ 0.0001,***P ≤ 0.001, **P<0.01, and *P<0.05.*

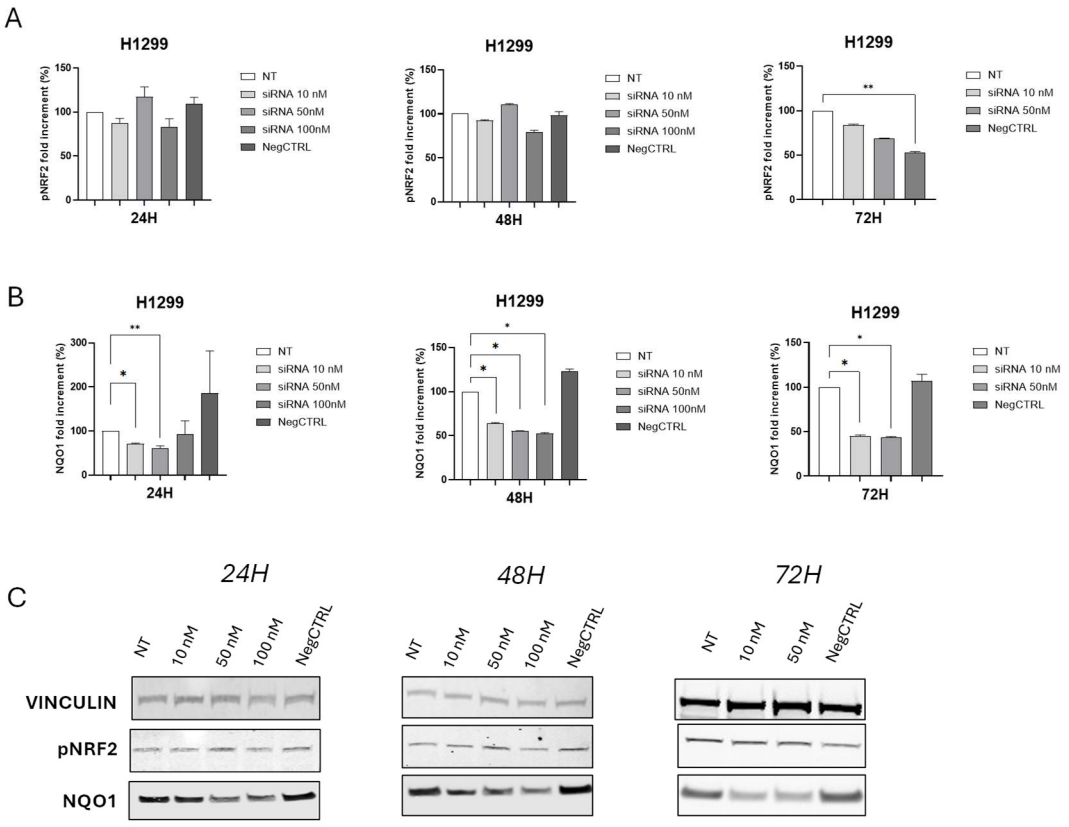

*Figure 24: Western blot evaluation of NRF2 silencing. Protein expression of pNRF2 (A) and NQO1 (B)in H1299 cells transfected with different concentrations of siRNA at different time points. Representative Western blots showing the protein expression levels (C). Data are normalized to untreated cells (NT) and GAPDH or Vinculin, results are represented as a mean ± SEM, ****P ≤ 0.0001,***P ≤ 0.001, **P<0.01, and *P<0.05.*

The optimization results showed that the lowest concentration, 10 nM of siRNA for NRF2, was sufficient to induce a significant inhibitory effect on NQO1 expression across all three cell lines, with the effect being clear at the 24-hours' time point. Note that for H1975 cells, data at the 100nM concentration were non included as this dose proved fatal to cell viability, indicating intrinsic toxicity of the siRNA or the transfection complex at that level. Since NQO1 serves as a robust and sensitive readout of NRF2 transcriptional activity, its effectiveness al 10 nM allowed us to select this concentration as optimal for subsequent functional assays, particularly those testing the impact of NRF2 genetic silencing on NSCLC cells exposed to the CM under various conditions. This provides a reliable instrument to mechanistically decouple the NRF2 axis from other pathways activated or suppressed by the CM.

4.4.6 Pirfenidone-Modulated CAFs impair NSCLC cell invasion: Dissection of the NRF2 role

With the aim to evaluate if the PFD-mediated alteration of the CAF secretome impacts the aggressive potential of tumoral cells and to dissect the contribution of NRF2 to this mechanism, we performed transwell invasion assays to investigate the effects of TME and NRF2 silencing on invasive capacity.

The invasiveness of A549, H1975 and H1299 cell lines was tested over 24 hours using matrigel-coated transwell inserts. These three cell conditions were compared:

- Un-transfected cells (NT)
- Scrambled siRNA (NegCTRL) cells transfected with a non-targeting siRNA
- Nrf2-silenced cells (siNrf2)

The invasive capacity of these three cellular conditions was tested in the presence of normal medium, in the presence of CM-CAFs/-PFD or CM-CAFs/+PFD. Furthermore, to establish a functional baseline for NRF2 involvement in invasion process, invasiveness of cells treated with ML385, in the presence of normal medium were also evaluated.

The pharmacological inhibition of NRF2 with ML385, in standard medium, resulted in a significant inhibitory effect on A549 cells invasiveness. This confirmed the role of NRF2 as a contributor to the basal invasive capacity of this cell line. We then examined the effect of genetically disrupting NRF2 in combination with the CM conditions (siNrf2 and NegCTRL).

The greatest inhibitory effect on A549 invasiveness was consistently achieved by the combination of Nrf2 silencing and the PFD-modulated CM (siNrf2 in CM-CAF/+PFD). This combination resulted in a significant lower number of invading cells compared to all other conditions, particularly when cells were exposed to the CM derived from CAF#1 and CAF#2 (Fig.25 B,C)

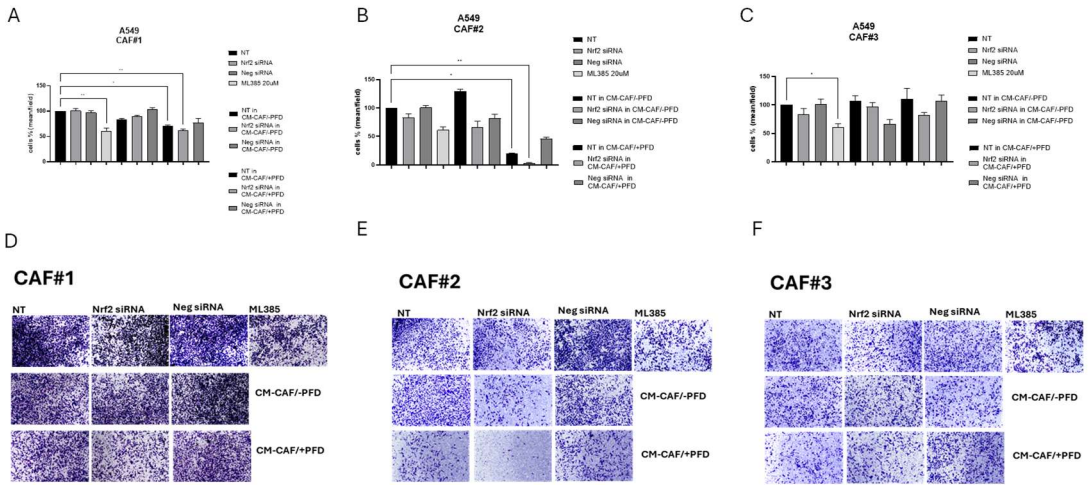

*Figure 25: Quantification of invaded A549 cells in percentage, under the indicated experimental conditions (CAF-conditioned media and NRF2 silencing) from the three different CAFs (A,B,C). Representative images of the Transwell invasion assay showing invaded A549 cells under the indicated experimental conditions (CAF-conditioned media and NRF2 silencing) from the three different CAFs (D,E,F), cells were stained with Crystal Violet. Data are normalized to untreated cells (NT), results are represented as a mean ± SEM, ****P ≤ 0.0001,***P ≤ 0.001, **P<0.01, and *P<0.05.*

Consistent with the results found in A549 cells, also in H1975 cell line the pharmacological inhibition of NRF2 with ML385 showed a significant inhibitory effect on H1975 cell invasion. We also found that, H1975 cells exposed to the CM-CAF/+PFD derived from CAF#1 and CAF#2, in combination of Nrf2 silencing resulted in a synergic or additive inhibitory effect, leading to the lowest levels of invasion observed. In sharp contrast with these findings, in H1975 cells exposed to the CM derived from CAF#3 there was no significant difference in invasiveness between Nrf2 silenced cells exposed to CM-CAF/-PFD and CM-CAF/+PFD, in both cases a significant inhibitory effect on invasiveness was already achieved (Fig.26)

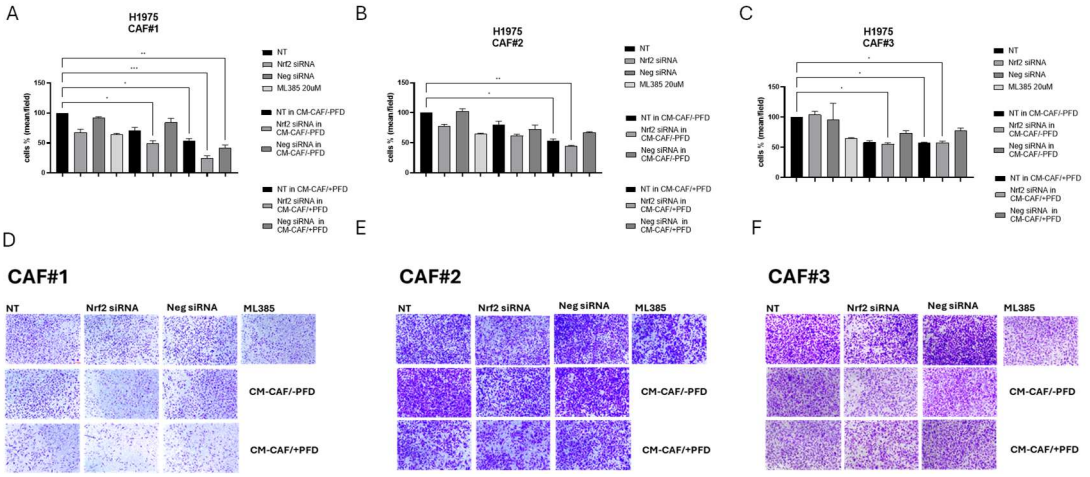

*Figure 26: Quantification of invaded H1975 cells in percentage, under the indicated experimental conditions (CAF-conditioned media and NRF2 silencing) from the three different CAFs (A,B,C). Representative images of the Transwell invasion assay showing invaded H1975 cells under the indicated experimental conditions (CAF-conditioned media and NRF2 silencing) from the three different CAFs (D,E,F), cells were stained with Crystal Violet. Data are normalized to untreated cells (NT), results are represented as a mean ± SEM, ****P ≤ 0.0001,***P ≤ 0.001, **P<0.01, and *P<0.05.*

In H1299 cell lines we observed the most complex profile of response. In un-transfected cells the treatment with ML385 in standard medium caused only a slight decrease in invasive capacity, the combination of siNrf2 and CM-CAF/+PFD represented the condition with the lowest number of invading cells, particularly with the CM of CAF#1. Under the treatment with CM-CAF#2 the effect of CM-CAF/+PFD was not significantly different between siNrf2 cells and unsilenced cells, indeed, the inhibition of invasiveness is due to the CM-CAF/+PFD alone. The response to CM-CAF#3 was completely different. The treatment with CM-CAF/+PFD showed no significant inhibitory effect on invasive capacity compared to the treatments with other medium.

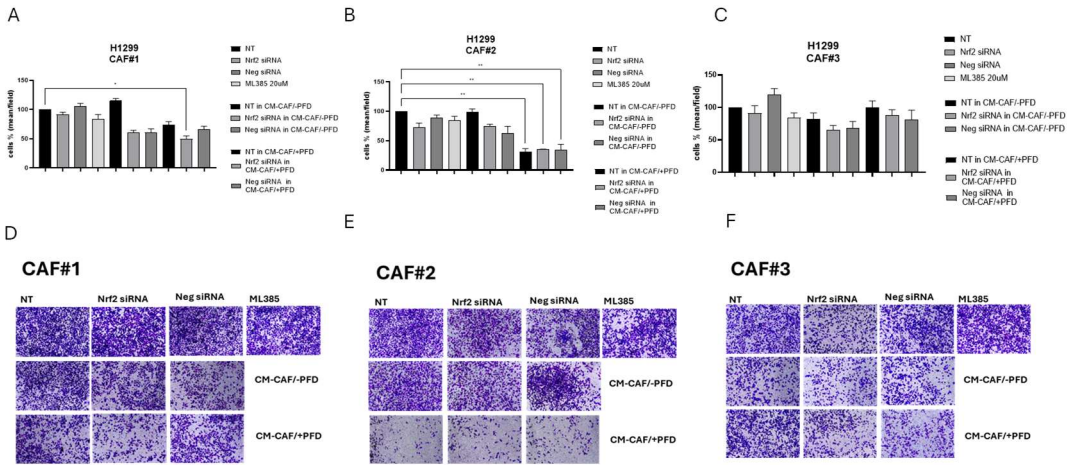

*Figure 27 : Quantification of invaded H1299 cells in percentage, under the indicated experimental conditions (CAF-conditioned media and NRF2 silencing) from the three different CAFs (A,B,C). Representative images of the Transwell invasion assay showing invaded H1299 cells under the indicated experimental conditions (CAF-conditioned media and NRF2 silencing) from the three different CAFs (D,E,F), cells were stained with Crystal Violet. Data are normalized to untreated cells (NT), results are represented as a mean ± SEM, ****P ≤ 0.0001,***P ≤ 0.001, **P<0.01, and *P<0.05.*

The comprehensive analysis of transwell invasiveness assay consistently revealed a critical level of heterogeneity in the CAF secretome response to PFD across all NSCLC cell lines. CM-CAF/+PFD derived from CAF#1 and CAF#2 generally resulted in a robust inhibitory effect, often accompanied by an additive effect when the treatment was associated with Nrf2 silencing. Conversely, the treatment with CM from CAF#3 presented a distinct pattern. Indeed, the treatment with CM-CAF/+PFD from CAF#3 failed to induce a significant inhibitory effect on invasiveness when compared to its corresponding CM-CAF/-PFD in all three cell lines.

4.5 Establishing a 3D multicellular spheroid model to study TME modulation

To establish a physiologically relevant, reliable model for future studies of NSCLC progression and its interaction with the TME, we optimized the formation of multicellular tumor spheroids (MCTS) using patient-derived CAFs from patient #1 and the three NSCLC cell lines (A549, H1975 and H1299). The primary objective of this preliminary experiment was to validate the MCTS system as a functional tool capable of recapitulating the TME response to anti-fibrotic modulation.

MCTS were constructed using CAFs that had been pre-treated for 48h with PFD or in normal medium; following this pretreatment the CAF were co-cultured with the NSCLC cells at a 2:1 ratio (2 CAF and 1 tumor cell), mimicking the high stromal density found in fibrotic tumors. The cells were allowed to aggregate and form stable spheroids over a period of 24/48 hours.

In all the tested conditions and cell lines, the mixed CAF/cancer cells aggregates successfully formed compact, well-defined MCTS within 24 hours, confirming the stability and viability of the 3D model.

Subsequent quantification of the spheroid dimensions after the 24 hours aggregation phase revealed a highly significant difference in size based on the CAF pretreatment (Fig.28).

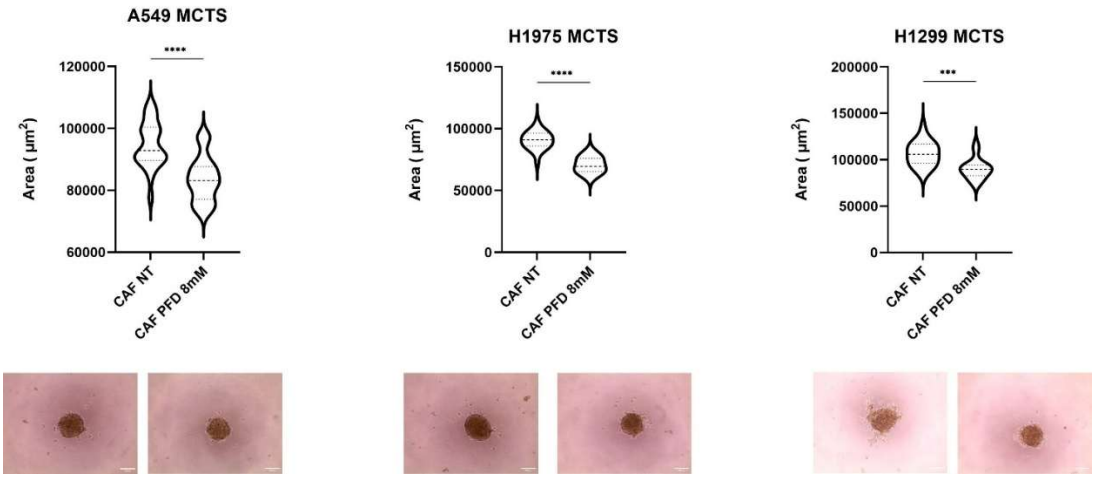

*Figure 28 Quantification and representative images of 3D multicellular spheroids. Co-cultures of NSCLC cells and primary CAFs (1:2 ratio) under the indicated experimental conditions (± Pirfenidone). Images were captured using brightfield microscopy. Data are normalized to untreated cells (CAF NT), results are represented as a mean ± SEM, ****P ≤ 0.0001,***P ≤ 0.001, **P<0.01, and *P<0.05.*

Spheroids constructed with CAF treated with PFD were consistently and significantly smaller in diameter compared to the MCTS constructed using with normal CAF, across all three NSCLC cell lines.

This result not only validates the MCTS system as an appropriate model for our cell lines but also demonstrates that the pre-treatment of CAF with PFD fundamentally alters their ability to support 3D aggregation and initial growth of the tumor cell mass. The reduced spheroid size observed with CAF treated confirms that this model is sensitive enough to capture the effects of CAF modulation, making it a robust platform for subsequent functional studies of the TME and NRF2 implications.

5 DISCUSSION

Lung cancer remains the leading cause of cancer-related mortality worldwide with Non-Small Cell Lung Cancer (NSCLC) accounting for approximately 85% of all cases. NSCLC is a highly heterogeneous disease, traditionally classified into histological subtypes such as adenocarcinoma, squamous cell carcinoma and large cell carcinoma. Despite significant improvements in early detection and molecular characterization, the prognosis for many patients remains poor, largely due to late-stage diagnosis and the inevitable emergence of therapeutic resistance.

The treatment paradigm for NSCLC has undergone a radical transformation over the last decade. The shift from conventional platinum-based chemotherapy toward targeted therapies and immunotherapy (e.g., Immune Checkpoint Inhibitors targeting PD-1/PD-L1) has significantly extended survival for subsets of patients. However, the high plasticity of tumor cells and the protective influence of the surrounding environment often lead to treatment failure, highlighting the need for strategies that address the tumor not as an isolated entity, but as a complex ecosystem [157], [158], [159] .For this reasons it is important to consider and investigate the role of the tumor microenvironment (TME) in tumor progression and resistance to therapies. The TME is a sophisticated network of cellular and non-cellular components, including immune cells, blood vessels, extracellular matrix (ECM) and cancer-associated fibroblasts (CAFs). CAFs represent the most prominent cellular component of the TME, characterized by the expression of specific markers such as alphaSMA, these cells undergo a "fibroblast-to-myofibroblast" transition, acquiring a highly secretory and contractile phenotype. TGFbeta, secreted *in primis* by cancer cells, is the master regulator driving the transformation of resident fibroblasts into activated CAFs, once activated, CAFs themselves secrete high levels of TGFbeta creating a self-sustaining autocrine loop that maintains their activated state. In NSCLC the TME is frequently characterized by a "desmoplastic reaction", an aberrant fibrotic response driven primarily by activate CAFs [160], [161]. In addition to TGFbeta, these cells secrete excessive ECM proteins creating a stiffened physical barrier that impairs drug delivery and provides biochemical cues that promote tumor cell survival, epithelial-to-mesenchymal transition (EMT), and the promotion of metastatic diffusion [162].

The critical stressed microenvironmental conditions, in association with the selective pressure of the therapeutic treatments lead NSCLC cells to adopt signalling pathways for survival. One of these pathways is the activation of NRF2 (Nuclear factor erythroid 2-related factor 2).

Traditionally recognized for its role in protecting normal cells from oxidative damage, NRF2 is often hijacked in cancer. Its hyperactivation driven by canonical mutations (KEAP1) or non-canonical signalling from the stroma-leads to a robust antioxidant response, metabolic reprogramming and enhanced detoxification. This “NRF2 addiction” allows tumor cells to survive in the hostile, pro-oxidant environment of the fibrotic stroma and resist the cytotoxic effects of chemotherapy and radiotherapy[163], [164], [165] .

While the role of NRF2 in tumor cells is well-documented, its regulation within the complex landscape of the TME remains an area requiring urgent investigation, this study emphasizes the role of “stromal normalization”. The “stromal normalization” is not merely the reduction of physical density of the extracellular matrix but relates to the interference on biochemical crosstalk between host cells (fibroblasts) and cancer cells that take place in the fibrotic microenvironment driven by TGF-beta and NRF2 pathway.

Initially, it was essential to evaluate the impact of key cytokines representative of the inflammatory and fibrotic TME, specifically TGF-beta and TNF-alpha, on the modulation of NRF2, within A549 and H1975 cell lines, which serve as established *in vitro* models of NSCLC. Western blot analysis confirmed that both cytokines significantly upregulated the expression of NRF2. Notably, this increase was specifically observed in its active, phosphorylated form (p-NRF2), suggesting that these TME-derived stimuli can trigger the intracellular antioxidant and cytoprotective signalling pathways of tumor cells. The phosphorylated form of NRF2 at Ser-40, verified by using the specific antibody, is mediated by the protein Kinase C and is responsible for activating the nuclear translocation mechanism of NRF2 and the subsequent activation of transcription following binding to ARE sites[166] .For this reason, in the ongoing work, the expression of NRF2 in this form was analyzed. Simultaneously, we investigated the impact of these cytokines on the expression of p21 (CDKN1A). Beyond its established role as a pivotal cell cycle regulator, p21 has been characterized as a key mediator in the oxidative stress response through its direct interaction with the NRF2 signalling axis [167].To further elucidate this crosstalk, we employed K67, a specific chemical inhibitor that targets the Keap1/p62 interaction, thereby blocking the non-canonical activation of the NRF2 pathway. Our findings revealed that the downregulation of p21 expression induced by cytokine treatment was significantly reverted when cells were co-treated with K67. This suggests that the modulation of p21 is functionally linked to the aberrant activation of the NRF2 pathway in this context. Furthermore, to ensure that these fluctuations in protein expression were not biased by cellular suffering, MTT assays were performed, confirming that the observed molecular changes were not secondary to a decrease in cell viability. The pharmacological inhibition of NRF2 (via K67) leading to a recovery of p21 levels strongly indicates the existence of a negative feedback loop.

Having stablished that TGF-beta serves as a potent inducer of the NRF2 pathway and modulates the p21/NRF2 axis, we sought to validate these findings within a more physiological relevant context. To this end, our study integrated CAFs isolated from patients affected by NSCLC. While the use of recombinant TGFbeta allowed us to isolate specific signalling events, transitioning to patient-derived CAFs was essential for several reason. First, CAFs provide a complex secretome that includes not only TGFbeta but also a cocktail of cytokines, chemokines and ECM components that more accurately mimic the lung cancer milieu. Second, utilizing patient-derived cells, we account for the inter-patient heterogeneity inherent in lung adenocarcinoma, this approach allows us to confirm whether the NRF2 dynamics we observed are a fundamental feature of the CAF-cancer cell interaction rather than a transient response to a single exogenous stimulus.

To translate our molecular findings into a clinical context, we established primary cultures of CAFs from three patient lung cancer biopsies. The reliability of the subsequent experiments hinged on the rigorous isolation and characterization of these cells to ensure a pure mesenchymal population, free from epithelial contamination. The isolation process relied on the differential ability of fibroblasts to rapidly adhere to plastic surface, a standard technique for enriching mesenchymal cells from dissociated tissue. To confirm the success of this enrichment, we performed flow cytometry analysis focusing on two key membrane antigens: CD90(Thy-1), a well established glycosylphosphatidylinositol-anchored glycoprotein used as a positive marker for fibroblasts and mesenchymal-derived stem cells and CD326 (EpCAM), an epithelial cell adhesion molecule used here as a negative marker to exclude any contaminating tumor cells or normal epithelial cells. FACS analyses demonstrated that the isolated populations were nearly 100% positive for CD90and negative for CD326. To defining feature of CAF as “activated” (or myofibroblastic phenotype), we analyzed the expression of alphaSMA using both western blot and immunofluorescence assays. To provide a baseline for normal fibroblast behavior, we used the MRC5 (human fetal lung fibroblasts) cell line as a control. MRC5 cells represent a quiescent or non-activated fibroblast phenotype, making them the ideal benchmark to quantify the degree of activation in our patient-derived samples. Interestingly, we observed a relative increase in alphaSMA expression across our samples. While all the three samples revealed high expression of alphaSMA and were defined as “activated”, there were differences in expression intensity: CAF#1 lowest activation prophile, CAF#2 intermediate and CAF#3 highest activation profile. This variability between three primary CAF is particularly noteworthy as it reflects the clinical heterogeneity of lung cancer.

The pivotal role of the TGFbeta axis in maintaining CAF activation led us to explore a targeted pharmacological intervention using Pirfenidone (PFD), as a clinically approved antifibrotic agent. PFD was chosen for its known ability to inhibit the TGFbeta signalling cascade and

reduce extracellular matrix deposition and is already under study as a drug directed against TME[168], [169], [170] .Our goal was to determine if the pro-tumorigenic CAF phenotype could be “reverted” toward a more quiescent state. Our results demonstrate that PFD effectively disrupt the myofibroblastic signature across the primary CAF lines. The consistent downregulation of alphaSMA and TGFbeta protein levels indicates a successful disruption of the autocrine loop that sustains CAF activation. By reducing these makers, PFD effectively “deactivates” the stroma, potentially limiting its ability to drive the NRF2-mediated stress response in neighbouring cancer cells. While *Col1A1* transcripts decreased in all CAF populations, the protein levels paradoxically increased in CAF#3 (the most activated line), this discrepancy suggests a post-translational stabilization, allowing the fibrotic matrix to persist despite the inhibition by the antifibrotic agent PFD. While the consistent increase in TGFbeta mRNA across all three lines indicates a robust compensatory feedback loop, the CAFs likely attempt to overcome the blockade by upregulating the transcription of the ligand itself.

To better simulate the paracrine interactions within the tumor microenvironment we developed an indirect in vitro co-culture model using conditioned media (CM) from primary CAFs. A crucial methodological aspect of this approach was the use of CM harvested from CAFs previously treated with PFD. Because each CM was used “as-is”, following the incubation period, it inevitably contained residual non-metabolized PFD. Given that the exact concentration of the remaining drug was unknown, we determined whether the modulation of NRF2 in NSCLC cells is a result of the altered CAF secretome or a direct pharmacological effect of the drug. Thus, NSCLC cell lines were treated directly with Pirfenidone at two concentration: the dose used in CAFs experiments [171] and the specific IC_{50} dose calculated for the tumor cells. Our findings demonstrated that PFD, even at the highest concentration, had no direct effect on NRF2 expression in the cancer cells.

We next evaluated the impact of the normal and “reverted” CAF secretome on NSCLC cell behaviour. The viability assays demonstrate that the secretome of PFD-treated CAFs generally caused a significant decrease in cell viability, a striking exception was observed in the interaction between A549 cells and CAF#3, the most activated line; untreated CM from this CAFs significantly increased A549 viability, highlighting a particularly potent pro-tumorigenic secretome, in this specific combination, the CM-CAF#3/+PFD failed to reduce viability, instead showing no net effect. Taken together, these findings highlight that non-toxic pharmacological interventions frequently reach a plateau of ineffectiveness. This plateau reflects a biological adaptation to the drug, where the malignant environment develops a 'habituation' that neutralizes the treatment's impact over time. Furthermore, we focused on the activation of NRF2 signalling pathway in the cross-talk between cancer cells and CAF-CM. In a complex signalling environment, measuring NRF2 protein levels alone is often

insufficient to confirm true pathway flux. Therefore, we expanded our analysis to include key downstream effectors and regulator, specifically NQO1 (NAD(P)H Quinone Dehydrogenase1) and p62(SQSTM1). Analyzing NQO1 is essential as it serves as a primary transcriptional target of NRF2; its downregulation provides definitive evidence of reduced NRF2 transcriptional activity. Simultaneously, monitoring p62 is crucial because it facilitates a "non-canonical" activation of NRF2 by sequestering Keap1. By observing the dynamics of these proteins, we explored whether CAF secretome influences NRF2 through classical or alternative regulatory loops. Our results reveal a consistent trend: treatment with CM/+PFD from all three primary CAF lines led to a significant reduction in NRF2 activation, and this was mirrored by a clear decrease in NQO1 expression. Moreover, the non-canonical activation of NRF2 typically involves p62, and we found that pNRF2 levels changed independently of p62 suggesting that the NRF2 induction driven by the CAF is directed by other direct secretome-driven events. A central finding of this study is the correlation between CAF activation status and the magnitude of NRF2 induction in cancer cells. As we predicted from our preliminary TGFbeta experiments, the secretome from untreated CAFs function as a potent inducer of NRF2. Crucially the level of NRF2 activation followed a kind of gradient of CAF aggressiveness, indeed CAF #3 triggered the most robust NRF2 upregulation. This suggests that the "richer" and more aggressive the CAF secretome is, the more intensely it will force the cancer cell into an NRF2-high, pro-survival state.

It is fundamental to mention that while the CAF secretome acted as a inducer of NRF2, H1299 cell line exhibited a distinct lack of response. In these cells, exposure to the CM from all three CAF lines failed to trigger a significant increase in NRF2 activation, the lack of NRF2 induction in H1299 cells underscores the critical role of the genetic background in determining the response to the CAF secretome.

Among the complex of the results obtained we suggest that NRF2 downregulation in NSCLC cells is a paracrine effect. Indeed, PFD which "reprograms" CAF secretome deprives the cancer cells of the external stimuli normally required to sustain high NRF2 levels.

To confirm that the NRF2 signalling directly dictates the proliferative capacity of NSCLC cells, we performed cell count assays and protein analysis using NRF2 inhibitor ML385 as a strategic control. It is important to distinguish the mechanism of ML385 action from the previously used K67. While K67 typically interferes with the NRF2-Keap1 protein-protein interaction to block the pathway's activation, ML385 acts as a direct transcriptional inhibitor, it binds specifically to the Neh1 domain of NRF2, preventing it from binding to the ARE of its target genes. This allows us to verify if the effects on proliferation are specifically due to the transcriptional output of NRF2. Whereas K67, that was used to define the relationship

between NRF2 and p21 in response to cytokine stimulation, failed to inhibit pNRF2 expression at basal level, we found that ML385 inhibits NRF2 activation. In both A549 and H1975 lines, we observed a consistent functional pattern, the CM from untreated CAFs exerted a stromal support with a clear pro-proliferaive effect, reinforcing the idea that an activated stroma actively pushes cancer cells through the cell cycle. This pro-tumorigenic effect was effectively downregulated by PFD. CM from treated CAFs induced a drastic and significant reduction in cell proliferation. Crucially, direct inhibition of NRF2 via ML385 yielded an almost identical inhibitory effect to that obtained in PFD-treated CM. The most compelling evidence for our proposed mechanism is the expression of p21. We observed a significant upregulation of p21 in two specific conditions: when cancer cells were exposed to the "reverted" secretome and when NRF2 was directly blocked. Stromal deactivation, via PFD and direct NRF2 inhibition with ML385 lead to a similar phenotypic outcomes, characterized by an upregulation of p21 and reduced proliferation. These results suggest a potential association between CAF-derived signals and the modulation of these proteins. In addition, these findings indicate that the pro-proliferative influence of the stroma might be, at least in part, related to a interplay between NRF2 and p21, although the precise molecular hierarchy of this interaction remains to be fully elucidated. The H1299 cell line exhibit a distinct response profile. While direct NRF2 inhibition via ML385 did eventually lead to an antiproliferative effect, this response was notably delayed compared to the other lines and occurred without any detectable upregulation of p21. This result suggests that in the p53-null background of H1299, the potential NRF2/p21 regulatory axis is disrupted or entirely absent. In contrast, the more rapid and robust growth inhibition observed with CM-CAFs/+PFD suggests that the "reverted" CAF secretome targets a broader range of survival signals beyond just NRF2. Furthermore, we cannot exclude that residual PFD within CM contributes to this immediate effect by acting directly on H1299. However, it should be taken into account that the viability analysis carried out with PFD on the tumor cells showed a weak cytostatic effect. It is plausible to think that while CAF-reversion is a key driver of tumor suppression, the presence of the drug itself provides a "second hit" that ensures growth inhibition even in those cells like H1299 cell lines, where the NRF2/p21 axis is less responsive.

To further validate the role of NRF2 in cancer progression, we employed a genetic approach with a knockdown strategy, we targeted Exon4 of the *NRF2* gene, which encodes the Neh3 domain, essential for the transcriptional activation; the effectiveness of silencing was validated by observing a significant reduction in NQO1 expression, confirming the successful distribution of NRF2-transcription process. In the invasion assays, we tested the capacity of these NRF2-silenced cells to migrate through a reconstructed basement membrane in response to the CAF secretome and in most experimental conditions. We observed that "disarming" the

cancer cell through NRF2 silencing and “deactivating” the stroma via the perturbation with PFD were effective individually. However, the most significant reduction in invasiveness occurred when these strategies were combined. This suggests that the maximal therapeutic benefit may be achieved only when the tumor’s internal antioxidant defence (NRF2) is silenced simultaneously with the withdrawal of stimuli from the CAF secretome. Despite the general success of this synergy, the heterogeneity of the tumor microenvironment introduced notable exceptions. In A549 cells, the secretome of the most aggressive line CAF#3 appeared to partially override the treatments. Significant inhibition in this specific pairing was only achieved via NRF2 silencing in basal condition, suggesting that CAF#3 produces a “threshold” of pro-invasive factors that can bypass some of the inhibitory effects of PFD. The behaviour of H1299 cells reinforces their unique profile. Unlike the other lines, silenced condition alone failed to decrease invasion, a result mirrored by the lack of response to the ML385 control. This confirms that while H1299 cells are sensitive to the broader changes in the CAF secretome, they may do not primary rely on the NRF2 axis to execute their invasive program. These results illustrate that while the NRF2-p21-invasion axis is the powerful driver in A549 and H1975 lines, the most aggressive CAFs (CAF#3) and p53-null backgrounds (H1299) present more complex challenges. Collectively, these data support a model where stromal deactivation is most effective when tailored to the specific genetic vulnerabilities of the tumor, with the combination of NRF2 inhibition and antifibrotics representing a potent, although context-dependent strategy to block metastasis.

In conclusion of this study, we established a preliminary 3D multicellular co-culture model using primary #2 CAFs. To better simulate the tumor architecture. A strategic 1:2 ratio of tumor cells to CAF was employed to ensure the stromal component remained well-represented, and effectively counteracting the naturally faster proliferation of the cancer cells. This approach proved highly feasible and revealed that multicellular spheroids containing PFD-treated CAF were significantly smaller than those with untreated CAF, demonstrating that stromal deactivation effectively limits tumor-stroma growth even within a spatial arrangement.

The successful implementation of this 3D model provides a sophisticated platform for dissecting the symbiotic relationship between the stroma and the tumor. By precisely mapping the molecular cross-talk and the spatial activation of NRF2 at the tumor-CAF interface, this system may be useful in identifying novel therapeutic targets designed to disrupt this cooperation. Beyond target discovery, this model offers a translational window into personalized medicine. By accounting for variables like matrix stiffness and mechanical signalling, it allows for the screening of stroma-targeted therapies and explores how a reduced fibrotic environment might enhance the penetration and efficacy of traditional chemotherapy.

6 REFERENCES

[1] A. A. Thai, B. J. Solomon, L. V Sequist, J. F. Gainor, and R. S. Heist, "Lung cancer," *The Lancet*, vol. 398, no. 10299, pp. 535–554, Aug. 2021, doi: 10.1016/S0140-6736(21)00312-3.

[2] C. Li *et al.*, "Risk mapping of lung cancer: a comprehensive appraisal of published meta-analyses incorporating Mendelian randomization studies," *J Cancer Res Clin Oncol*, vol. 149, no. 10, pp. 6857–6873, Aug. 2023, doi: 10.1007/s00432-023-04606-4.

[3] E. D. Neama *et al.*, "Understanding the current landscape of lung cancer research and treatment: A systematic review," *International Journal of Advanced Biochemistry Research*, vol. 8, no. 4, pp. 268–272, Jan. 2024, doi: 10.33545/26174693.2024.v8.i4d.948.

[4] B. Smolarz, H. Łukasiewicz, D. Samulak, E. Piekarska, R. Kołaciński, and H. Romanowicz, "Lung Cancer—Epidemiology, Pathogenesis, Treatment and Molecular Aspect (Review of Literature)," *Int J Mol Sci*, vol. 26, no. 5, p. 2049, Feb. 2025, doi: 10.3390/ijms26052049.

[5] J. A. Barta, C. A. Powell, and J. P. Wisnivesky, "Global Epidemiology of Lung Cancer," *Ann Glob Health*, vol. 85, no. 1, Jan. 2019, doi: 10.5334/aogh.2419.

[6] L. M. Tesfaw, Z. G. Dessie, and H. Mekonnen Fenta, "Lung cancer mortality and associated predictors: systematic review using 32 scientific research findings," *Front Oncol*, vol. 13, Dec. 2023, doi: 10.3389/fonc.2023.1308897.

[7] O. Rodak, M. D. Peris-Díaz, M. Olbromski, M. Podhorska-Okołów, and P. Dzięgiel, "Current Landscape of Non-Small Cell Lung Cancer: Epidemiology, Histological Classification, Targeted Therapies, and Immunotherapy," *Cancers (Basel)*, vol. 13, no. 18, p. 4705, Sep. 2021, doi: 10.3390/cancers13184705.

[8] Y. Shen, J.-Q. Chen, and X.-P. Li, "Differences between lung adenocarcinoma and lung squamous cell carcinoma: Driver genes, therapeutic targets, and clinical efficacy," *Genes Dis*, vol. 12, no. 3, p. 101374, May 2025, doi: 10.1016/j.gendis.2024.101374.

[9] V. Relli, M. Trerotola, E. Guerra, and S. Alberti, "Abandoning the Notion of Non-Small Cell Lung Cancer," *Trends Mol Med*, vol. 25, no. 7, pp. 585–594, Jul. 2019, doi: 10.1016/j.molmed.2019.04.012.

[10] W. Wang, H. Liu, and G. Li, "What's the difference between lung adenocarcinoma and lung squamous cell carcinoma? Evidence from a retrospective analysis in a cohort of Chinese patients," *Front Endocrinol (Lausanne)*, vol. 13, Aug. 2022, doi: 10.3389/fendo.2022.947443.

[11] W. Nabi *et al.*, "Comparative survival outcomes among histological subtypes of non-small cell lung cancer in the United States.," *Journal of Clinical Oncology*, vol. 43, no. 16_suppl, Jun. 2025, doi: 10.1200/JCO.2025.43.16_suppl.e20072.

[12] J. Goodwin *et al.*, "The distinct metabolic phenotype of lung squamous cell carcinoma defines selective vulnerability to glycolytic inhibition," *Nat Commun*, vol. 8, no. 1, p. 15503, May 2017, doi: 10.1038/ncomms15503.

[13] W. Wang, H. Liu, and G. Li, “What’s the difference between lung adenocarcinoma and lung squamous cell carcinoma? Evidence from a retrospective analysis in a cohort of Chinese patients,” *Front Endocrinol (Lausanne)*, vol. 13, Aug. 2022, doi: 10.3389/fendo.2022.947443.

[14] A. W. Chan *et al.*, “The Landscape of Actionable Molecular Alterations in Immunomarker-Defined Large-Cell Carcinoma of the Lung,” *Journal of Thoracic Oncology*, vol. 14, no. 7, pp. 1213–1222, Jul. 2019, doi: 10.1016/j.jtho.2019.03.021.

[15] D. H. Hwang, D. P. Szeto, A. S. Perry, J. L. Bruce, and L. M. Sholl, “Pulmonary Large Cell Carcinoma Lacking Squamous Differentiation Is Clinicopathologically Indistinguishable From Solid-Subtype Adenocarcinoma,” *Arch Pathol Lab Med*, vol. 138, no. 5, pp. 626–635, May 2014, doi: 10.5858/arpa.2013-0179-OA.

[16] D. H. Hwang, D. P. Szeto, A. S. Perry, J. L. Bruce, and L. M. Sholl, “Pulmonary Large Cell Carcinoma Lacking Squamous Differentiation Is Clinicopathologically Indistinguishable From Solid-Subtype Adenocarcinoma,” *Arch Pathol Lab Med*, vol. 138, no. 5, pp. 626–635, May 2014, doi: 10.5858/arpa.2013-0179-OA.

[17] J. L. Johnson, S. Pillai, and S. P. Chellappan, “Genetic and Biochemical Alterations in Non-Small Cell Lung Cancer,” *Biochem Res Int*, vol. 2012, pp. 1–18, 2012, doi: 10.1155/2012/940405.

[18] S. Workman, S. K. Jabbour, and M. P. Deek, “A narrative review of genetic biomarkers in non-small cell lung cancer: an update and future perspectives,” *AME Med J*, vol. 8, pp. 6–6, Mar. 2023, doi: 10.21037/amj-2022-01.

[19] V. Lazar *et al.*, “Integrated molecular portrait of non-small cell lung cancers,” *BMC Med Genomics*, vol. 6, no. 1, p. 53, Dec. 2013, doi: 10.1186/1755-8794-6-53.

[20] F. Xu *et al.*, “Prognostic biomarkers correlated with immune infiltration in non-small cell lung cancer,” *FEBS Open Bio*, vol. 13, no. 1, pp. 72–88, Jan. 2023, doi: 10.1002/2211-5463.13501.

[21] K. Wang, M. Ye, Z. Mo, X. Huang, Y. Li, and S. Wei, “Comprehensive analysis of genomic alterations and novel prognostic biomarkers, and establishment of prediction models of metastasis in metastatic non-small cell lung cancer,” *J Cancer*, vol. 16, no. 1, pp. 339–350, Jan. 2025, doi: 10.7150/jca.97070.

[22] R. Liao *et al.*, “Genomic Characteristics and the Potential Clinical Implications in Oligometastatic Non–Small Cell Lung Cancer,” *Cancer Res Treat*, vol. 55, no. 3, pp. 814–831, Jul. 2023, doi: 10.4143/crt.2022.1315.

[23] K. J. Song *et al.*, “Proteogenomic analysis reveals non-small cell lung cancer subtypes predicting chromosome instability, and tumor microenvironment,” *Nat Commun*, vol. 15, no. 1, p. 10164, Nov. 2024, doi: 10.1038/s41467-024-54434-4.

[24] A. Sultana *et al.*, “Single-cell RNA-seq analysis to identify potential biomarkers for diagnosis, and prognosis of non-small cell lung cancer by using comprehensive bioinformatics approaches,” *Transl Oncol*, vol. 27, p. 101571, Jan. 2023, doi: 10.1016/j.tranon.2022.101571.

[25] R. Pirlog *et al.*, “Cellular and Molecular Profiling of Tumor Microenvironment and Early-Stage Lung Cancer,” *Int J Mol Sci*, vol. 23, no. 10, p. 5346, May 2022, doi: 10.3390/ijms23105346.

[26] J. L. Johnson, S. Pillai, and S. P. Chellappan, “Genetic and Biochemical Alterations in Non-Small Cell Lung Cancer,” *Biochem Res Int*, vol. 2012, pp. 1–18, 2012, doi: 10.1155/2012/940405.

[27] V. Lazar *et al.*, “Integrated molecular portrait of non-small cell lung cancers,” *BMC Med Genomics*, vol. 6, no. 1, p. 53, Dec. 2013, doi: 10.1186/1755-8794-6-53.

[28] H. Jeon, S. Wang, J. Song, H. Gill, and H. Cheng, “Update 2025: Management of Non-Small-Cell Lung Cancer,” *Lung*, vol. 203, no. 1, p. 53, Dec. 2025, doi: 10.1007/s00408-025-00801-x.

[29] N. Deboever, K. G. Mitchell, H. A. Feldman, T. Cascone, and B. Sepesi, “Current Surgical Indications for Non-Small-Cell Lung Cancer,” *Cancers (Basel)*, vol. 14, no. 5, p. 1263, Feb. 2022, doi: 10.3390/cancers14051263.

[30] S. Tang *et al.*, “Immune Checkpoint Inhibitors in Non-Small Cell Lung Cancer: Progress, Challenges, and Prospects,” *Cells*, vol. 11, no. 3, p. 320, Jan. 2022, doi: 10.3390/cells11030320.

[31] Y. Cheng, T. Zhang, and Q. Xu, “Therapeutic advances in non-small cell lung cancer: Focus on clinical development of targeted therapy and immunotherapy,” *MedComm (Beijing)*, vol. 2, no. 4, pp. 692–729, Dec. 2021, doi: 10.1002/mco2.105.

[32] J. C. Restrepo, D. Dueñas, Z. Corredor, and Y. Liscano, “Advances in Genomic Data and Biomarkers: Revolutionizing NSCLC Diagnosis and Treatment,” *Cancers (Basel)*, vol. 15, no. 13, p. 3474, Jul. 2023, doi: 10.3390/cancers15133474.

[33] M. Yuan, L.-L. Huang, J.-H. Chen, J. Wu, and Q. Xu, “The emerging treatment landscape of targeted therapy in non-small-cell lung cancer,” *Signal Transduct Target Ther*, vol. 4, no. 1, p. 61, Dec. 2019, doi: 10.1038/s41392-019-0099-9.

[34] S.-Y. M. Liu, M.-M. Zheng, Y. Pan, S.-Y. Liu, Y. Li, and Y.-L. Wu, “Emerging evidence and treatment paradigm of non-small cell lung cancer,” *J Hematol Oncol*, vol. 16, no. 1, p. 40, Apr. 2023, doi: 10.1186/s13045-023-01436-2.

[35] P.-L. Su *et al.*, “Recent advances in therapeutic strategies for non-small cell lung cancer,” *J Hematol Oncol*, vol. 18, no. 1, p. 35, Mar. 2025, doi: 10.1186/s13045-025-01679-1.

[36] S.-R. Yang, A. M. Schultheis, H. Yu, D. Mandelker, M. Ladanyi, and R. Büttner, “Precision medicine in non-small cell lung cancer: Current applications and future directions,” *Semin Cancer Biol*, vol. 84, pp. 184–198, Sep. 2022, doi: 10.1016/j.semcancer.2020.07.009.

[37] B. Arneth, “Tumor Microenvironment,” *Medicina (B Aires)*, vol. 56, no. 1, p. 15, Dec. 2019, doi: 10.3390/medicina56010015.

[38] A. A. Rasheed and V. P. B. Koyyala, “The Tumor Microenvironment,” *Indian Journal of Medical and Paediatric Oncology*, vol. 41, no. 02, pp. 213–214, Mar. 2020, doi: 10.4103/ijmpo.ijmpo_25_20.

[39] C. M. Neophytou, M. Panagi, T. Stylianopoulos, and P. Papageorgis, “The Role of Tumor Microenvironment in Cancer Metastasis: Molecular Mechanisms and Therapeutic Opportunities,” *Cancers (Basel)*, vol. 13, no. 9, p. 2053, Apr. 2021, doi: 10.3390/cancers13092053.

[40] H. Sabit *et al.*, “Beyond Cancer Cells: How the Tumor Microenvironment Drives Cancer Progression,” *Cells*, vol. 13, no. 19, p. 1666, Oct. 2024, doi: 10.3390/cells13191666.

[41] B. Emon, J. Bauer, Y. Jain, B. Jung, and T. Saif, “Biophysics of Tumor Microenvironment and Cancer Metastasis - A Mini Review,” *Comput Struct Biotechnol J*, vol. 16, pp. 279–287, 2018, doi: 10.1016/j.csbj.2018.07.003.

[42] M. Wang *et al.*, “Role of tumor microenvironment in tumorigenesis,” *J Cancer*, vol. 8, no. 5, pp. 761–773, 2017, doi: 10.7150/jca.17648.

[43] Habibah Nadeem, Muhammad Kashif Shahzad Virk, Faizan Abbas, Zahra Nawaz, Muhammad Waseel Ahmad, and Musab Binyameen, “The Role of Tumour Microenvironment in Cancer Progression and Therapeutic Resistance Mechanisms and Implications for Treatment Strategies,” *Indus Journal of Bioscience Research*, vol. 3, no. 4, pp. 107–117, Apr. 2025, doi: 10.70749/ijbr.v3i4.991.

[44] D. C. Hinshaw and L. A. Shevde, “The Tumor Microenvironment Innately Modulates Cancer Progression,” *Cancer Res*, vol. 79, no. 18, pp. 4557–4566, Sep. 2019, doi: 10.1158/0008-5472.CAN-18-3962.

[45] V. Petrova, M. Annicchiarico-Petruzzelli, G. Melino, and I. Amelio, “The hypoxic tumour microenvironment,” *Oncogenesis*, vol. 7, no. 1, p. 10, Jan. 2018, doi: 10.1038/s41389-017-0011-9.

[46] S. Huang *et al.*, “Cellular dynamics of tumor microenvironment driving immunotherapy resistance in non-small-cell lung carcinoma,” *Cancer Lett*, vol. 604, p. 217272, Nov. 2024, doi: 10.1016/j.canlet.2024.217272.

[47] C. Madeddu, C. Donisi, N. Liscia, E. Lai, M. Scartozzi, and A. Macciò, “EGFR-Mutated Non-Small Cell Lung Cancer and Resistance to Immunotherapy: Role of the Tumor Microenvironment,” *Int J Mol Sci*, vol. 23, no. 12, p. 6489, Jun. 2022, doi: 10.3390/ijms23126489.

[48] A. De Lucia *et al.*, “Non-small cell lung cancer and the tumor microenvironment: making headway from targeted therapies to advanced immunotherapy,” *Front Immunol*, vol. 16, Feb. 2025, doi: 10.3389/fimmu.2025.1515748.

[49] R. Paredes, R. Borea, F. Drago, A. Russo, G. Nigita, and C. Rolfo, “Genetic drivers of tumor microenvironment and immunotherapy resistance in non-small cell lung cancer: the role of *KEAP1* , *SMARCA4* , and *PTEN* mutations,” *J Immunother Cancer*, vol. 13, no. 8, p. e012288, Aug. 2025, doi: 10.1136/jitc-2025-012288.

[50] T. Lv *et al.*, “Tumor-Associated Macrophages: Key Players in the Non-Small Cell Lung Cancer Tumor Microenvironment,” *Cancer Med*, vol. 14, no. 3, Feb. 2025, doi: 10.1002/cam4.70670.

[51] Y. Chen, K. M. McAndrews, and R. Kalluri, “Clinical and therapeutic relevance of cancer-associated fibroblasts,” *Nat Rev Clin Oncol*, vol. 18, no. 12, pp. 792–804, Dec. 2021, doi: 10.1038/s41571-021-00546-5.

[52] R. Rimal *et al.*, “Cancer-associated fibroblasts: Origin, function, imaging, and therapeutic targeting,” *Adv Drug Deliv Rev*, vol. 189, p. 114504, Oct. 2022, doi: 10.1016/j.addr.2022.114504.

[53] K. Wright, T. Ly, M. Kriet, A. Czirok, and S. M. Thomas, “Cancer-Associated Fibroblasts: Master Tumor Microenvironment Modifiers,” *Cancers (Basel)*, vol. 15, no. 6, p. 1899, Mar. 2023, doi: 10.3390/cancers15061899.

[54] T. Liu, L. Zhou, D. Li, T. Andl, and Y. Zhang, “Cancer-Associated Fibroblasts Build and Secure the Tumor Microenvironment,” *Front Cell Dev Biol*, vol. 7, Apr. 2019, doi: 10.3389/fcell.2019.00060.

[55] C. Zeltz, I. Primac, P. Erusappan, J. Alam, A. Noel, and D. Gullberg, “Cancer-associated fibroblasts in desmoplastic tumors: emerging role of integrins,” *Semin Cancer Biol*, vol. 62, pp. 166–181, May 2020, doi: 10.1016/j.semcancer.2019.08.004.

[56] R.-P. Czekay, D.-J. Cheon, R. Samarakoon, S. M. Kutz, and P. J. Higgins, “Cancer-Associated Fibroblasts: Mechanisms of Tumor Progression and Novel Therapeutic Targets,” *Cancers (Basel)*, vol. 14, no. 5, p. 1231, Feb. 2022, doi: 10.3390/cancers14051231.

[57] E. Sahai *et al.*, “A framework for advancing our understanding of cancer-associated fibroblasts,” *Nat Rev Cancer*, vol. 20, no. 3, pp. 174–186, Mar. 2020, doi: 10.1038/s41568-019-0238-1.

[58] H. Luo *et al.*, “Pan-cancer single-cell analysis reveals the heterogeneity and plasticity of cancer-associated fibroblasts in the tumor microenvironment,” *Nat Commun*, vol. 13, no. 1, p. 6619, Nov. 2022, doi: 10.1038/s41467-022-34395-2.

[59] D. Lavie, A. Ben-Shmuel, N. Erez, and R. Scherz-Shouval, “Cancer-associated fibroblasts in the single-cell era,” *Nat Cancer*, vol. 3, no. 7, pp. 793–807, Jul. 2022, doi: 10.1038/s43018-022-00411-z.

[60] L. Cords *et al.*, “Cancer-associated fibroblast classification in single-cell and spatial proteomics data,” *Nat Commun*, vol. 14, no. 1, p. 4294, Jul. 2023, doi: 10.1038/s41467-023-39762-1.

[61] X. Lan, W. Li, K. Zhao, J. Wang, S. Li, and H. Zhao, “Revisiting the role of cancer-associated fibroblasts in tumor microenvironment,” *Front Immunol*, vol. 16, Apr. 2025, doi: 10.3389/fimmu.2025.1582532.

[62] E. Sahai *et al.*, “A framework for advancing our understanding of cancer-associated fibroblasts,” *Nat Rev Cancer*, vol. 20, no. 3, pp. 174–186, Mar. 2020, doi: 10.1038/s41568-019-0238-1.

[63] R. S. A. El Alaa, W. Al-Mannai, N. Darwish, and L. Al-Mansoori, “Adipose-Derived Stromal Cells and Cancer-Associated Fibroblasts: Interactions and Implications in Tumor Progression,” *Int J Mol Sci*, vol. 25, no. 21, p. 11558, Oct. 2024, doi: 10.3390/ijms252111558.

[64] X. Shi, C. D. Young, H. Zhou, and X.-J. Wang, “Transforming Growth Factor-β Signaling in Fibrotic Diseases and Cancer-Associated Fibroblasts,” *Biomolecules*, vol. 10, no. 12, p. 1666, Dec. 2020, doi: 10.3390/biom10121666.

[65] J. Y.-F. Chung *et al.*, “TGF-β Signaling: From Tissue Fibrosis to Tumor Microenvironment,” *Int J Mol Sci*, vol. 22, no. 14, p. 7575, Jul. 2021, doi: 10.3390/ijms22147575.

[66] F. Wu *et al.*, “Signaling pathways in cancer-associated fibroblasts and targeted therapy for cancer,” *Signal Transduct Target Ther*, vol. 6, no. 1, p. 218, Jun. 2021, doi: 10.1038/s41392-021-00641-0.

[67] J. Wu *et al.*, “<scp>CD248</scp> -expressing cancer-associated fibroblasts induce non-small cell lung cancer metastasis via Hippo pathway-mediated extracellular matrix stiffness,” *J Cell Mol Med*, vol. 28, no. 16, Aug. 2024, doi: 10.1111/jcmm.70025.

[68] C. Chen, Y. Feng, F. C. F. Ko, S. K. Lam, S. Yan, and J. C. M. Ho, “Lung cancer-associated fibroblasts-mediated collagen deposition drives mediastinal lymph node metastasis in non-small cell lung cancer,” *Front Oncol*, vol. 15, Jun. 2025, doi: 10.3389/fonc.2025.1597585.

[69] Z. Wu, M. Luo, H. Hu, Z. Jiang, Y. Lu, and Z.-J. Xiao, “Hidden forces: the impact of cancer-associated fibroblasts on non-small cell lung cancer development and therapy,” *J Transl Med*, vol. 23, no. 1, p. 830, Jul. 2025, doi: 10.1186/s12967-025-06791-x.

[70] C. Li, Y. Qiu, and Y. Zhang, “Research Progress on Therapeutic Targeting of Cancer-Associated Fibroblasts to Tackle Treatment-Resistant NSCLC,” *Pharmaceuticals*, vol. 15, no. 11, p. 1411, Nov. 2022, doi: 10.3390/ph15111411.

[71] K. Y. Wong *et al.*, “Cancer-associated fibroblasts in nonsmall cell lung cancer: From molecular mechanisms to clinical implications,” *Int J Cancer*, vol. 151, no. 8, pp. 1195–1215, Oct. 2022, doi: 10.1002/ijc.34127.

[72] C. Chen, Y. Feng, F. C. F. Ko, S. K. Lam, S. Yan, and J. C. M. Ho, “Lung cancer-associated fibroblasts-mediated collagen deposition drives mediastinal lymph node metastasis in non-small cell lung cancer,” *Front Oncol*, vol. 15, Jun. 2025, doi: 10.3389/fonc.2025.1597585.

[73] F. Wu *et al.*, “Signaling pathways in cancer-associated fibroblasts and targeted therapy for cancer,” *Signal Transduct Target Ther*, vol. 6, no. 1, p. 218, Jun. 2021, doi: 10.1038/s41392-021-00641-0.

[74] Y. Shintani, T. Kimura, S. Funaki, N. Ose, T. Kanou, and E. Fukui, “Therapeutic Targeting of Cancer-Associated Fibroblasts in the Non-Small Cell Lung Cancer Tumor Microenvironment,” *Cancers (Basel)*, vol. 15, no. 2, p. 335, Jan. 2023, doi: 10.3390/cancers15020335.

[75] J. W. Kaspar, S. K. Niture, and A. K. Jaiswal, “Nrf2:INrf2 (Keap1) signaling in oxidative stress,” Nov. 01, 2009. doi: 10.1016/j.freeradbiomed.2009.07.035.

[76] S. Murakami, Y. Kusano, K. Okazaki, T. Akaike, and H. Motohashi, “NRF2 signalling in cytoprotection and metabolism,” *Br J Pharmacol*, Oct. 2023, doi: 10.1111/bph.16246.

[77] C. Tonelli, I. I. C. Chio, and D. A. Tuveson, “Transcriptional Regulation by Nrf2,” *Antioxid Redox Signal*, vol. 29, no. 17, pp. 1727–1745, Dec. 2018, doi: 10.1089/ars.2017.7342.

[78] J.-M. Lee, M. J. Calkins, K. Chan, Y. W. Kan, and J. A. Johnson, “Identification of the NF-E2-related Factor-2-dependent Genes Conferring Protection against Oxidative Stress in Primary Cortical Astrocytes Using Oligonucleotide Microarray Analysis,” *Journal of Biological Chemistry*, vol. 278, no. 14, pp. 12029–12038, Apr. 2003, doi: 10.1074/jbc.M211558200.

[79] T. Nguyen, H. C. Huang, and C. B. Pickett, “Transcriptional regulation of the antioxidant response element. Activation by Nrf2 and repression by MafK.,” *J Biol Chem*, vol. 275, no. 20, pp. 15466–73, May 2000, doi: 10.1074/jbc.M000361200.

[80] J. Alam, D. Stewart, C. Touchard, S. Boinapally, A. M. Choi, and J. L. Cook, “Nrf2, a Cap’n’Collar transcription factor, regulates induction of the heme oxygenase-1 gene.,” *J Biol Chem*, vol. 274, no. 37, pp. 26071–8, Sep. 1999, doi: 10.1074/jbc.274.37.26071.

[81] X. Yang *et al.*, “Targeting epigenetic and post-translational modifications of NRF2: key regulatory factors in disease treatment,” *Cell Death Discov*, vol. 11, no. 1, p. 189, Apr. 2025, doi: 10.1038/s41420-025-02491-z.

[82] F. He, X. Ru, and T. Wen, “NRF2, a Transcription Factor for Stress Response and Beyond,” *Int J Mol Sci*, vol. 21, no. 13, p. 4777, Jul. 2020, doi: 10.3390/ijms21134777.

[83] Q. Liu, Y. Gao, and X. Ci, “Role of Nrf2 and Its Activators in Respiratory Diseases,” *Oxid Med Cell Longev*, vol. 2019, pp. 1–17, Jan. 2019, doi: 10.1155/2019/7090534.

[84] V. Ngo and M. L. Duennwald, “Nrf2 and Oxidative Stress: A General Overview of Mechanisms and Implications in Human Disease,” *Antioxidants*, vol. 11, no. 12, p. 2345, Nov. 2022, doi: 10.3390/antiox11122345.

[85] L. Baird and M. Yamamoto, “The Molecular Mechanisms Regulating the KEAP1-NRF2 Pathway,” *Mol Cell Biol*, vol. 40, no. 13, Jun. 2020, doi: 10.1128/MCB.00099-20.

[86] C. Shan, Y. Wang, and Y. Wang, “The Crosstalk between Autophagy and Nrf2 Signaling in Cancer: from Biology to Clinical Applications,” *Int J Biol Sci*, vol. 20, no. 15, pp. 6181–6206, Nov. 2024, doi: 10.7150/ijbs.103187.

[87] T. Jiang, B. Harder, M. Rojo de la Vega, P. K. Wong, E. Chapman, and D. D. Zhang, “p62 links autophagy and Nrf2 signaling,” *Free Radic Biol Med*, vol. 88, pp. 199–204, Nov. 2015, doi: 10.1016/j.freeradbiomed.2015.06.014.

[88] A. Jain *et al.*, “p62/SQSTM1 Is a Target Gene for Transcription Factor NRF2 and Creates a Positive Feedback Loop by Inducing Antioxidant Response Element-driven Gene Transcription,” *Journal of Biological Chemistry*, vol. 285, no. 29, pp. 22576–22591, Jul. 2010, doi: 10.1074/jbc.M110.118976.

[89] Y. Chen *et al.*, “Nrf2 signaling pathway activation through Keap1-dependent and -independent mechanisms in response to acute benzo[a]pyrene exposure in Mytilus coruscus,” *Aquatic Toxicology*, vol. 287, p. 107513, Oct. 2025, doi: 10.1016/j.aquatox.2025.107513.

[90] J. Zhang, M. Zhang, M. Tatar, and R. Gong, “Keap1-independent Nrf2 regulation: A novel therapeutic target for treating kidney disease,” *Redox Biol*, vol. 82, p. 103593, May 2025, doi: 10.1016/j.redox.2025.103593.

[91] J. Y. Lo, B. N. Spatola, and S. P. Curran, “WDR23 regulates NRF2 independently of KEAP1,” *PLoS Genet*, vol. 13, no. 4, p. e1006762, Apr. 2017, doi: 10.1371/journal.pgen.1006762.

[92] A. I. Rojo *et al.*, “Signaling pathways activated by the phytochemical nordihydroguaiaretic acid contribute to a Keap1-independent regulation of Nrf2 stability:

Role of glycogen synthase kinase-3," *Free Radic Biol Med*, vol. 52, no. 2, pp. 473–487, Jan. 2012, doi: 10.1016/j.freeradbiomed.2011.11.003.

[93] H.-C. Huang, T. Nguyen, and C. B. Pickett, "Phosphorylation of Nrf2 at Ser-40 by Protein Kinase C Regulates Antioxidant Response Element-mediated Transcription," *Journal of Biological Chemistry*, vol. 277, no. 45, pp. 42769–42774, Nov. 2002, doi: 10.1074/jbc.M206911200.

[94] H. K. Bryan, A. Olayanju, C. E. Goldring, and B. K. Park, "The Nrf2 cell defence pathway: Keap1-dependent and -independent mechanisms of regulation," *Biochem Pharmacol*, vol. 85, no. 6, pp. 705–717, Mar. 2013, doi: 10.1016/j.bcp.2012.11.016.

[95] X. Yuan *et al.*, "Butylated hydroxyanisole regulates ARE-mediated gene expression via Nrf2 coupled with ERK and JNK signaling pathway in HepG2 cells," *Mol Carcinog*, vol. 45, no. 11, pp. 841–850, Nov. 2006, doi: 10.1002/mc.20234.

[96] Y.-S. Keum *et al.*, "Mechanism of Action of Sulforaphane: Inhibition of p38 Mitogen-Activated Protein Kinase Isoforms Contributing to the Induction of Antioxidant Response Element–Mediated Heme Oxygenase-1 in Human Hepatoma HepG2 Cells," *Cancer Res*, vol. 66, no. 17, pp. 8804–8813, Sep. 2006, doi: 10.1158/0008-5472.CAN-05-3513.

[97] M. Komatsu *et al.*, "The selective autophagy substrate p62 activates the stress responsive transcription factor Nrf2 through inactivation of Keap1," *Nat Cell Biol*, vol. 12, no. 3, pp. 213–223, Mar. 2010, doi: 10.1038/ncb2021.

[98] C. A. Silva-Islas and P. D. Maldonado, "Canonical and non-canonical mechanisms of Nrf2 activation," *Pharmacol Res*, vol. 134, pp. 92–99, Aug. 2018, doi: 10.1016/j.phrs.2018.06.013.

[99] W. Chen *et al.*, "Direct Interaction between Nrf2 and p21Cip1/WAF1 Upregulates the Nrf2-Mediated Antioxidant Response," *Mol Cell*, vol. 34, no. 6, pp. 663–673, Jun. 2009, doi: 10.1016/j.molcel.2009.04.029.

[100] H. Robertson, A. T. Dinkova-Kostova, and J. D. Hayes, "NRF2 and the Ambiguous Consequences of Its Activation during Initiation and the Subsequent Stages of Tumourigenesis," *Cancers (Basel)*, vol. 12, no. 12, p. 3609, Dec. 2020, doi: 10.3390/cancers12123609.

[101] R. Pillai, M. Hayashi, A.-M. Zavitsanou, and T. Papagiannakopoulos, "NRF2: KEAPing Tumors Protected," *Cancer Discov*, vol. 12, no. 3, pp. 625–643, Mar. 2022, doi: 10.1158/2159-8290.CD-21-0922.

[102] M. Rojo de la Vega, E. Chapman, and D. D. Zhang, "NRF2 and the Hallmarks of Cancer," *Cancer Cell*, vol. 34, no. 1, pp. 21–43, Jul. 2018, doi: 10.1016/j.ccell.2018.03.022.

[103] C. Glorieux, C. Enríquez, C. González, G. Aguirre-Martínez, and P. Buc Calderon, "The Multifaceted Roles of NRF2 in Cancer: Friend or Foe?," *Antioxidants*, vol. 13, no. 1, p. 70, Jan. 2024, doi: 10.3390/antiox13010070.

[104] E. Panieri *et al.*, "Potential Applications of NRF2 Modulators in Cancer Therapy," *Antioxidants*, vol. 9, no. 3, p. 193, Feb. 2020, doi: 10.3390/antiox9030193.

[105] S. P. Hallis, J. M. Kim, and M.-K. Kwak, “Emerging Role of NRF2 Signaling in Cancer Stem Cell Phenotype,” *Mol Cells*, vol. 46, no. 3, pp. 153–164, Mar. 2023, doi: 10.14348/molcells.2023.2196.

[106] R. Wang, L. Liang, M. Matsumoto, K. Iwata, A. Umemura, and F. He, “Reactive Oxygen Species and NRF2 Signaling, Friends or Foes in Cancer?,” *Biomolecules*, vol. 13, no. 2, p. 353, Feb. 2023, doi: 10.3390/biom13020353.

[107] J. Zhang, H.-X. Xu, J.-Q. Zhu, Y.-X. Dou, Y.-F. Xian, and Z.-X. Lin, “Natural Nrf2 Inhibitors: A Review of Their Potential for Cancer Treatment,” *Int J Biol Sci*, vol. 19, no. 10, pp. 3029–3041, 2023, doi: 10.7150/ijbs.82401.

[108] S. V. Ramisetti, T. Patra, V. Munirathnam, J. V. Sainath, D. Veeraiyan, and A. Namani, “NRF2 Signaling Pathway in Chemo/Radio/Immuno-Therapy Resistance of Lung Cancer: Looking Beyond the Tip of the Iceberg,” *Arch Bronconeumol*, vol. 60, pp. S59–S66, Oct. 2024, doi: 10.1016/j.arbres.2024.06.021.

[109] M. Yildiz and H. Segmen, “Two Faces of Nrf2 in Cancer,” in *Molecular Mechanisms in Cancer*, IntechOpen, 2022. doi: 10.5772/intechopen.102753.

[110] H. Kumar, R. M. Kumar, D. Bhattacharjee, P. Somanna, and V. Jain, “Role of Nrf2 Signaling Cascade in Breast Cancer: Strategies and Treatment,” *Front Pharmacol*, vol. 13, Apr. 2022, doi: 10.3389/fphar.2022.720076.

[111] H. Kitamura and H. Motohashi, “NRF2 addiction in cancer cells,” *Cancer Sci*, vol. 109, no. 4, pp. 900–911, Apr. 2018, doi: 10.1111/cas.13537.

[112] K. Taguchi and M. Yamamoto, “The KEAP1–NRF2 System in Cancer,” *Front Oncol*, vol. 7, May 2017, doi: 10.3389/fonc.2017.00085.

[113] S. H. Hamad *et al.*, “TP53, CDKN2A/P16, and NFE2L2/NRF2 regulate the incidence of pure- and combined-small cell lung cancer in mice,” *Oncogene*, vol. 41, no. 25, pp. 3423–3432, Jun. 2022, doi: 10.1038/s41388-022-02348-0.

[114] T. Shibata *et al.*, “Cancer related mutations in *NRF2* impair its recognition by Keap1-Cul3 E3 ligase and promote malignancy,” *Proceedings of the National Academy of Sciences*, vol. 105, no. 36, pp. 13568–13573, Sep. 2008, doi: 10.1073/pnas.0806268105.

[115] M. J. Kerins and A. Ooi, “A catalogue of somatic NRF2 gain-of-function mutations in cancer,” *Sci Rep*, vol. 8, no. 1, p. 12846, Aug. 2018, doi: 10.1038/s41598-018-31281-0.

[116] J. Zhao *et al.*, “Nrf2 Mediates Metabolic Reprogramming in Non-Small Cell Lung Cancer,” *Front Oncol*, vol. 10, Nov. 2020, doi: 10.3389/fonc.2020.578315.

[117] F. Goeman *et al.*, “Mutations in the KEAP1-NFE2L2 Pathway Define a Molecular Subset of Rapidly Progressing Lung Adenocarcinoma,” *Journal of Thoracic Oncology*, vol. 14, no. 11, pp. 1924–1934, Nov. 2019, doi: 10.1016/j.jtho.2019.07.003.

[118] X. Jiang *et al.*, “High expression of nuclear NRF2 combined with NFE2L2 alterations predicts poor prognosis in esophageal squamous cell carcinoma patients,” *Modern Pathology*, vol. 35, no. 7, pp. 929–937, Jul. 2022, doi: 10.1038/s41379-022-01010-0.

[119] M. Sánchez-Ortega, A. C. Carrera, and A. Garrido, “Role of NRF2 in lung cancer,” Aug. 01, 2021, *MDPI*. doi: 10.3390/cells10081879.

[120] A. Hammad, A. Namani, M. Elshaer, X. J. Wang, and X. Tang, "'NRF2 addiction' in lung cancer cells and its impact on cancer therapy," *Cancer Lett*, vol. 467, pp. 40–49, Dec. 2019, doi: 10.1016/j.canlet.2019.09.016.

[121] B. Singh, N. K. Bhat, and H. K. Bhat, "Induction of NAD(P)H-quinone oxidoreductase 1 by antioxidants in female ACI rats is associated with decrease in oxidative DNA damage and inhibition of estrogen-induced breast cancer.," *Carcinogenesis*, vol. 33, no. 1, pp. 156–63, Jan. 2012, doi: 10.1093/carcin/bgr237.

[122] X. Sun *et al.*, "NRF2 preserves genomic integrity by facilitating ATR activation and G2 cell cycle arrest," *Nucleic Acids Res*, vol. 48, no. 16, pp. 9109–9123, Sep. 2020, doi: 10.1093/nar/gkaa631.

[123] F. Liu *et al.*, "Increased Susceptibility of Nrf2-Null Mice to 1-Bromopropane–Induced Hepatotoxicity," *Toxicological Sciences*, vol. 115, no. 2, pp. 596–606, Jun. 2010, doi: 10.1093/toxsci/kfq075.

[124] J. Wang and T. Konishi, "Nuclear factor (erythroid-derived 2)-like 2 antioxidative response mitigates cytoplasmic radiation-induced <scp>DNA</scp> double-strand breaks," *Cancer Sci*, vol. 110, no. 2, pp. 686–696, Feb. 2019, doi: 10.1111/cas.13916.

[125] H. Satoh *et al.*, "NRF2 Intensifies Host Defense Systems to Prevent Lung Carcinogenesis, but After Tumor Initiation Accelerates Malignant Cell Growth.," *Cancer Res*, vol. 76, no. 10, pp. 3088–96, May 2016, doi: 10.1158/0008-5472.CAN-15-1584.

[126] H. Ikeda, S. Nishi, and M. Sakai, "Transcription factor Nrf2/MafK regulates rat placental glutathione S-transferase gene during hepatocarcinogenesis.," *Biochem J*, vol. 380, no. Pt 2, pp. 515–21, Jun. 2004, doi: 10.1042/BJ20031948.

[127] M. Ramos-Gomez, P. M. Dolan, K. Itoh, M. Yamamoto, and T. W. Kensler, "Interactive effects of nrf2 genotype and oltipraz on benzo[a]pyrene-DNA adducts and tumor yield in mice.," *Carcinogenesis*, vol. 24, no. 3, pp. 461–7, Mar. 2003, doi: 10.1093/carcin/24.3.461.

[128] R. Saddawi-Konefka *et al.*, "Nrf2 Induces IL-17D to Mediate Tumor and Virus Surveillance," *Cell Rep*, vol. 16, no. 9, pp. 2348–2358, Aug. 2016, doi: 10.1016/j.celrep.2016.07.075.

[129] S. Menegon, A. Columbano, and S. Giordano, "The Dual Roles of NRF2 in Cancer," *Trends Mol Med*, vol. 22, no. 7, pp. 578–593, Jul. 2016, doi: 10.1016/j.molmed.2016.05.002.

[130] A. Hammad, A. Namani, M. Elshaer, X. J. Wang, and X. Tang, "'NRF2 addiction' in lung cancer cells and its impact on cancer therapy," *Cancer Lett*, vol. 467, pp. 40–49, Dec. 2019, doi: 10.1016/j.canlet.2019.09.016.

[131] J. M. DeBlasi and G. M. DeNicola, "Dissecting the Crosstalk between NRF2 Signaling and Metabolic Processes in Cancer," *Cancers (Basel)*, vol. 12, no. 10, p. 3023, Oct. 2020, doi: 10.3390/cancers12103023.

[132] A. Singh *et al.*, "NRF2 Activation Promotes Aggressive Lung Cancer and Associates with Poor Clinical Outcomes," *Clinical Cancer Research*, vol. 27, no. 3, pp. 877–888, Feb. 2021, doi: 10.1158/1078-0432.CCR-20-1985.

[133] C. Kandoth *et al.*, “Mutational landscape and significance across 12 major cancer types,” *Nature*, vol. 502, no. 7471, pp. 333–339, Oct. 2013, doi: 10.1038/nature12634.

[134] L. M. Solis *et al.*, “Nrf2 and Keap1 abnormalities in non-small cell lung carcinoma and association with clinicopathologic features.,” *Clin Cancer Res*, vol. 16, no. 14, pp. 3743–53, Jul. 2010, doi: 10.1158/1078-0432.CCR-09-3352.

[135] M. S. Binkley *et al.*, “*KEAP1/NFE2L2* Mutations Predict Lung Cancer Radiation Resistance That Can Be Targeted by Glutaminase Inhibition,” *Cancer Discov*, vol. 10, no. 12, pp. 1826–1841, Dec. 2020, doi: 10.1158/2159-8290.CD-20-0282.

[136] R. Romero *et al.*, “Keap1 loss promotes Kras-driven lung cancer and results in dependence on glutaminolysis,” *Nat Med*, vol. 23, no. 11, pp. 1362–1368, Nov. 2017, doi: 10.1038/nm.4407.

[137] A. Singh, M. Bodas, N. Wakabayashi, F. Bunz, and S. Biswal, “Gain of Nrf2 Function in Non-Small-Cell Lung Cancer Cells Confers Radioresistance,” *Antioxid Redox Signal*, vol. 13, no. 11, pp. 1627–1637, Dec. 2010, doi: 10.1089/ars.2010.3219.

[138] Z. Li *et al.*, “NQO1 protein expression predicts poor prognosis of non-small cell lung cancers.,” *BMC Cancer*, vol. 15, p. 207, Mar. 2015, doi: 10.1186/s12885-015-1227-8.

[139] T. Shibata, S. Saito, A. Kokubu, T. Suzuki, M. Yamamoto, and S. Hirohashi, “Global Downstream Pathway Analysis Reveals a Dependence of Oncogenic NF-E2–Related Factor 2 Mutation on the mTOR Growth Signaling Pathway,” *Cancer Res*, vol. 70, no. 22, pp. 9095–9105, Nov. 2010, doi: 10.1158/0008-5472.CAN-10-0384.

[140] H. M. Aljohani *et al.*, “Genetic mutations associated with lung cancer metastasis to the brain,” *Mutagenesis*, vol. 33, no. 2, pp. 137–145, Apr. 2018, doi: 10.1093/mutage/gey003.

[141] C. Lior, D. Barki, C. Halperin, C. A. Iacobuzio-Donahue, D. Kelsen, and R. S.-Shouval, “Mapping the tumor stress network reveals dynamic shifts in the stromal oxidative stress response,” *Cell Rep*, vol. 43, no. 5, p. 114236, May 2024, doi: 10.1016/j.celrep.2024.114236.

[142] F. He, L. Antonucci, and M. Karin, “NRF2 as a regulator of cell metabolism and inflammation in cancer,” *Carcinogenesis*, vol. 41, no. 4, pp. 405–416, Jun. 2020, doi: 10.1093/carcin/bgaa039.

[143] T. Bae, S. P. Hallis, and M.-K. Kwak, “Hypoxia, oxidative stress, and the interplay of HIFs and NRF2 signaling in cancer,” *Exp Mol Med*, vol. 56, no. 3, pp. 501–514, Mar. 2024, doi: 10.1038/s12276-024-01180-8.

[144] S. A. Best and K. D. Sutherland, “‘Keaping’ a lid on lung cancer: the Keap1-Nrf2 pathway,” *Cell Cycle*, vol. 17, no. 14, pp. 1696–1707, Jul. 2018, doi: 10.1080/15384101.2018.1496756.

[145] M. Choi *et al.*, “Mutation profiles in early-stage lung squamous cell carcinoma with clinical follow-up and correlation with markers of immune function.,” *Ann Oncol*, vol. 28, no. 1, pp. 83–89, Jan. 2017, doi: 10.1093/annonc/mdw437.

[146] J. Feng, O. J. Read, and A. T. Dinkova-Kostova, “Nrf2 in TIME: The Emerging Role of Nuclear Factor Erythroid 2-Related Factor 2 in the Tumor Immune

Microenvironment," *Mol Cells*, vol. 46, no. 3, pp. 142–152, Mar. 2023, doi: 10.14348/molcells.2023.2183.

[147] J. Feng, O. J. Read, and A. T. Dinkova-Kostova, "Nrf2 in TIME: The Emerging Role of Nuclear Factor Erythroid 2-Related Factor 2 in the Tumor Immune Microenvironment," *Mol Cells*, vol. 46, no. 3, pp. 142–152, Mar. 2023, doi: 10.14348/molcells.2023.2183.

[148] L. Baird and M. Yamamoto, "Immunoediting of KEAP1-NRF2 mutant tumours is required to circumvent NRF2-mediated immune surveillance," *Redox Biol*, vol. 67, p. 102904, Nov. 2023, doi: 10.1016/j.redox.2023.102904.

[149] M. Hayashi *et al.*, "Microenvironmental Activation of Nrf2 Restricts the Progression of Nrf2-Activated Malignant Tumors," *Cancer Res*, vol. 80, no. 16, pp. 3331–3344, Aug. 2020, doi: 10.1158/0008-5472.CAN-19-2888.

[150] C. Ma *et al.*, "NRF2-GPX4/SOD2 axis imparts resistance to EGFR-tyrosine kinase inhibitors in non-small-cell lung cancer cells," *Acta Pharmacol Sin*, vol. 42, no. 4, pp. 613–623, Apr. 2021, doi: 10.1038/s41401-020-0443-1.

[151] L. Zuo *et al.*, "The Nrf2-HMOX1 pathway as a therapeutic target for reversing cisplatin resistance in non-small cell lung cancer via inhibiting ferroptosis," *Cell Death Discov*, vol. 11, no. 1, p. 287, Jun. 2025, doi: 10.1038/s41420-025-02564-z.

[152] Y. Tian *et al.*, "Modification of platinum sensitivity by KEAP1/NRF2 signals in non-small cell lung cancer," *J Hematol Oncol*, vol. 9, no. 1, p. 83, Dec. 2016, doi: 10.1186/s13045-016-0311-0.

[153] Y. Chen *et al.*, "5-Methylcytosine transferase NSUN2 drives NRF2-mediated ferroptosis resistance in non-small cell lung cancer," *Journal of Biological Chemistry*, vol. 300, no. 4, p. 106793, Apr. 2024, doi: 10.1016/j.jbc.2024.106793.

[154] S. Huang *et al.*, "Metformin reverses chemoresistance in non-small cell lung cancer via accelerating ubiquitination-mediated degradation of Nrf2," *Transl Lung Cancer Res*, vol. 9, no. 6, pp. 2337–2355, Dec. 2020, doi: 10.21037/tlcr-20-1072.

[155] L. Zuo *et al.*, "The Nrf2-HMOX1 pathway as a therapeutic target for reversing cisplatin resistance in non-small cell lung cancer via inhibiting ferroptosis," *Cell Death Discov*, vol. 11, no. 1, p. 287, Jun. 2025, doi: 10.1038/s41420-025-02564-z.

[156] J.-S. Choi *et al.*, "KEAP1-NRF2 Pathway as a Novel Therapeutic Target for EGFR-Mutant Non-small Cell Lung Cancer," *Tuberc Respir Dis (Seoul)*, vol. 88, no. 1, pp. 138–149, Jan. 2025, doi: 10.4046/trd.2024.0087.

[157] S. L. Wood, M. Pernemalm, P. A. Crosbie, and A. D. Whetton, "The role of the tumor-microenvironment in lung cancer-metastasis and its relationship to potential therapeutic targets," *Cancer Treat Rev*, vol. 40, no. 4, pp. 558–566, May 2014, doi: 10.1016/j.ctrv.2013.10.001.

[158] L. Wang, Q. Jia, Q. Chu, and B. Zhu, "Targeting tumor microenvironment for non-small cell lung cancer immunotherapy," *Chinese Medical Journal Pulmonary and Critical Care Medicine*, vol. 1, no. 1, pp. 18–29, Mar. 2023, doi: 10.1016/j.pccm.2022.11.001.

[159] N. K. Altorki *et al.*, "The lung microenvironment: an important regulator of tumour growth and metastasis.," *Nat Rev Cancer*, vol. 19, no. 1, pp. 9–31, Jan. 2019, doi: 10.1038/s41568-018-0081-9.

[160] A. Abu Qubo *et al.*, "Idiopathic pulmonary fibrosis and lung cancer: future directions and challenges," *Breathe*, vol. 18, no. 4, p. 220147, Dec. 2022, doi: 10.1183/20734735.0147-2022.

[161] B. H. Herzog *et al.*, "Tumor-associated fibrosis impairs immune surveillance and response to immune checkpoint blockade in non–small cell lung cancer," *Sci Transl Med*, vol. 15, no. 699, Jun. 2023, doi: 10.1126/scitranslmed.adh8005.

[162] A. Calon, D. V. F. Tauriello, and E. Batlle, "TGF-beta in CAF-mediated tumor growth and metastasis," *Semin Cancer Biol*, vol. 25, pp. 15–22, Apr. 2014, doi: 10.1016/j.semcancer.2013.12.008.

[163] S. Homma *et al.*, "Nrf2 Enhances Cell Proliferation and Resistance to Anticancer Drugs in Human Lung Cancer," *Clinical Cancer Research*, vol. 15, no. 10, pp. 3423–3432, May 2009, doi: 10.1158/1078-0432.CCR-08-2822.

[164] A. Singh, M. Bodas, N. Wakabayashi, F. Bunz, and S. Biswal, "Gain of Nrf2 Function in Non-Small-Cell Lung Cancer Cells Confers Radioresistance," *Antioxid Redox Signal*, vol. 13, no. 11, pp. 1627–1637, Dec. 2010, doi: 10.1089/ars.2010.3219.

[165] M. M. Silva, C. R. R. Rocha, G. S. Kinker, A. L. Pelegrini, and C. F. M. Menck, "The balance between NRF2/GSH antioxidant mediated pathway and DNA repair modulates cisplatin resistance in lung cancer cells," *Sci Rep*, vol. 9, no. 1, p. 17639, Nov. 2019, doi: 10.1038/s41598-019-54065-6.

[166] H.-C. Huang, T. Nguyen, and C. B. Pickett, "Phosphorylation of Nrf2 at Ser-40 by Protein Kinase C Regulates Antioxidant Response Element-mediated Transcription," *Journal of Biological Chemistry*, vol. 277, no. 45, pp. 42769–42774, Nov. 2002, doi: 10.1074/jbc.M206911200.

[167] W. Chen *et al.*, "Direct Interaction between Nrf2 and p21Cip1/WAF1 Upregulates the Nrf2-Mediated Antioxidant Response," *Mol Cell*, vol. 34, no. 6, pp. 663–673, Jun. 2009, doi: 10.1016/j.molcel.2009.04.029.

[168] N. Rastegar-Pouyani, M. H. Abdolvahab, M. A. Farzin, H. Zare, P. Kesharwani, and A. Sahebkar, "Targeting cancer-associated fibroblasts with pirfenidone: A novel approach for cancer therapy," *Tissue Cell*, vol. 91, p. 102624, Dec. 2024, doi: 10.1016/j.tice.2024.102624.

[169] A. Fujiwara *et al.*, "Effects of pirfenidone targeting the tumor microenvironment and tumor-stroma interaction as a novel treatment for non-small cell lung cancer," *Sci Rep*, vol. 10, no. 1, p. 10900, Jul. 2020, doi: 10.1038/s41598-020-67904-8.

[170] H. A. Es, T. R. Cox, E. Sarafraz-Yazdi, J. P. Thiery, and M. E. Warkiani, "Pirfenidone Reduces Epithelial–Mesenchymal Transition and Spheroid Formation in Breast Carcinoma through Targeting Cancer-Associated Fibroblasts (CAFs)," *Cancers (Basel)*, vol. 13, no. 20, p. 5118, Oct. 2021, doi: 10.3390/cancers13205118.

[171] M. Mediavilla-Varela, K. Boateng, D. Noyes, and S. J. Antonia, "The anti-fibrotic agent pirfenidone synergizes with cisplatin in killing tumor cells and cancer-associated fibroblasts," *BMC Cancer*, vol. 16, no. 1, p. 176, Dec. 2016, doi: 10.1186/s12885-016-2162-z.

La borsa di dottorato è stata finanziata con risorse dell'Unione europea-*NextGeneration EU*
Piano Nazionale di Ripresa e Resilienza Missione 4 – Componente 2 – "Dalla ricerca all'impresa" – Investimento "Centri Nazionali" – *CUP_ PNRR_CN3_RNA_Spoke_2 - PNRR_CN 3_Centro Nazionale di Ricerca Sviluppo di terapia genica e farmaci con tecnologia a RNA - B13C22001010001*